JPL
IN-74-CR
[illegible]
P 124

Metal Thin-film Optical Polarizers for Space Applications

Phase II -- Final Report

Contract # NAS7-1037

May 28, 1991

Robert E. Slocum, Ph D
Principal Investigator

Polatomic, Inc.
2201 Waterview Parkway, #1.712
Richardson, TX 75080

Preface

The Final Report consists of two parts. Part 1 is a Technical Summary of the Phase II effort describing the background, technical innovations, and technical accomplishments. Part 2 records the technical objectives, approachs, and results for each task listed in the Statement of Work in the Phase II Proposal. Each section or subsection is numbered in accordance with the corresponding task in the original Statement of Work A complete bibliography of reference articles, books and patents is included in Part 2.

This work was directed by Principal Investigator Robert E. Slocum. Measurement and instrumentation work was performed by Dmetro Andrychuk. Sample preparation and silver deposition work was performed by Fred Browning.

TABLE OF CONTENTS

PART 1: TECHNICAL SUMMARY

ABSTRACT

A light polarizing material was developed for wavelengths in the visible and near-infrared spectral band (400 nm to 3,000 nm). The material is comprised of ellipsoidal silver particles uniformly distributed and aligned on the surface of an optical material. A method is set forth for making polarizing material by evaporatively coating a smooth glass surface with ellipsoidal silver particles. The wavelength of peak absorption is chosen by selecting the aspect ratio of the ellipsoidal metal particles and the refractive index of the material surrounding the metal particles. The wavelength of peak absorption can be selected to fall at a desired wavelength in the range from 400 nm to 3,000 nm by control of the deposition process. This method is demonstrated by evaporative deposition of silver particles directly on to a smooth optical surface. By applying a multilayer silver coating on a glass disc, a contrast of greater than 40,000 was achieved at 590 nm. A polarizing filter was designed, fabricated and assembled which achieved contrast of 100,000 at 590 nm and can serve as a replacement for crystal polarizers.

1. BACKGROUND

Sheet polarizers were developed to replace crystal beam-splitter polarizers which are expensive, bulky and of limited size. The art of sheet polarizer material is well known dating from Land's invention of the H-sheet dichroic polarizer in 1938. Production of plastic polarizing materials in sheet form is a two step process. First, a suspension medium containing long chain molecules is stretched to align those long chain molecules. Second, polarizing dichroic molecules are added to the medium or included in the medium and attach themselves so as to orient along the aligned chain molecules. The light polarizing particles may also first disperse in the medium and align by extruding, rolling or stretching the medium. For space applications the plastic polarizer is not robust and degrades in the space environment. Crystal polarizers are relatively long and increase the optical path and increase the size of space instruments.

Although the major portion of sheet polarizer material marketed commercially has been the organic plastic material type, Corning has performed research on high performance polarizers for ophthalmic applications where high surface hardness and good scratch resistance are desired. Polarizing glasses have been prepared where ellipsoidal metallic particles dissolved in the glass comprise the polarizing material. The polarizing action is based on the fact that the ellipsoidal metal particle absorbs light polarized along the long axis and transmits light polarized perpendicular to the long axis.

Three methods for making polarizing glass have been disclosed in recent patent literature. U.S. Pat. Nos. 4,125,404 and 4,125,405 disclose a polarizing action in photochromic glasses containing silver halides which are darkened with actinic radiation in the range 350 nm to 410 nm and bleached with linearly polarized bleaching light. U.S. Pat. Nos. 3,653,863 and 4,282,022 disclose the manufacture of highly polarizing glasses starting with glass which is phase separable or photochromic and contains a silver halide which is heat treated to form silver halide particles of the desired size. The glass is then subjected to a two step process. First, the glass is heated at an elevated temperature between the annealing point and the melting point (500 to 600 C) followed by stretching, extruding or rolling the glass containing the silver halide particles to elongate them and orient the particles to an ellipsoidal shape. Second, the glass is subjected to irradiation by actinic radiation to produce silver metal on the surface of the silver halide particles. An improvement of the second step is disclosed in U.S. Patent No. 4,304,584 where the extruded glass is heat treated in a reducing environment at temperatures below the annealing point of the glass in order to produce elongated metallic silver in the glass or on the silver halide particles in a surface layer of the glass at least ten microns thick. It includes the practice of making composite glass bodies where polarizing and photochromic glass layers are combined and laminated.

A further improvement is disclosed in U.S. Pat. No. 4,479,584 for making effective polarizing glasses for the near infrared spectral region described as 700 nm to 3000 nm by improved glass drawing and high temperature reduction techniques. U.S. Pat. No. 4,486,213 describes the cladding of a core polarizing glass with a skin glass in order to achieve high aspect ratios for the elongated metal particles. U.S. Pat. No. 4,908,054 disclosed methods for improving the contrast and the bandwidth of polarization action for the product described in U.S. Patent. No. 4,479,584.

A third class of polarizers are Hertzian polarizers which place metal wires on the surface of a transparent optical material. Prior to 1900 Hertz demonstrated his method for polarizing radiation using an array of parallel reflective wires which were long compared to the wavelength of the radiation to be polarized and were separated by a distance much less than the wavelength to be polarized. The Hertzian polarizer is often configured as a grid of wires but can also be irregularly spaced wires which meet the polarization conditions. The Hertzian polarizer transmits the radiation with electrical vector perpendicular to the wires and reflects radiation with electrical vector parallel to the wires.

U.S. Pat. No. 3,046,839 discribes a method of manufacturing a Hertzian polarizer on the surface of an optical material by first forming a diffraction grating on the surface. The diffraction grating consists of grooves and the groove tips are evaporatively coated with metal to form an array of metal filaments. U.S. Pat. No. 3,353,895 discribes a method of manufacturing a Hertzian polarizer material by forming metal filaments using an evaporative shadowing method. Evaporated metal is directed near the grazing angle toward a bumpy transparent material covered regularly with protuberances. Metal filaments of a Hertzian polarizer are produced by forming filaments which lie along side the protuberances and are separated by the shadows cast by the protuberances.

U.S. Pat. Nos. 3,969,545 and 4,049,338 discribe a Hertzian polarizer comprised of filaments of metal which are evaporatively deposited on smooth surfaces of transparent optical material. The metal elements of the Hertzian polarizer are silver whiskers grown on the surface by grazing angle vacuum deposition of silver.

Each of the three classes of sheet polarizer has characteristics which prevent the realization of the goal of a high performance polarizing material suitable for both the visible and near-infrared spectral region (400 nm to 3,000 nm). The plastic sheet polarizer has poor performance in the near-infrared spectral region and is easily damaged because of the softness of plastic. The Hertzian polarizers applied to optically transparent materials reflects rather that absorbs the unwanted polarization components of radiation which is particularly undesirable for ophthalmic and display applications. The Hertzian method, although successfully applied to the near-infrared spectral region, has not been effectively extended to the visible portion of the spectrum because of the difficulty of producing a uniform density of metal filaments spaced at

separations much less than the wavelength of light. Finally the polarizing glass method is limited to glasses which are highly specialized compositions containing silver. Although the polarizing glasses marketed by Corning under the trademark Polacor are effective near-infrared polarizers, the original goal of manufacturing ophthalmic quality glass for use in quality and prescription sunglasses has not been met. This unmet goal is due to the complexity and difficulty of the shaping and heating of specialty glasses and failure to control the shape and uniformity of the polarizing metal particles for the visible spectral region. We obtained two samples from Corning for evaluation and observed contrast greater than 500 at 590 nm. Unfortunately, Polacor samples for visible light are no longer available for loan or sale.

2. TECHNICAL OBJECTIVE

The anisotropic polarization dependence of the optical absorbance of spheroidal metal particles is well known from such texts as van de Hulst and the suspension of such particles in glass (Corning) or plastics (Land). The properties of spheroidal metal particles on flat surfaces has been investigated by practioners of Surfaced Enhanced Ramann Scattering (SERS). Scientific investigators have observed weak polarization effects in metal thin films. The novel material to be described here places the metal particles on the surface of a transparent optical material in such a way as to achieve significant anisotropic absorption of light with large absorbance of the polarization component vibrating parallel to the alignment axis and large transmission of the component vibrating perpendicular to alignment axis so as to make the material useful as a polarizer. We have demonstrated a process for selecting the particle volume and aspect ratio to effectly tune the wavelength of peak polarization of the material to the desired wavelength in the range covering 450 nm to 3000 nm.

The object of the present effort is to provide a sheet polarizer with excellent contrast over the visible to near infrared spectral region and achieve contrast greater than 10^5 at 590 nm. The light polarizing material can be applied to a smooth surface by forming a coating of aligned ellipsoidal silver particles on that surface. The array of silver particles transmits the desired polarization component and absorbs the unwanted component of polarization. The array of silver particles is formed on a smooth transparent surface by evaporative deposition in a vacuum system. The wavelength of peak polarization can

be selected by the choosing the aspect ratio of the ellipsoidal metal particles and the refractive index of the material surrounding the ellipsoidal metal particles. Heat treatment of the evaporated metal particles can be used to enhance the contrast in the visible spectra region where small aspect ratios (length to width ratios of 5) are required to peak the polarization effect.

3. DESCRIPTION OF SILVER FILM POLARIZER

We report here investigations of methods of making polarizing material by covering the surface of an optical material with ellipsoidal silver particles which are aligned. The light polarization component parallel the alignment direction (absorbed) and the polarization component perpendicular to the alignment direction (transmitted) are measured. The wavelength of peak polarization, determined by the length-to-width ratio (aspect ratio) of the ellipsoidal metal particles and the refractive index of transparent material surrounding the metal particles, was set at 590 nm. A light polarizing, single layer material was demonstrated which has contrast greater than 1,000 for wavelength in the visible and near-infrared spectral band. The material is comprised of ellipsoidal silver particles uniformly distributed and aligned on the surface of an optical material. An analytical model was developed which predicts the polarization effect in an array of aligned ellipsoidal particles. The theoretical predictions for absorption along the particle long axis is shown in Figure 1-a and absorption perpendicular to the long axis is shown in Figure 1-b for a film with contrast of 1000 at 600 nm. An eight layer coat on a single substrate produced a contrast of greater than 40,000. A multi-substrate combination was assembled and tested with contrast greater than 300,000. The polarizing filter delivered to JPL for evaluation has a contrast of 100,000.

A variety of methods were investigated for making polarizing material by evaporatively coating a smooth glass surface with multiple layers of ellipsoidal silver particles. The wavelength of peak absorption can be selected to fall at a desired wavelength in the range from 400 nm to 3,000 nm by control of the deposition process. This method is demonstrated by evaporative deposition of metal particles directly on to a smooth optical surface and locating the wavelength of peak absorption by variation of

No = 1

T_{60} = 0.001

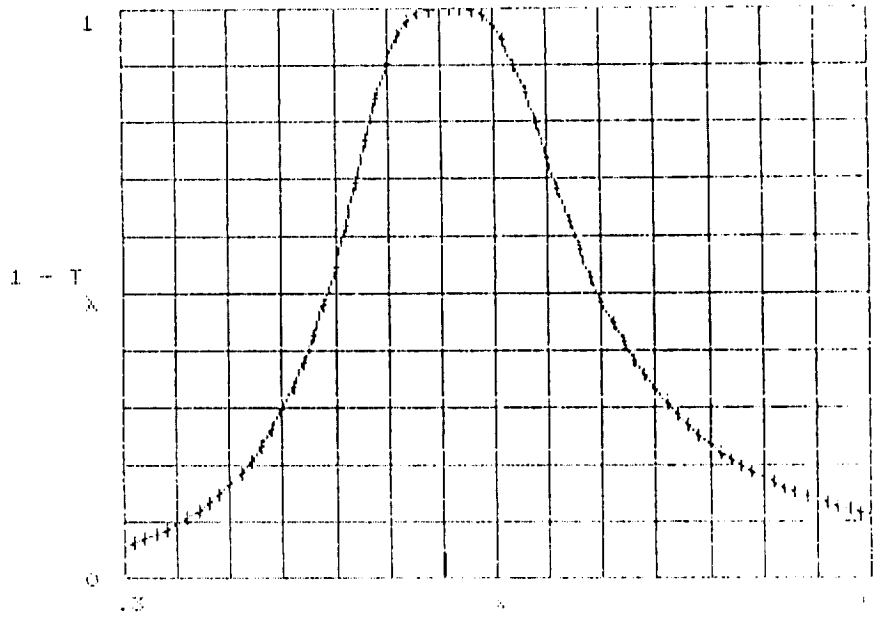

Wavelength in Microns

Figure 1-a

No = 1

T_{60} = 0.995

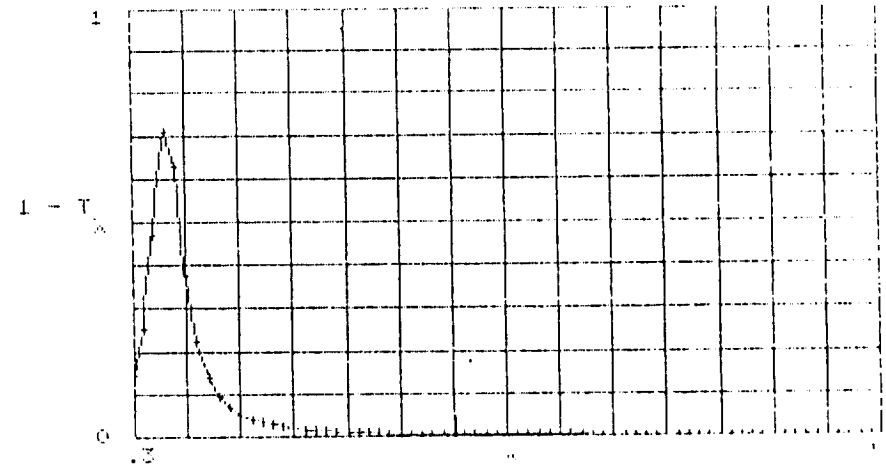

Wavelength in Microns

Figure 1-b

the multilayer deposition process. For silver particles in air, the ratio of particle width-to-length ratio of 0.2 sets the wavelength of peak absorption at 600 nm.

4. FABRICATION OF POLARIZING FILMS AND FILTERS

The transparent optical element selected for the substrate of the polarizing material is a 25 mm diameter disc of BK-7 glass which has been polished to an optical quality, microscopically smooth finish. The method of application of a coating of ellipsoidal metal particles to the surface of the glass disc is evaporative vacuum deposition by means of the apparatus shown in Fig. 2. The unique feature of the deposition technique is the impinging of the evaporated metal on the glass surface at an angle near the grazing angle (greater than 85 degrees to the normal to the glass disc surface).

The glass disc is mounted to a substrate holder and positioned at the correct angle to the metal deposition beam at a distance of 20 cm from the deposition source inside a bell jar. The substrate holder is designed so that the part can be rotated 180 degrees about the normal to the disc at the center of the disc. Position 1 will refer to the alignment of the glass disc is at 0 degrees between the direction of impinging metal vapor stream and an axis on the substrate surface as shown in Fig. 2. Position 2 will refer to alignment of the part when rotated 180 degrees from position 1 about an axis in the center of the substrate normal to the surface. The glass surface is cleaned with alcohol before mounting in the vacuum chamber.

The metal to be vapor deposited is placed in a resistance heating element which in turn is connected to a source of current. Before activating the current source the vacuum chamber is evacuated to a pressure less than 0.00001 torr using known techniques. When the deposition process is activated, metal atoms adhere to the surface and form an elliptical shape particle with the long axis of the ellipsoid aligned with the direction of the evaporated metal beam. The metal of choice is pure silver. The samples described here were prepared by evaporating 0.125 cc of silver, but only a small faction of the silver actually is deposited on the surface of an individual glass disc.

The investigation of thin metal films on surfaces has been an active field of research through out this century. A variety of deposition techniques have been developed for

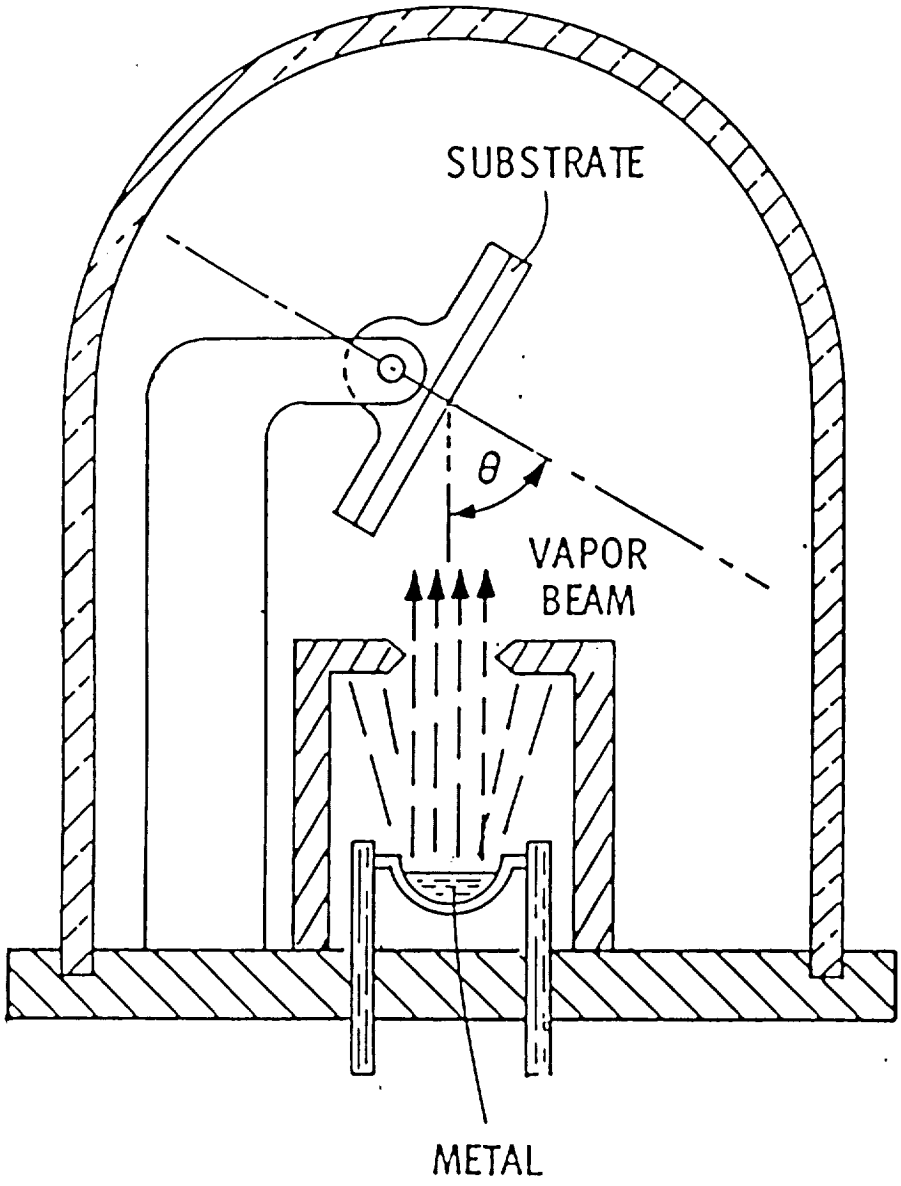

Figure 2

preparing island film of disconnected metal particle with shapes which are spherical, ellipsoidal and in the shape of whiskers. We have devised a novel method for preparation of silver metal particles which exhibit the distinctive polarization behavior of prolate metal spheroids as observed in polarizing glasses (component parallel alignment axis absorbed).

In addition this process is unique in providing a process control method for selecting the wavelength of peak polarization by causing the evaporated metal to impinge on the glass surface in a specific sequence of impingement directions with a specific fraction of silver arriving at the surface in each sequence. This physically selects the effective length-to-width ratio of the ellipsoidal particles which determines the wavelength of peak polarization. The wavelength of peak absorption can be shifted to longer wavelength by increasing the refractive index of the medium which surrounds the particles. The metal particles deposited directly on the surface of the glass are effectively surrounded by air with a refractive index of 1.0. The refractive index can be increased by evaporatively or chemically coating the glass with a higher index material. This method of wavelength selection is demonstrated here by the application of an optical adhesive with refractive index of 1.5.

EXAMPLE 1

The first example divides the deposition into two parts so that half of the silver is deposited in position 1 and half of the silver is deposited in position 2. Peak polarization occurs at 950 nm with particle transmittances $k_1 = .68$ and $k_2 = .0047$. The contrast is 145.

EXAMPLE 2

The second example divides the deposition into four parts so that half the silver is deposited in position 1 and half of the silver is deposited in position 2. Four depositions were made in the position order 1, 2, 1, 2. Peak polarization occurs at 700 nm with principle transmittances $k_1 = .64$ and $k_2 = .0045$. The contrast is 142.

EXAMPLE 3

The third example divides the deposition into 6 parts so that one half of the silver is deposited in position 1 and on half of the silver is deposition in position 2. Six depositions were made in the position order 1, 2, 1, 2, 1, 2. Peak polarization occurs at 600 nm with principle transmittances $k_1 = .58$ and $k_2 = .014$. The contrast is 42.

EXAMPLE 4

The fourth sample was made by dividing the silver into eight parts so that half of the silver is deposited in position 1 and half of the silver is deposited in position 2. Eight depositions were made in the position order 1, 2, 1, 2, 1, 2, 1, 2. Peak polarization occurs at 575 nm with principle transmittances $k_1 = .52$, $k_2 = .0036$ and contrast of 145.

EXAMPLE 5

The fifth sample was made following the process of Example 2. Following completion of the deposition process, the surface of the metal film was coated with optical adhesive which has an index of refraction of 1.50. The wavelength of peak absorption shift from 800 nm to 1200 nm. This illustrates the analytical prediction stating that the wavelength of peak polarization will be proportional to the index of refraction of the material surrounding the spheroidal metal particles.

EXAMPLE 6

The sixth sample was prepared by the method of Example 3 with the following modification in the preparation of the substrate in order to improve the polarizing characteristics of the material at 600 nm. The substrate was first coated with silver and heat treated prior to application of the method of Example 3. The substrate was coated by the method of Example 1 using 0.025 cc of silver for the total evaporation. The sample was heated in a vacuum system for 4 minutes at a distance of 10 cm from an evaporation boat at the temperature normally required to evaporate silver. The precoat of heated silver forms particles with the silver deposited according to the method of Example 3 to produce improved contrast at 600 nm as shown in Figure 3. A Transmission Electron Microscope micrograph of the sample is shown in Figure 4. The

POLARIZER DATA

Date: 05/15/91 Job Number: 8801 Run Number: 1
Disk: #7

A:	Precoat 2" + 2" Ag	D:	
B:	Heat 3 min at 110	E:	
C:	Tilt (-1)	F:	

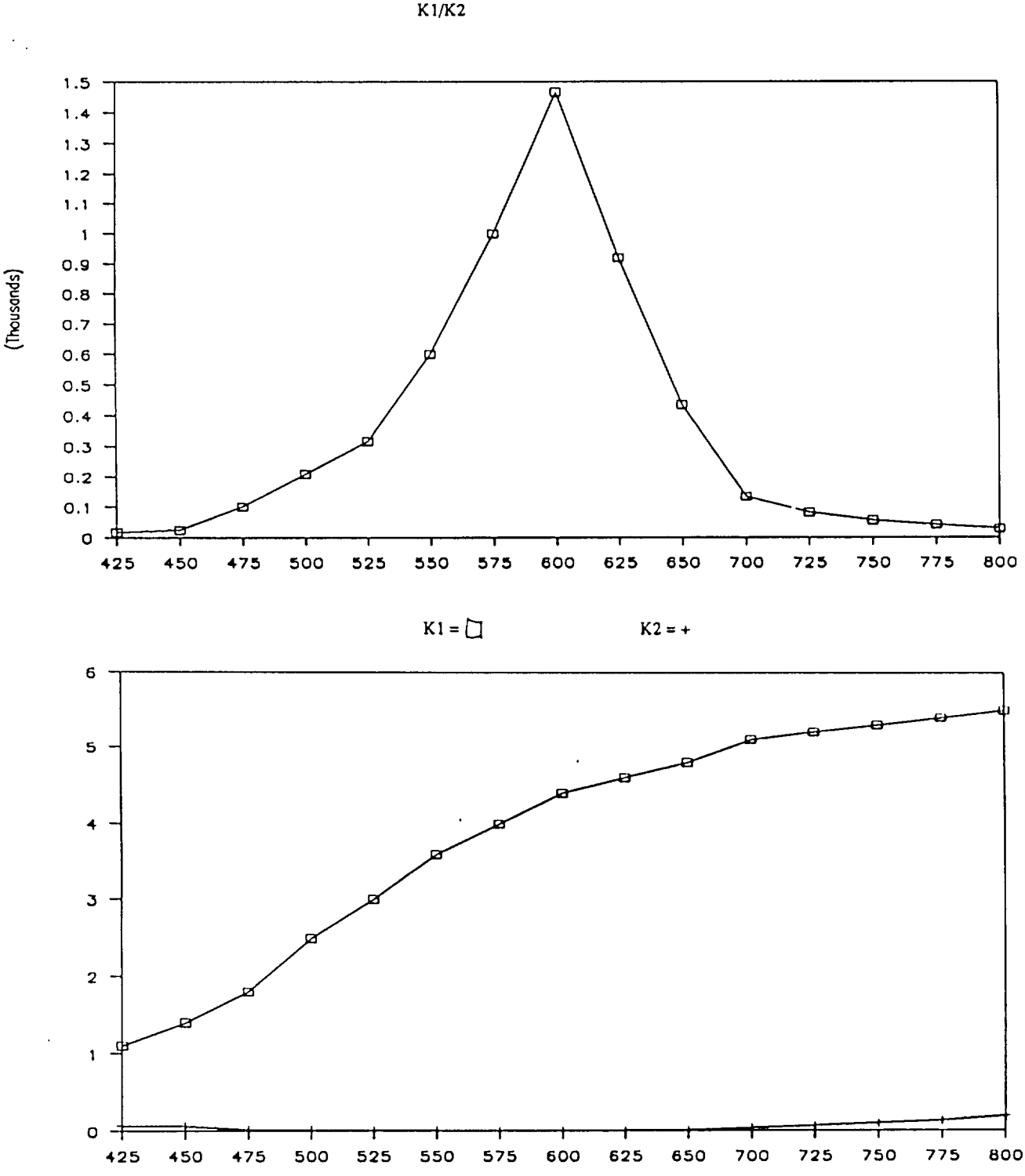

Figure 3

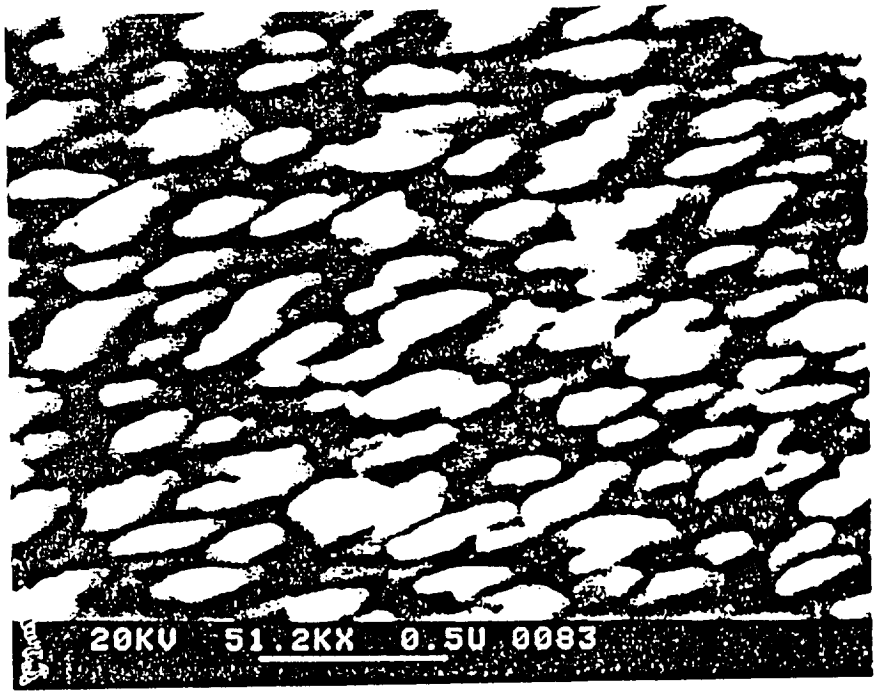

Figure 4

particle density is approximately 50 particles per micron square. The width-to-length ratio appears to be approximately 0.2 as required for a 600 nm peak absorption.

EXAMPLE 7

The final example is the polarizing filter designed using polarizing silver thin films to achieve contrast of 10^5 or greater. Using a laser polarization checker specially designed and constructed for this project, we were able to measure contrasts greater than 10^6.

As optical bench was used to evaluate and position substrates which make up the elements of a polarizing filter for 589 nm. By implementing the two substrate filter designs on the optical bench, the filter design was optimized and components were evaluated. Using Corning Polacor Sample #15 and disc 03-07-91 (1) with eight silver layers, a contrast of 337,500 was achieved. Unfortunately Corning was unable to make available any Polacor glass for assembly into a final polarizing filter.

Using the two silver coated discs 03-07-91 (4) and 03-07-91 (2) we achieved a contrast of 107,400. A ring mount was designed which could be hermetically sealed. The silver films are fragile and the angular alignment tolerances quite tight. Two polarizing filters were mounted and assembled which achieved contrasts of 100,000 and 97,000. These units will be delivered to JPL with the final report. The dependence of contrast on wavelength is shown in Figure 5.

5. CONCLUSIONS

Under the Phase II contract we developed a light polarizing material consisting of a transparent sheet material which is microscopically smooth to eliminate shadowing effects having attached to the surface an array of metal particles in the shape of prolate spheroids oriented in one direction with their long axis essentially parallel. These parallel metal spheroids absorb unwanted light with the electric vector E vibrating along the long axis of the metal spheroids and transmits light with the electric vector E vibrating perpendicular the long axis of the metal spheroids.

POLARIZER DATA

Date: 05/15/91 Job Number: 8801 Run Number: 1
Disk: #1 Assembly

A:	D:
B:	E:
C:	F:

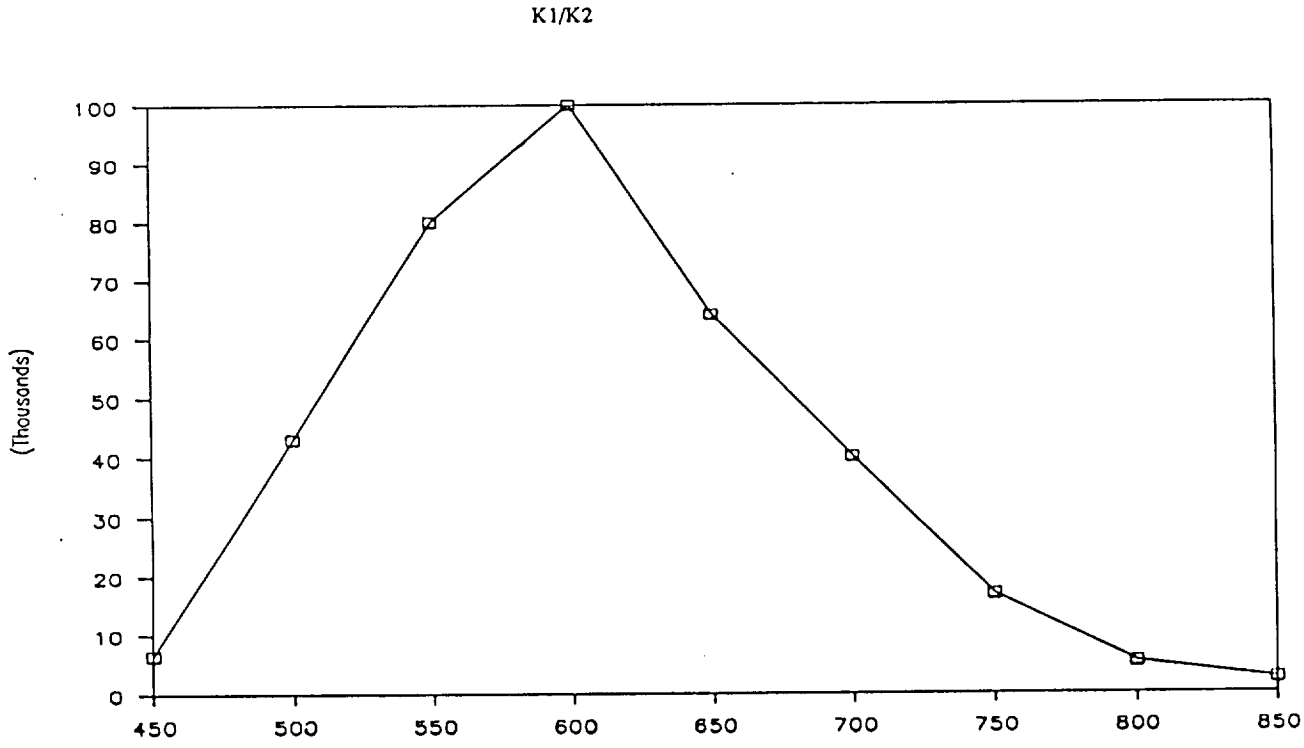

Figure 5

Light with the electric vector vibrating parallel the long axes has absorption which reaches a peak at a wavelength determined by the aspect ratio of the prolate spheroidal metal particles and the index of refraction of the material surrounding the metal particles. The metal spheroids are attached to a transparent sheet material which can be either glasses and plastics transparent to visible light.

The length-to-width ratio of the prolate spheroids are selected from values in the range from 1 to 20 in order to set wavelength of peak polarization in the wavelength band between 300 nm and the near-infrared spectral region. For peak absorption at 600 nm a ratio of 5 is required for silver particles in air.

We demonstrated single layer silver films with contrast in excess of 1000 at 600 nm. When multilayer films were separated by a high index material we achieved a contrast of greater than 40,000 at 600 nm with a single substrate.

The volume of the prolate spheroids seen in electromicrographs appeared to fall in the range of spheres with diameters ranging from 5 nm to 150 nm. The density was of the order of 50 per square micron which places the particles within a radius of each other causing dependent scattering.

A polarizing filter was designed, fabricated, mounted and assembled in a metal holder. Using two discs coated with multilayers of silver, a final contrast of 100,000 was achieved. Because of the high density of silver particles, k_1 was reduced and k_2 was broadened. Future developments would focus on increasing the density of silver particles and increasing the number of layers of silver particles.

The particles in these films had a volume equivalent to spheres of silver with diameters in the range of 150 nm. It was found that volume greater than a sphere of 30 nm diameter introduces unwanted scattering. The scattering could be reduced to a negligible level by reducing the volume of the particles by a factor of 5 and increasing the number of particles a factor of 5. The scattering effect was eliminated from the measurements of the silver film polarizing filters by locating the detector 1 m from the filter.

In conclusion, a novel material for polarizing visible and near infrared radiation has been developed and demonstrated under the Phase II contract. A patent application is being prepared for submission. This approach is found to achieve contrasts greater than 10^5. With reduction of scattering by reduction of particle size, this new high performance polarizing material will be suitable for a variety of scientific and commercial applications.

PART 2: WORK TASK REPORTS

SECTION 1 Filter Design and Theoretical Description

The first technical objective is development of an analytical description for the concept of a light polarizing material consisting of a distribution of metal particles on the surface of a transparent optical material or substrate. The polarizing effect derives from the ability of the dichroic metal particles to absorb one component of linearly polarized light and transmit the other linearly polarized component of polarized light. An analytical expression must be developed to describe the polarization effect of a thin film of metal particles having anisotropic absorption characteristics. The analytical expression will be used to reach the final goal of designing and fabricating a polarizing filter with contrast greater than 100,000 at 590 nm.

The experimental point of departure for this work is the Hertzian thin film polarizer described by Slocum (1976). The Hertzian thin film polarizer employs the parallel wire polarization effect described by Hertz more than a century ago. When parallel wires long compared to the wavelength of the radiation to be polarized are separated by a distance small compared to the radiation wavelength, radiation polarized parallel the wire is reflected, and radiation polarized perpendicular to the wires is transmitted. In order to fabricate a high performance Hertzian polarizer at 590 nm, wires must be separated by a distance much less than 590 nm, a very difficult task. Also, the Hertzian polarizer reflects the unwanted polarization component in the reverse direction of the incident light. For these reasons the Hertzian thin film approach was abandoned in favor of a metal thin film which absorbs the unwanted polarization component.

Our experimental work focused on evaporatively deposited silver particles in the shape of a prolate spheroid. In Section 1.1, the theoretical expression for the absorption of linearly polarized light by a silver prolate spheroid particle will be developed. A review of the literature describing absorption characteristics of metal particles is included in the References section. An absorption expression will be developed for the anisotropic silver prolate spheroid. The expression

takes into account the effect of the index of refraction of the material surrounding the particle on wavelength of peak absorption, the shape of the particle, and the variation of absorption with wavelength.

The absorption characteristics of an array of these silver particles distributed over an optically transparent surface is discussed in Section 1.2. The effect of particle density is investigated. We describe in Section 1.3 the use of particle shape to select the wavelength of maximum polarization. The effect of particle volume on anistropic absorption is considered, and volume dependent scattering effects are examined. Particle volume and density are major parameter influencing the design of polarizing material.

Finally, in Section 1.4 equations will be developed which describe the optical performance of metal thin film polarizers. The analytical expression for a multilayer polarizer must include the effects of absorption, scattering and reflection from all films and surfaces. The goal is to derive an analytical expression for multilayer thin film polarizers which can be used to interpret experimental results and guide in the design of high contrast polarizers for 590 nm light.

Section 1.1 Optical Absorption of Metal Particles

The technical objective of Task 1 was development of an analytical description of polarizing metal thin films. The analytical description would guide the experimental effort to develop high contrast metal film polarizers and lead to design equations for fabricating high contrast polarizing filters at 589 nm or any selected wavelength. In this section we will obtain an analytical expression for absorption of light by a single silver particle which approximates the shape of the silver particles found in the evaporated silver films.

SPHERICAL PARTICLES

Light absorption by metal particles has been investigated for a number of physical systems containing suspended spherical metal particles. Examples include silver particles in photographic emulsions, particles suspended as sols, and metal spheres suspended in glassy materials. In these experiments the spherical metal particles exhibit a characteristic polarization independent absorption variation with wavelength. The absorption is characterized by a wavelength of peak absorption which depends on the metal and the index of refraction of the material surrounding the particles.

When a beam of monochromatic light of wavelength λ and intensity I_0 irradiates a metal particle of volume V, the light absorbed is given by:

$$A = I_0 - I = I_0 \{1 - e \times p[-\gamma]\}, \tag{1.1-1}$$

where I is the intensity of the radiation after absorption occurs and γ is the absorption coefficient for a single particle. The beam transmission is given by T where:

$$T = 1 - A. \tag{1.1-2}$$

The absorption cross section per particle for a spherical particle has the form:

$$\gamma = \frac{2\pi V N_o^3}{0.111} \times \frac{B\lambda^2}{\{\varepsilon_o - A\lambda^2 + 2N_0^2\}^2 + B^2\lambda^6}, \tag{1.1-3}$$

where V is the volume of the particle N_0 is the refractive index of the material surrounding the particle, and A, B and ε_0 are constants which can be approximated by calculations from the free electron theory or obtained by fitting data from the bulk optical constants of silver.

The absorption peak occurs when the first term in the denominator of Eq (1.1-3) is zero. The wavelength of maximum resonance absorption λ_m is given by:

$$\lambda_m = \frac{1}{\sqrt{A}} \left\{ \varepsilon_o + 2N_0^2 \right\}^{1/2}. \tag{1.1-4}$$

These expressions were developed by Stookey (1968) and Seward (1984). The expressions are based on the assumption that the particles are small with respect to the radiation to be absorbed and the particles are separated by a distance great enough to be non-interacting.

SILVER SPHERICAL PARTICLES

The absorption cross-section per particle for a silver sphere can be expressed in the form of Eq (1.1-3) if the constants A, B and ε_0 are known for silver. Seward (1984) investigated absorption by silver particles suspended in certain oxide glasses and found that $\varepsilon_0 = 5$ and $A = 55$. Since we are interested in particles resting on a glass surface in the presence of air, we take $N_0 = 1.0$. The experimental absorption data reported by Seward was used to determine that $B = 12.8$. Therefore, for spherical silver particles, the value of γ is:

$$\gamma = \frac{2\pi V}{0.111} \times \frac{12.8\,\lambda^2}{\{-55\lambda^2 + 7\}^2 + 163.84\lambda^6} . \qquad (1.1\text{-}5)$$

The wavelength of peak absorption is found to be 357 nm using Eq. (1.1-4). This is the wavelength of peak resonance absorption in air with $N_0 = 1.0$. If, however, the silver spheres are suspended in glass with refractive index 1.5, the wavelength of peak absorption found from Eq (1.1-4) shift to a layer wavelength, 416 nm.

ELLIPSOIDAL PARTICLES

Polarization dependent absorption is introduced when metal particles take the shape of an ellipsoid. The ellipsoidal shape of interest here is the prolate spheroid which is formed when an ellipse is rotated about its major axis of length a. The aspect ratio of a prolate spheroid is the minor axis b divided by the major axis a. The expression for the absorption cross-section per particle now

contains a coefficient L which depends on the aspect ratio of the particle and is defined by the axis of linear polarization of incident light so that

$$\gamma = \frac{2\pi V N_0^3}{L^2} \times \frac{B\lambda^2}{\{\varepsilon_0 - A\lambda^2 + N_0^2(1/L-1)\}^2 + B^2\lambda^6} \quad . \tag{1.1-6}$$

The factor L is developed by van de Hulst (1957) and satisfies the relationship

$$L_a + L_b + L_c = 1 \quad , \tag{1.1-7}$$

where the subscripts a, b and c apply to the three cases where linearly polarized radiation is incident on the particle with the electric vector directed along the a, b or c axis of the particle. For a prolate spheroid, $L_b = L_c$, so these are actually two values of L coefficients where

$$L_a = 1 - 2L_b \quad . \tag{1.1-8}$$

SILVER PROLATE SPHEROIDS

Since the expression for the wavelength of peak absorption for a silver prolate spheroid is

$$\lambda_m = \frac{1}{\sqrt{55}} \left\{ 5 + N_0^2 (1/L - 1) \right\}^{1/2} , \tag{1.1-9}$$

polarized light incident along the a axis or b axis has an absorption peak occurring at different wavelengths. For a spherical particle

$$L_a = L_b = L_c = 1/3, \tag{1.1-10}$$

and, the peak resonance absorption occurs at λ_m = 357 nm as indicated above for spheres in air. When light polarized along the a axes is incident on the spheroidal particles λ_m is greater than 357 nm. However, when light is polarized along axis b, λ_m is found to be at a value less than 357 nm.

The prolate spheroid factor L_a is given by the following expression when a > b:

$$L_a = \frac{1-e^2}{e^2}\left\{-1+\frac{1}{2e}\bullet \ln\left(\frac{1+e}{1-e}\right)\right\}, \qquad (1.1\text{-}11)$$

where $$e^2 = 1-(b/a)^2 \ . \qquad (1.1\text{-}12)$$

The values of b/a, ε, L_a, L_b and l_m for $N_0 = 1$ and $N_0 = 1.5$ are shown in Table 1.1-1. The goal of this analysis is selection of a particle shape for peak absorption of the polarization component along the a axis of the prolate spheroid to occur at approximately 600 nm. By setting Eq. (1.1-9) to $\lambda_m = 600$ nm for $N_0 = 1.0$ we can solve for L_a. The coefficients for $\lambda_m = 600$ nm are:

$$L_a = 0.06 \ ; \ L_b = L_c = 0.47 \qquad (1.1\text{-}13)$$

It can be seen from Table 1.1-1 that for $\lambda_m = 600$ nm in air, b/a must be slightly greater than 0.2. This establishes the aspect ratio for the silver prolate spheroids to be used in polarizing thin films for 600 nm light if they are attached to a surface but essentially suspended in air with $N_0 = 1$.

If the silver spheroids are immersed in a material of refractive index $N_0 = 1.5$ typical of many optical materials and optical adhesives, Eq. (1.1-9) can again be used to find the L coefficients when $\lambda_m = 600$ and $N_o = 1.5$. In this case,

$$L_a = 0.135 \ ; \ L_b = L_c = 0.4325. \qquad (1.1\text{-}14)$$

It can be seen from Table 1.1-1 that the ratio b/a is slightly less than 0.4 when these conditions are satisfied. This analysis predicts that aspect ratio b/a of a silver prolate spheroid with peak absorption at 600 nm must be approximately double if the material surrounding the particle is changed from a refractive index of $N_0 = 1.0$ to $N_0 = 1.5$. This fact can be expressed as $a \cong 5b$ for $N_0 = 1$ and $a \cong 2.5b$ for $N_0 = 1.5$. In Section 3, the experimental preparation of particles satisfying these conditions will be reported and discussed.

Table 1.1-1

Anisotropic absorption values for silver prolate spheroids.

b/a	e	λm for $N_0 = 1.0$	L_a	λm for $N_0 = 1.5$
1.000	0.000	0.270	0.000	0.224
0.900	0.436	0.364	0.306	0.429
0.800	0.600	0.372	0.276	0.445
0.700	0.714	0.384	0.244	0.466
0.600	0.800	0.399	0.210	0.495
0.500	0.866	0.421	0.174	0.535
0.400	0.917	0.455	0.135	0.594
0.300	0.954	0.513	0.095	0.692
0.200	0.980	0.631	0.056	0.885
0.100	0.995	0.984	0.020	1.438
0.080	0.997	1.158	0.014	1.703
0.066	0.998	1.339	0.011	1.979
0.057	0.998	1.500	0.008	2.224
0.050	0.999	1.663	0.007	2.472

Section 1.2 Metal Particle Arrays

Having identified the silver prolate spheroid as the particle of choice for 600 nm resonance absorption peak, the issue of particle arrays will be considered. The light intensity I transmitted through the thin film is given by the expression:

$$I = I_0 \exp[-N\gamma] , \tag{1.2-1}$$

where γ is given by Eq. (1.1-5), N is the number of metal particles in the incident beam of intensity I_0. The fractional transmission of the metal film is $T = I/I_0$ and the fractional absorption $A = 1 - T$. The transmission can be written

$$T = \exp(-\psi)(\gamma/2\pi V) , \tag{1.2-2}$$

where

$$\psi = 2\pi NV . \tag{1.2-3}$$

The quantity NV is the volume of silver in the path of light of intensity I_0.

Five values of ψ have been used to calculate transmission curves which have values of T at 600 nm ranging from T = 0.1 to T = 0.00001. The values of ψ and T are shown in Table 1.2-1.

The absorption characteristics of arrays of similar particles in air ($N_0 = 1.0$) are seen in the absorption curves for each value of ψ shown in Table 1.2-1. In each case a MATHCAD program was used to calculate the absorption of light polarized along both the a axis and the b axis. For each value of ψ a third curve is calculated showing absorption for the same volume particle which is formed into a sphere (a = b = c). Absorption curves for $\psi = 0.015$ are shown in Figures 1.2-1, 2 and 3 where contrast ($C = k_1/k_2 = T_a/T_b$) at 600 nm is 9.8. Absorption curves for $\psi = 0.03$ are shown in Figures 1.2-4, 5 and 6, where contrast at 600 nm is 99.7. Absorption curves for $\psi = 0.045$ are shown in Figures 1.2-7, 8 and 9 where contrast at 600 nm is 995. Absorption curves for $\psi = 0.061$ are shown in Figures 1.2-10, 11 and 12, where contrast at 600 nm is 11,033. Absorption curves for $\psi = 0.076$ are shown in Figures 1.2-13, 14 and 15, where contrast is 110,222.

Table 1.2-1

Dependence of Transmission T on Wavelength and ψ for $N_0 = 1.0$ and $L_a = 0.6$.

ψ	T (600 nm) for L_a	T (600 nm) for L_b
.015	0.102	0.996
.030	0.010	0.997
.045	0.001	0.995
.061	0.00009	0.993
.076	0.000009	0.992

Table 1.2-2

Dependence of transmission on wavelength and ψ for $N_0 = 1.5$ and $L_a = 0.135$ and $L_b = 0.47$

ψ	T (600 nm) for L_a	T (600 nm) for L_b
0.020	0.112	0.989
0.041	0.011	0.977
0.061	0.001	0.966
0.082	0.00013	0.955
0.102	0.000014	0.944

No = 1 L = 0.06

T_{60} = 0.102

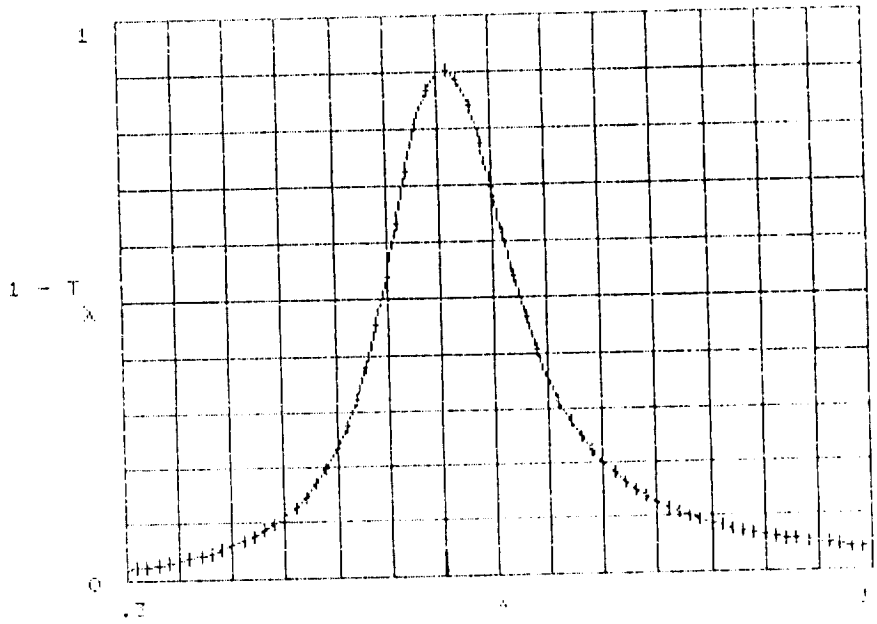

Wavelength in Microns

Figure 1.2-1

No = 1 L = 0.47

T_{60} = 0.998

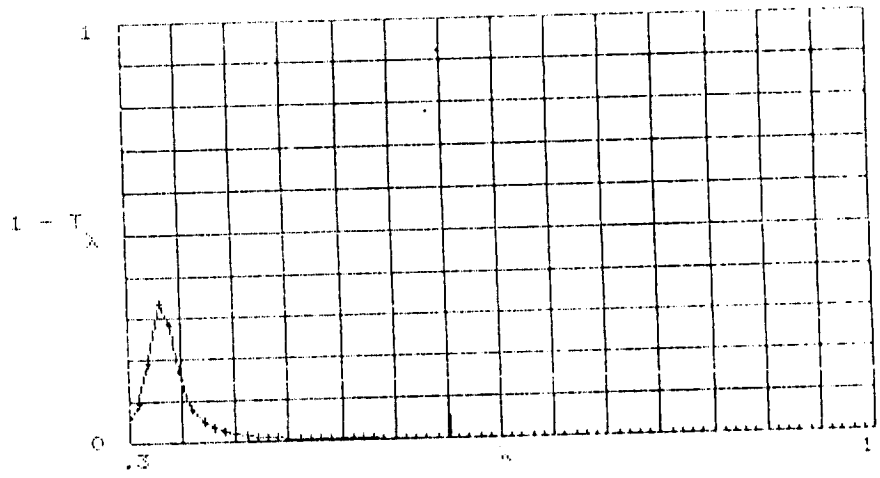

Wavelength in Microns

Figure 1.2-2

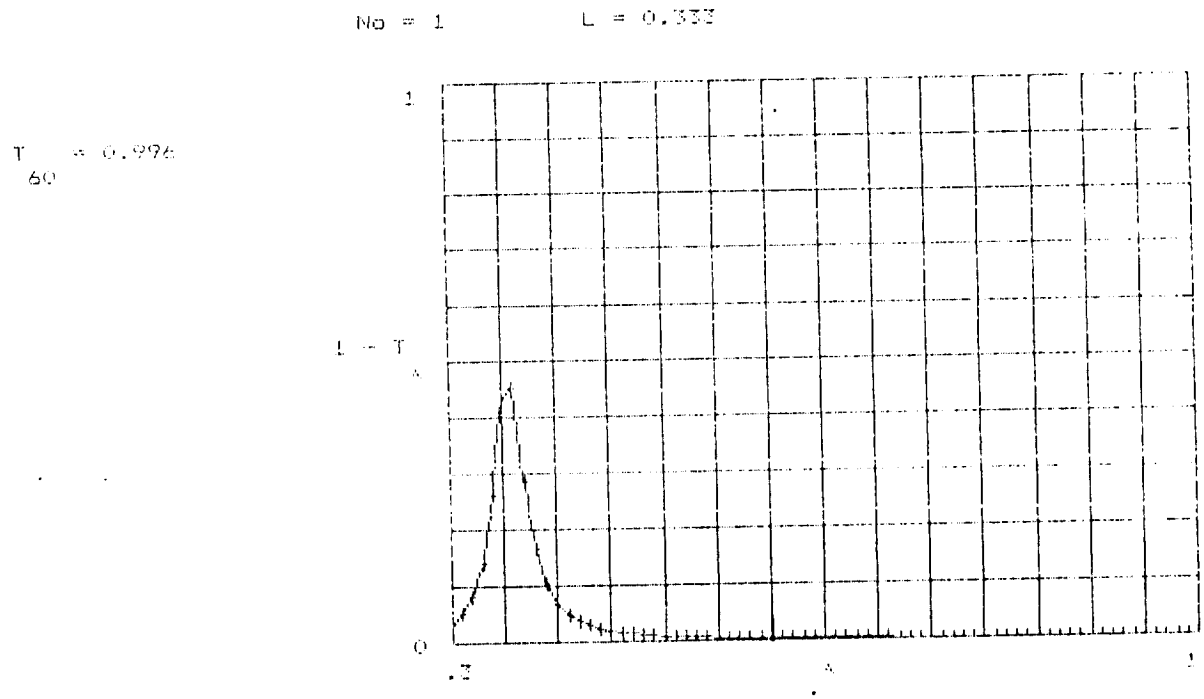

Wavelength in Microns

Figure 1.2-3

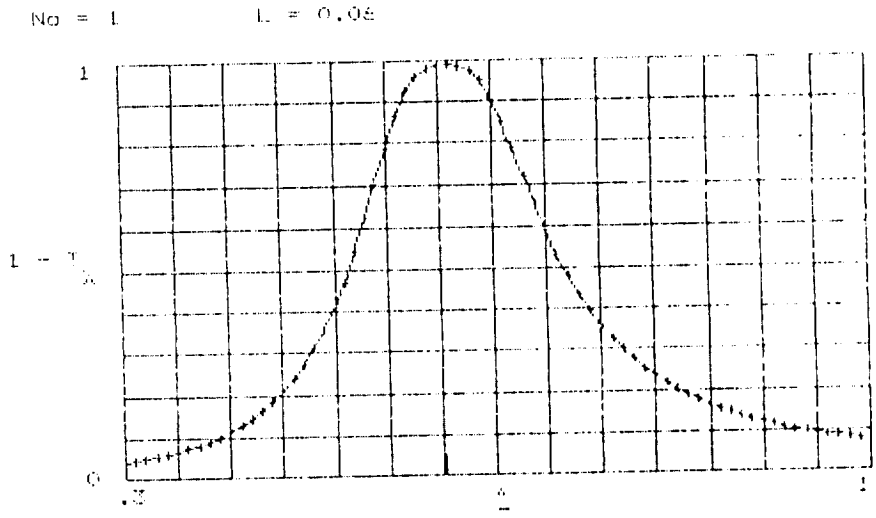

Wavelength in Microns

Figure 1.2-4

No = 1 L = 0.47

T_{60} = 0.997

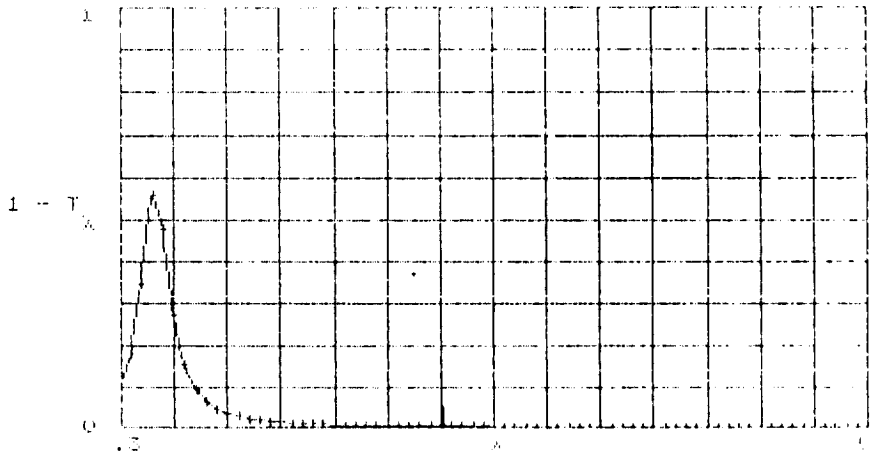

Wavelength in Microns

Figure 1.2-5

No = 1 L = 0.333

T_{60} = 0.993

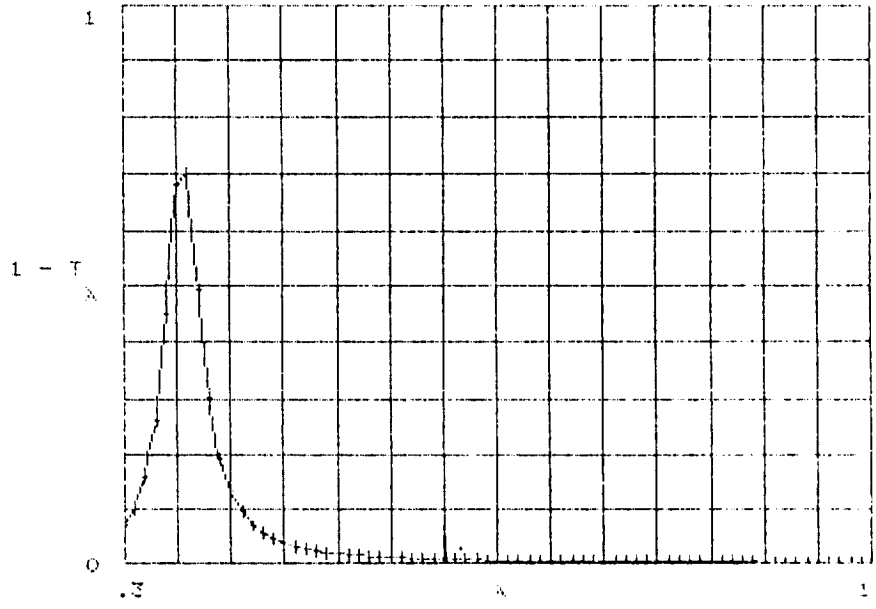

Wavelength in Microns

Figure 1.2-6

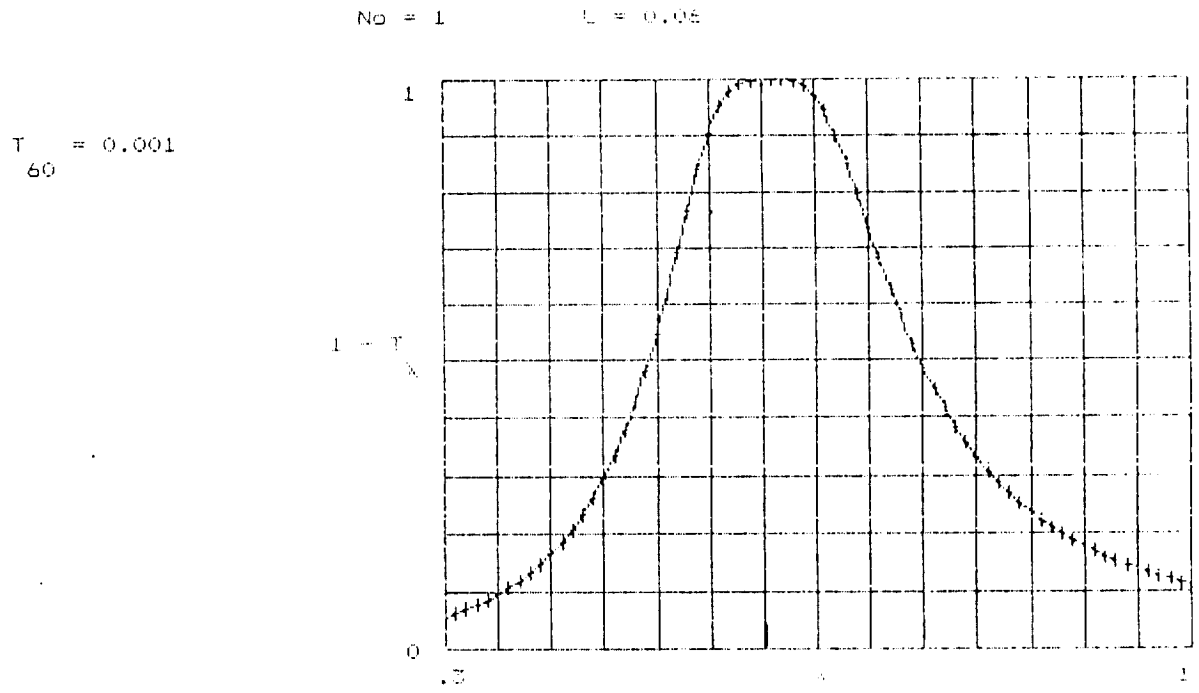

Wavelength in Microns

Figure 1.2-7

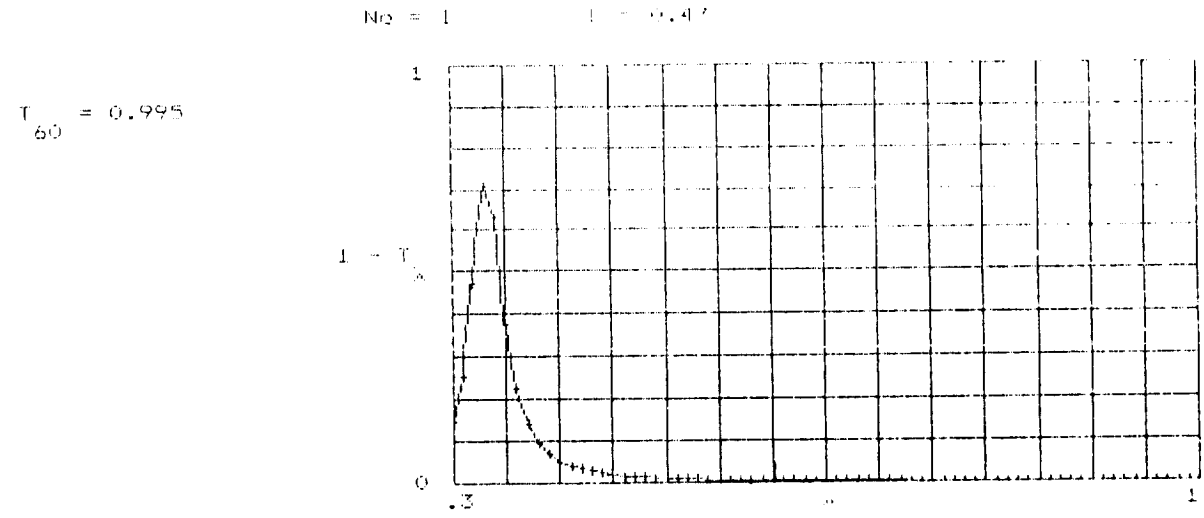

Wavelength in Microns

Figure 1.2-8

No = 1 L = 0.333

$T_{60} = 0.989$

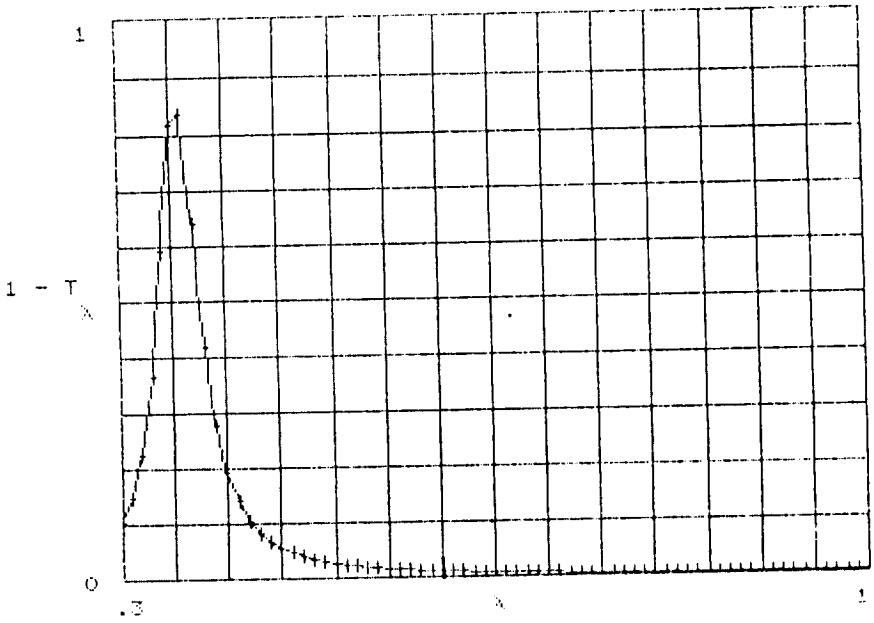

Wavelength in Microns

Figure 1.2-9

No = 1 L = 0.06

$T_{60} = 9.138 \cdot 10^{-5}$

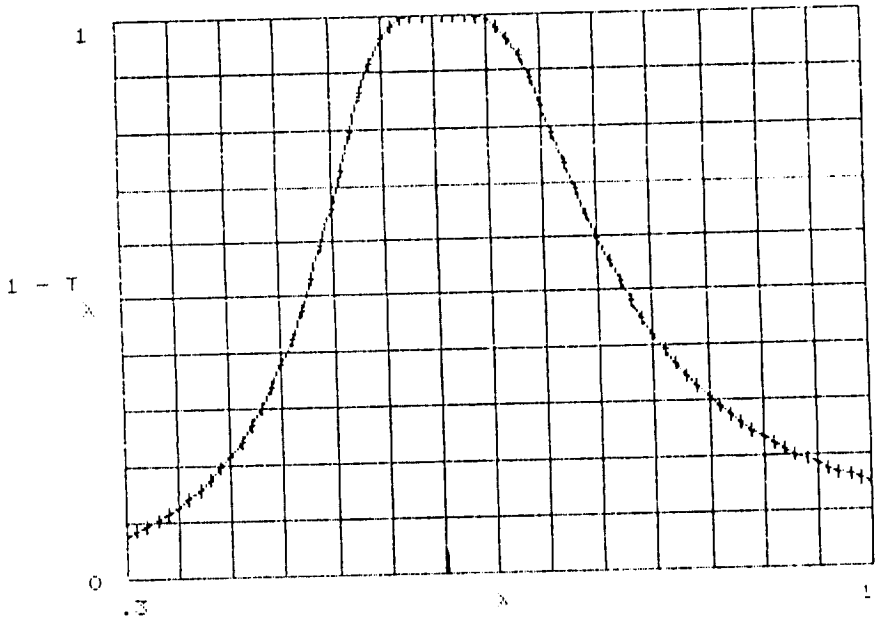

Wavelength in Microns

Figure 1.2-10

No = 1 L = 0.47

T_{60} = 0.993

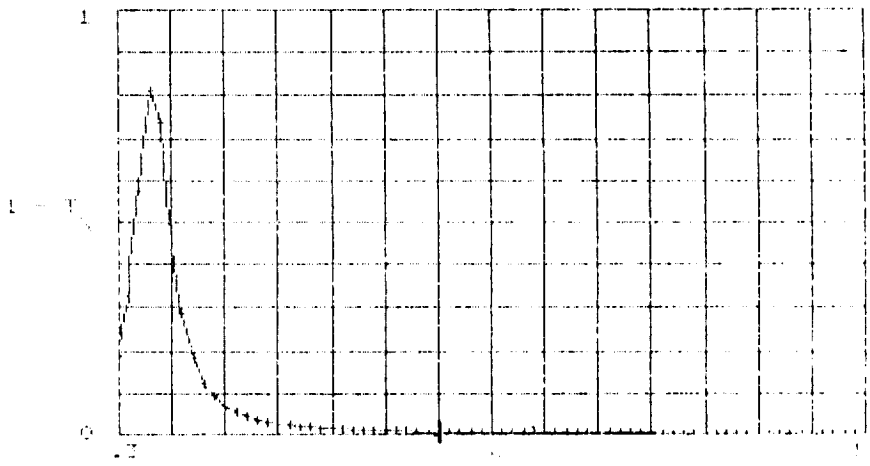

Wavelength in Microns

Figure 1.2-11

No = 1 L = 0.332

T_{60} = 0.985

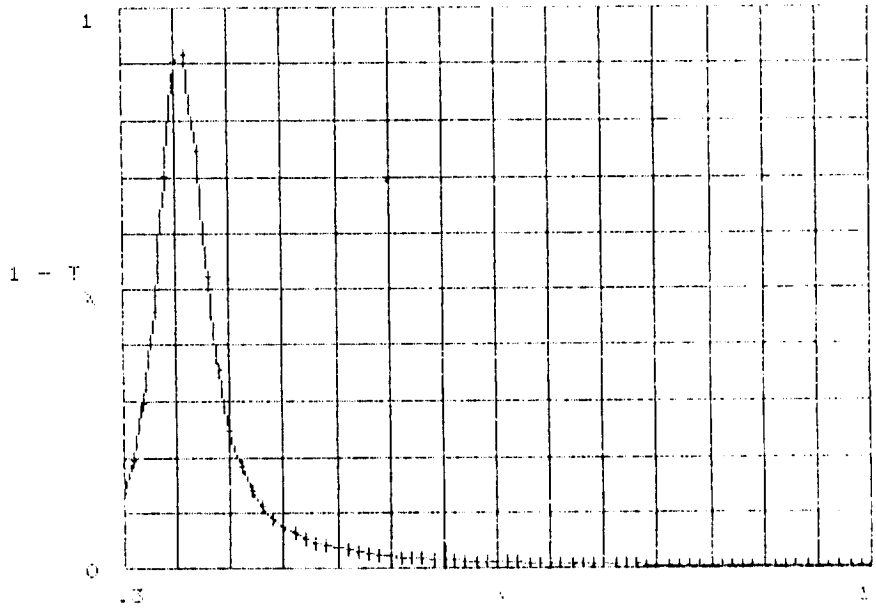

Wavelength in Microns

Figure 1.2-12

No = 1 L = 0.06

$T_{60} = 9.281 \cdot 10^{-6}$

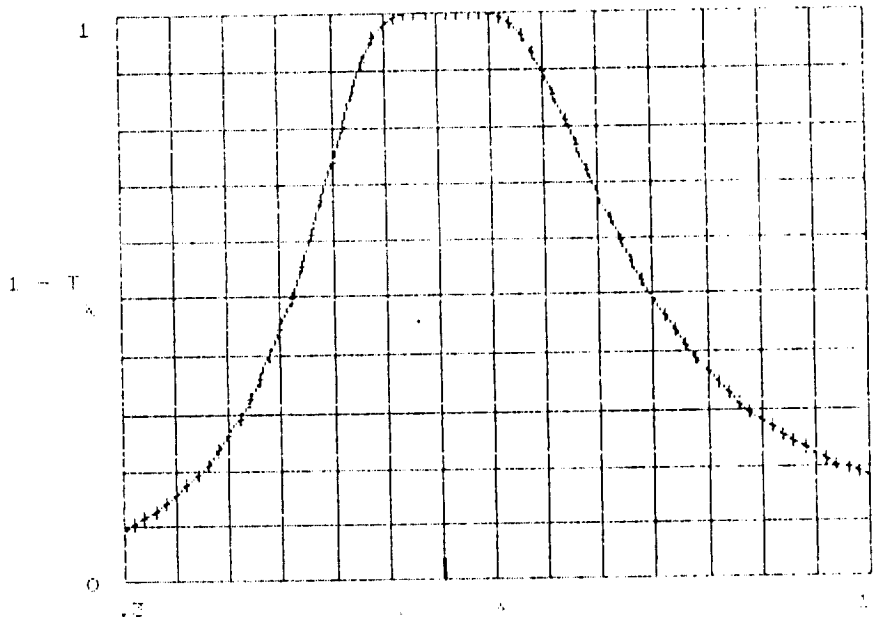

Wavelength in Microns

Figure 1.2-13

No = 1 L = 0.47

$T_{60} = 0.993$

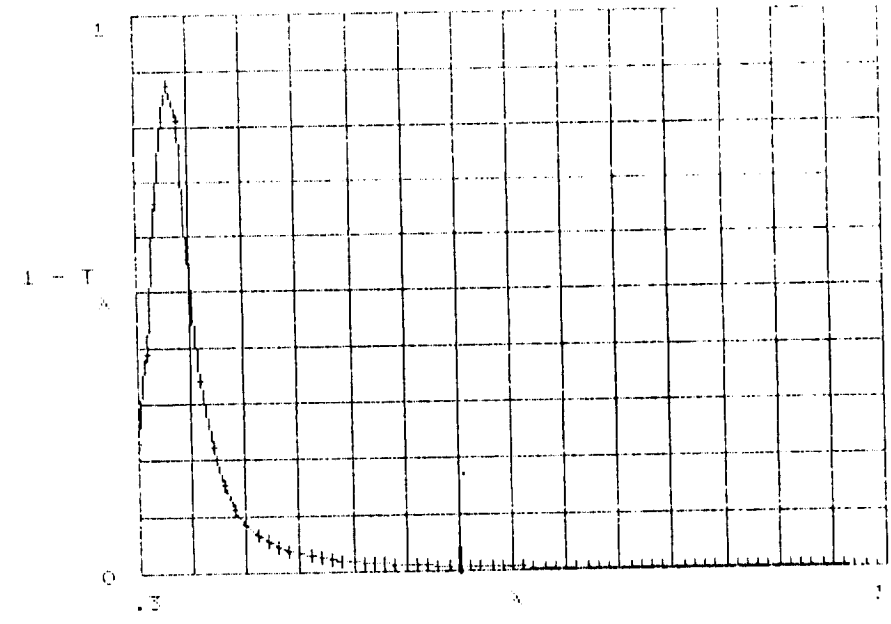

Wavelength in Microns

Figure 1.2-14

No = 1 L = 0.333

T_{60} = 0.982

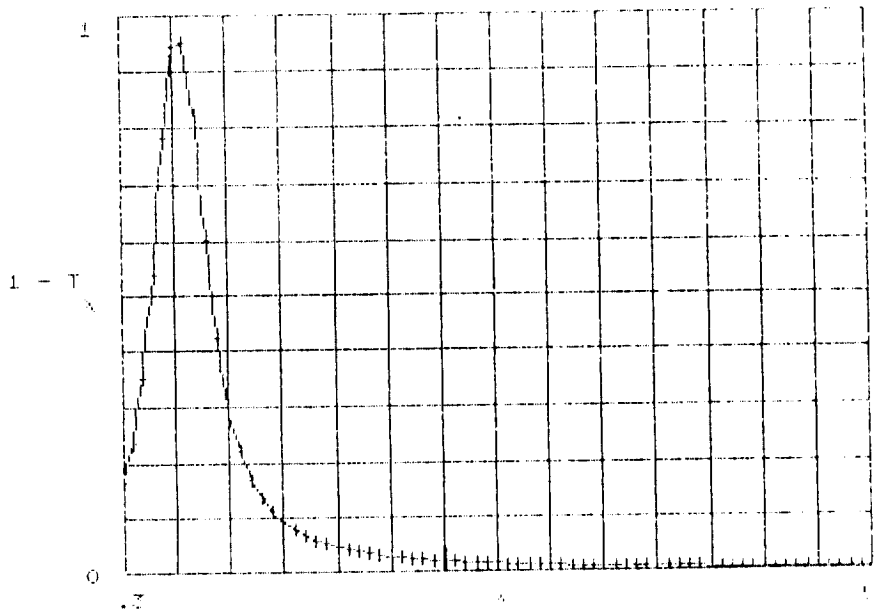

Wavelength in Microns

Figure 1.2-15

No = 1.5 L = 0.135

T_{60} = 0.112

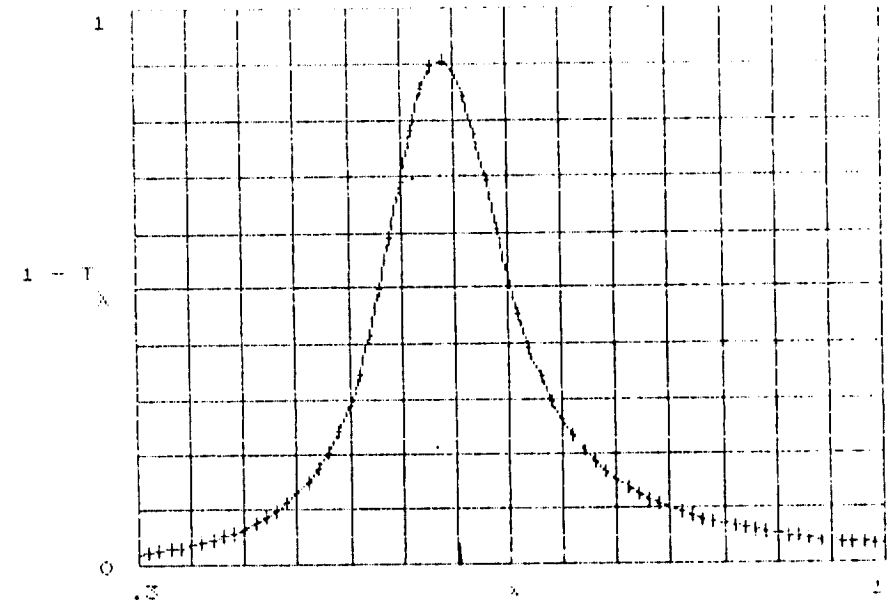

Wavelength in Microns

Figure 1.2-16

A second option is to embed the silver spheroids in a high index material and select the ellipsoid shape to provide maximum absorption for light polarized along the a axis for 600 nm. In this case we have used the MATHCAD program to calculate absorption for light polarized parallel axis a, parallel axis b and for the case of the particles shaped as a sphere (a = b = c) for a refractive index of 1.5. The absorption curves for ψ = 0.020 are shown in Figures 1.2-16, 17 and 18. Absorption curves for ψ = 0.04 are shown in Figures 1.2-19, 20 and 21. Absorption curves for ψ = 0.06 are shown in Figures 1.2-22, 23 and 24. Absorption curves for ψ = 0.081 are shown in Figures 1.2-25, 26 and 27. Absorption curves for ψ = 0.102 are shown in Figures 1.2-28, 29 and 30.

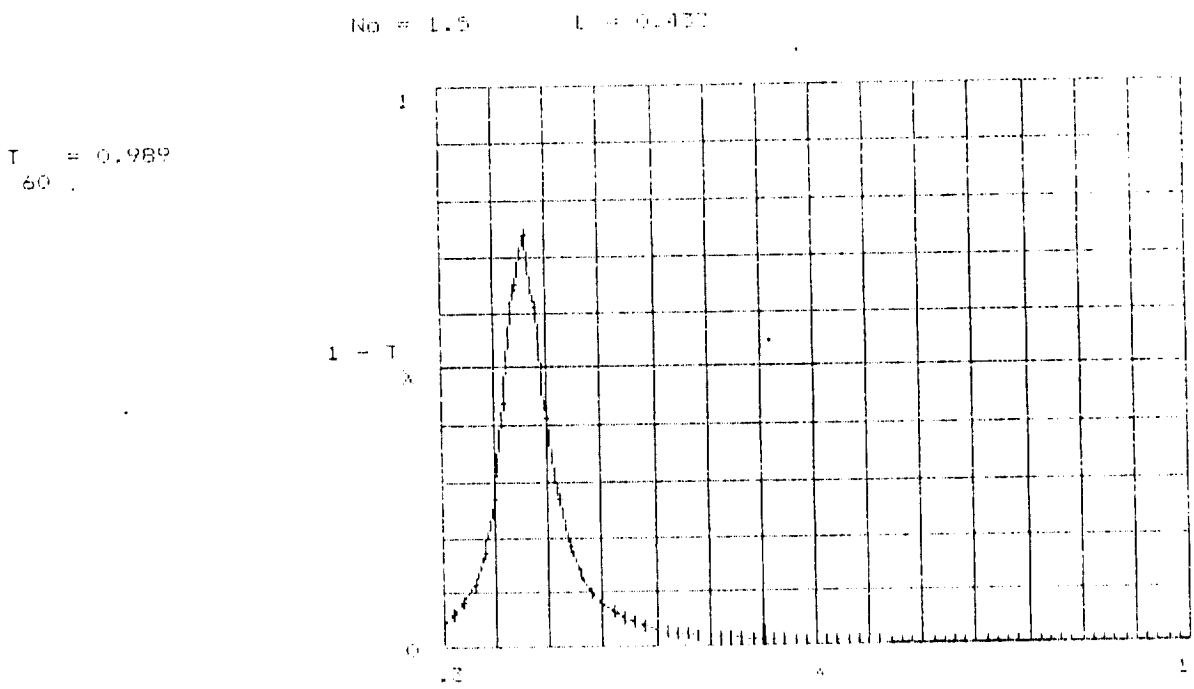

Wavelength in Microns

Figure 1.2-17

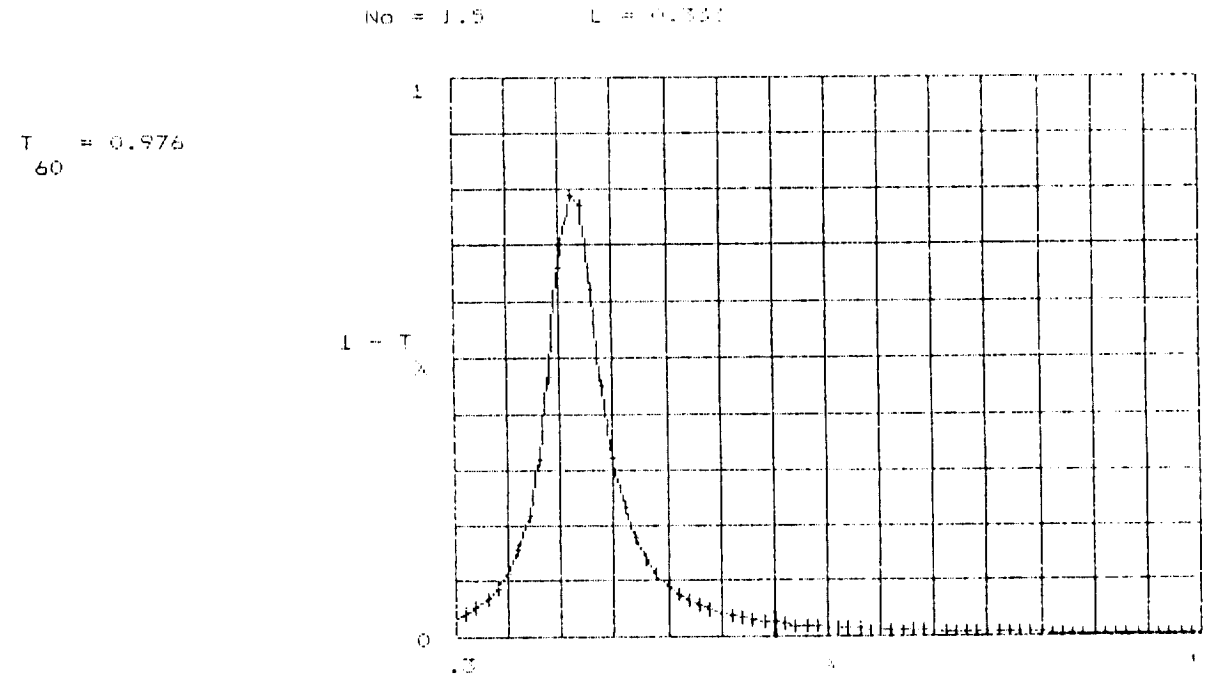

Wavelength in Microns

Figure 1.2-18

No = 1.5 L = 0.135

T_{60} = 0.011

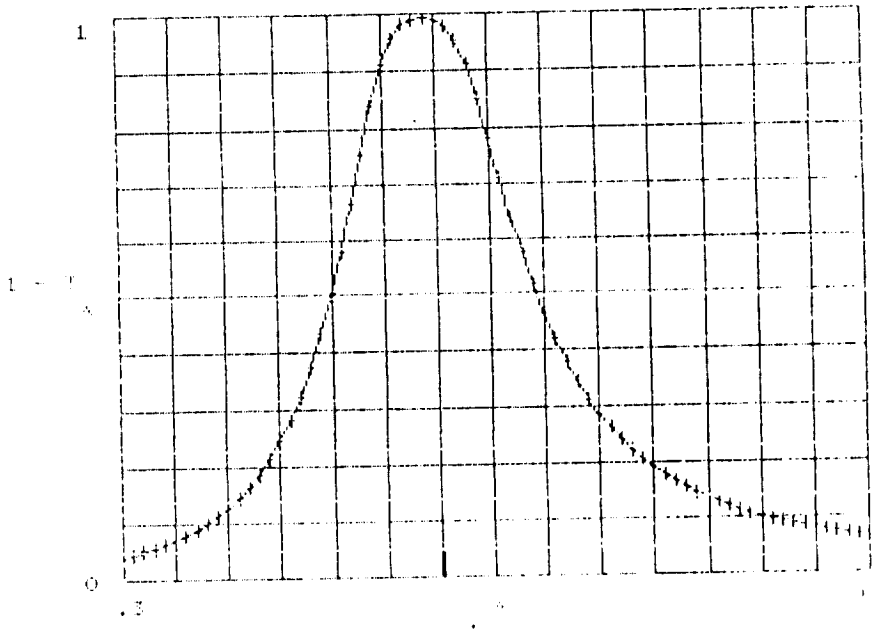

Wavelength in Microns

Figure 1.2-19

No = 1.5 L = 0.433

T_{60} = 0.977

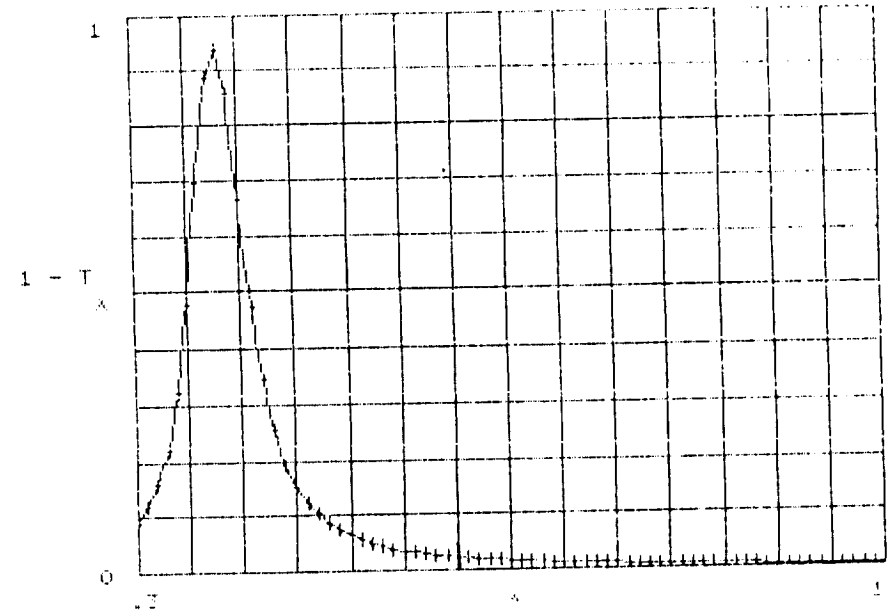

Wavelength in Microns

Figure 1.2-20

No = 1.5 L = 0.332

T_{60} = 0.951

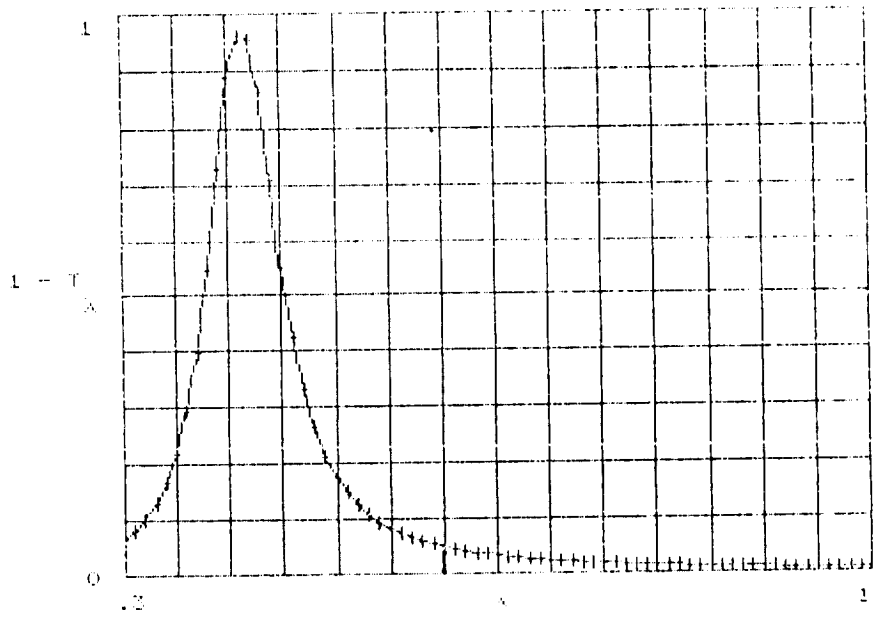

Wavelength in Microns

Figure 1.2-21

No = 1.5 L = 0.135

T_{60} = 0.001

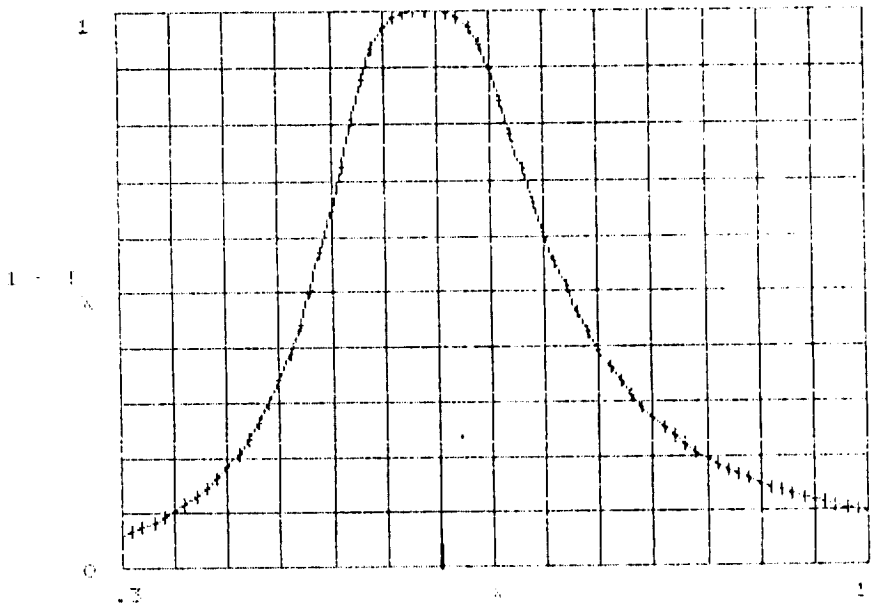

Wavelength in Microns

Figure 1.2-22

No = 1.5 L = 0.43

T_{60} = 0.966

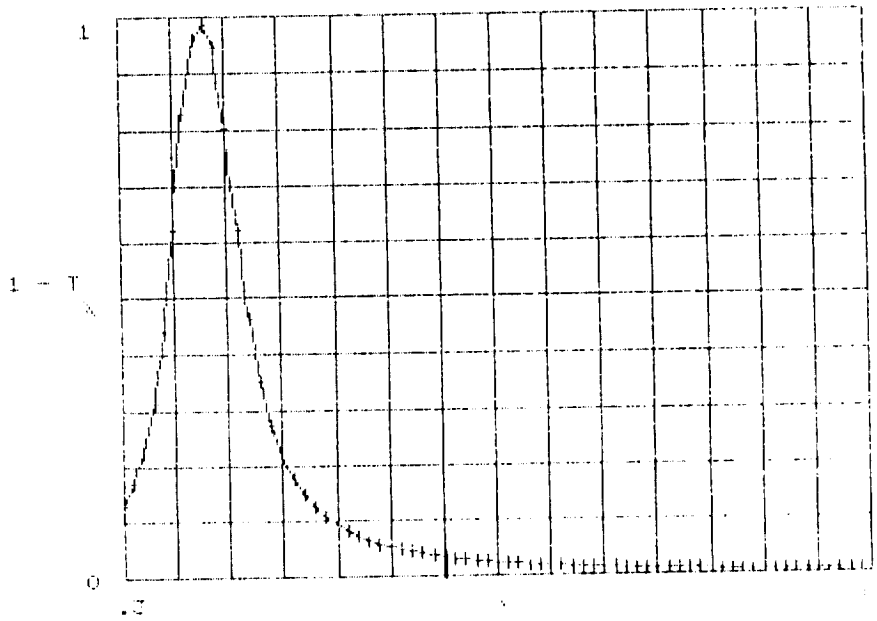

Wavelength in Microns

Figure 1.2-23

No = 1.5 L = 0.33

T_{60} = 0.928

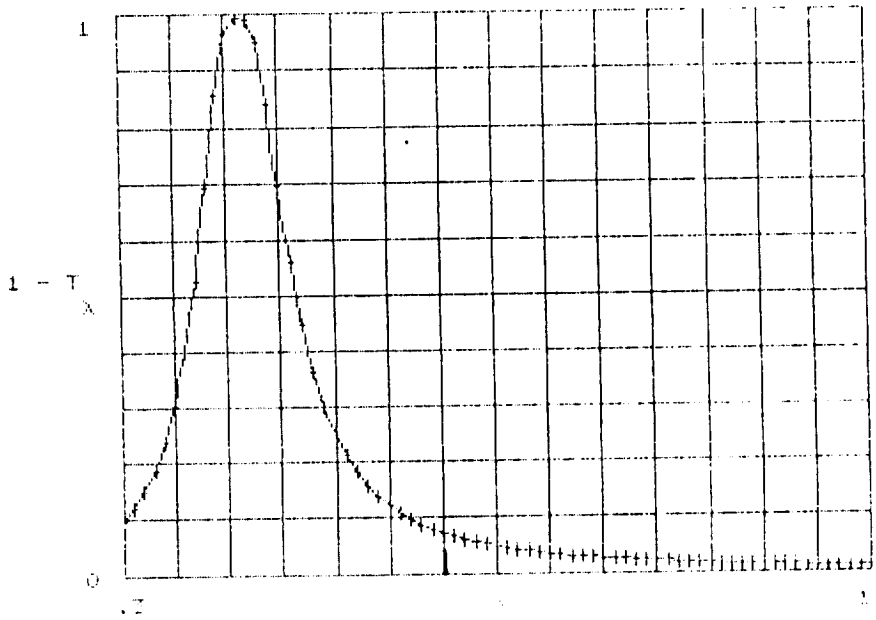

Wavelength in Microns

Figure 1.2-24

No = 1.5 L = 0.135

$T_{60} = 1.257 \cdot 10^{-4}$

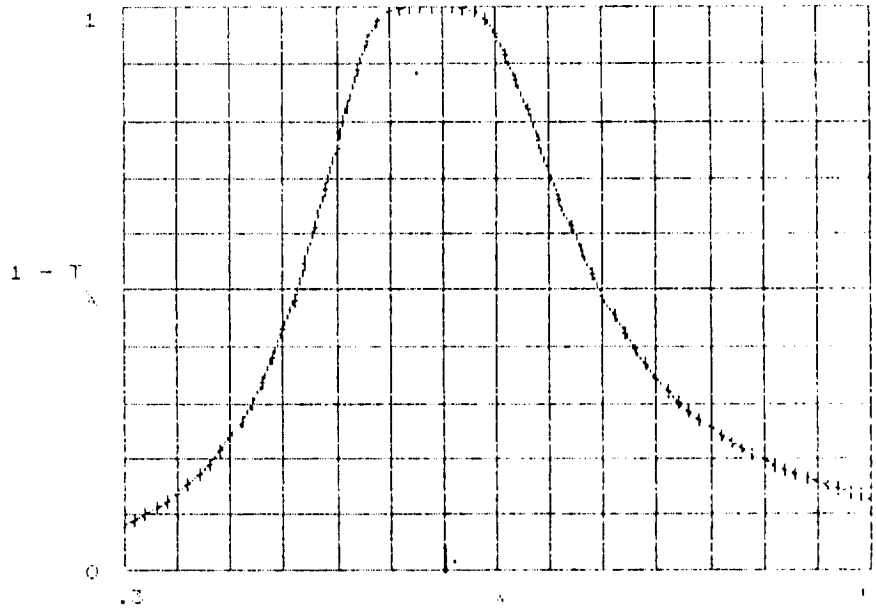

Wavelength in Microns

Figure 1.2-25

No = 1.5 L = 0.401

$T_{60} = 0.955$

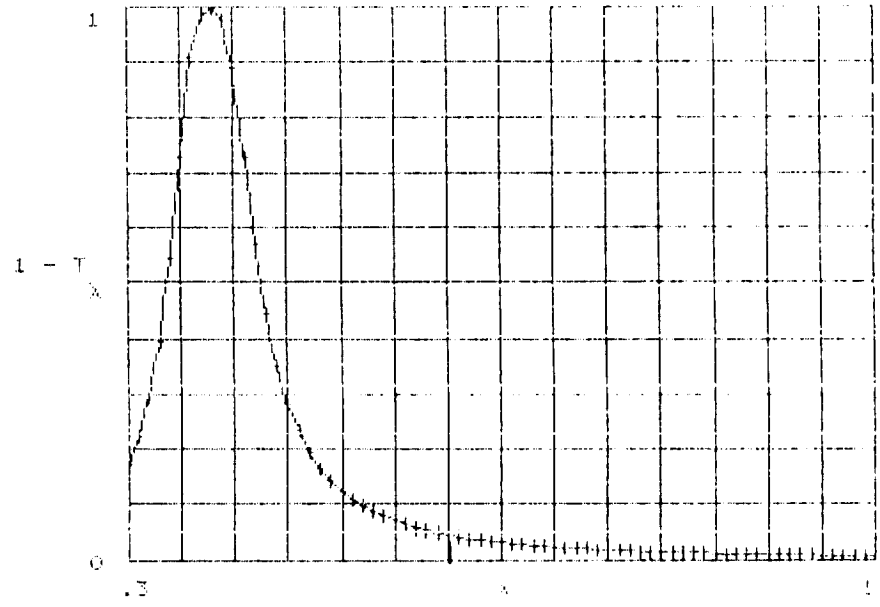

Wavelength in Microns

Figure 1.2-26

No = 1.5 L = 0.332

$T_{60} = 0.904$

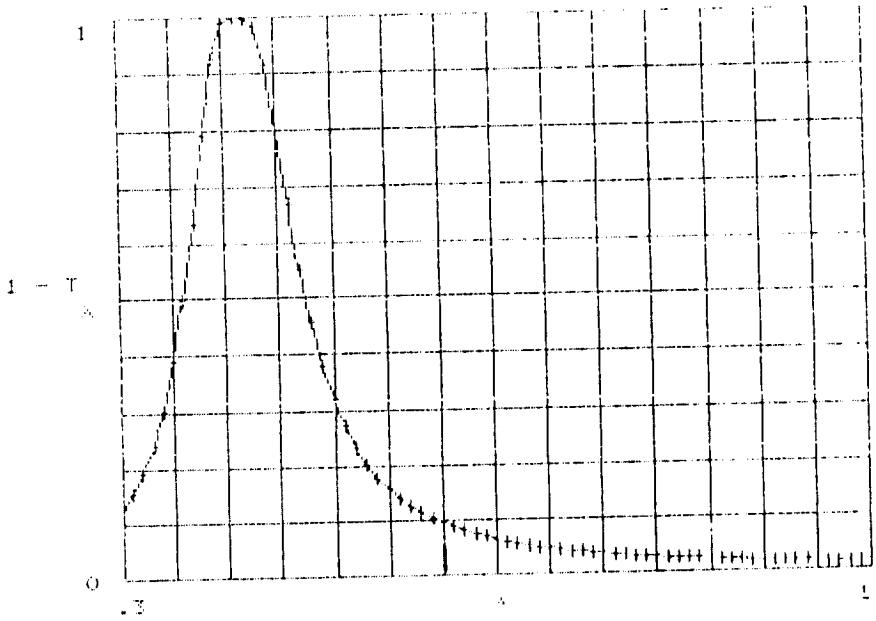

Wavelength in Microns

Figure 1.2-27

No = 1.5 L = 0.135

$T_{60} = 1.407 \cdot 10^{-5}$

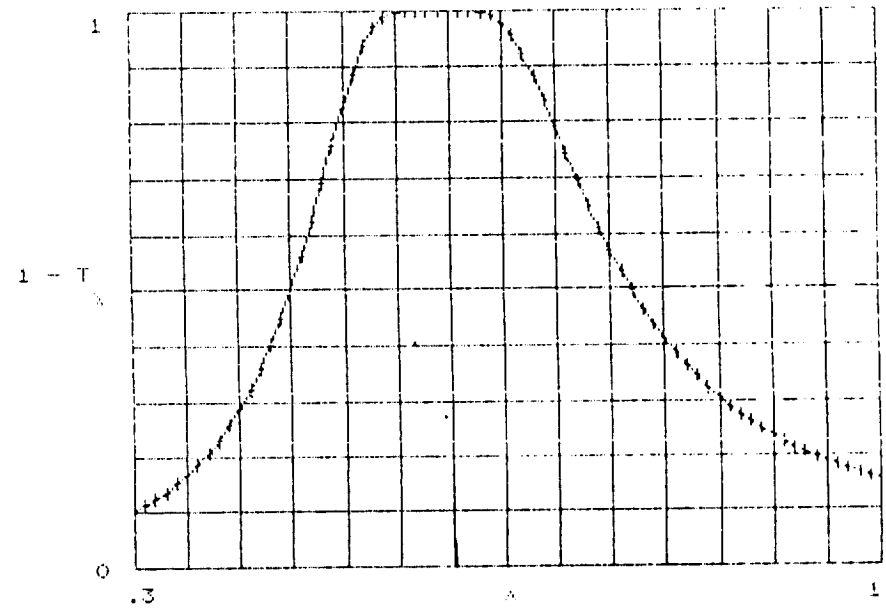

Wavelength in Microns

Figure 1.2-28

No = 1.5 L = 0.437

T_{60} = 0.944

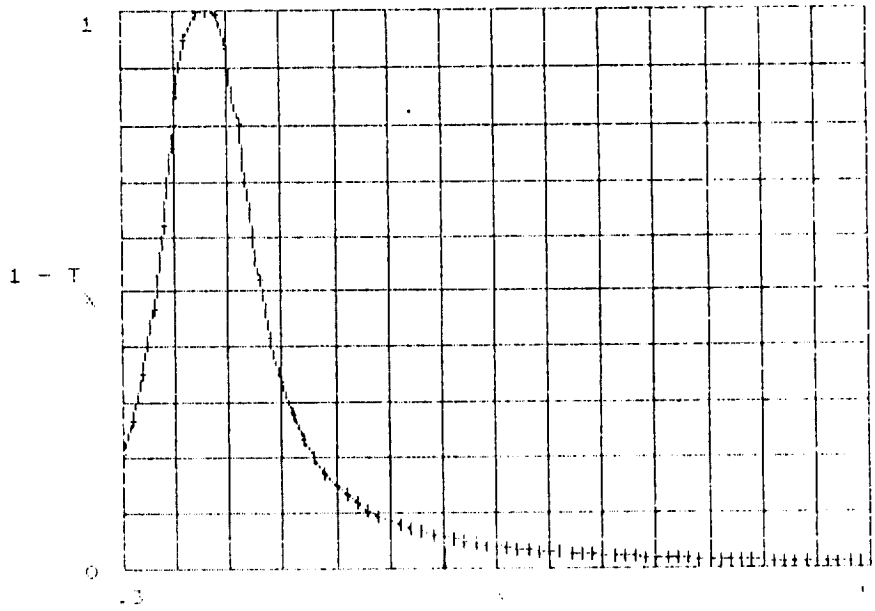

Wavelength in Microns

Figure 1.2-29

No = 1.5 L = 0.331

T_{60} = 0.882

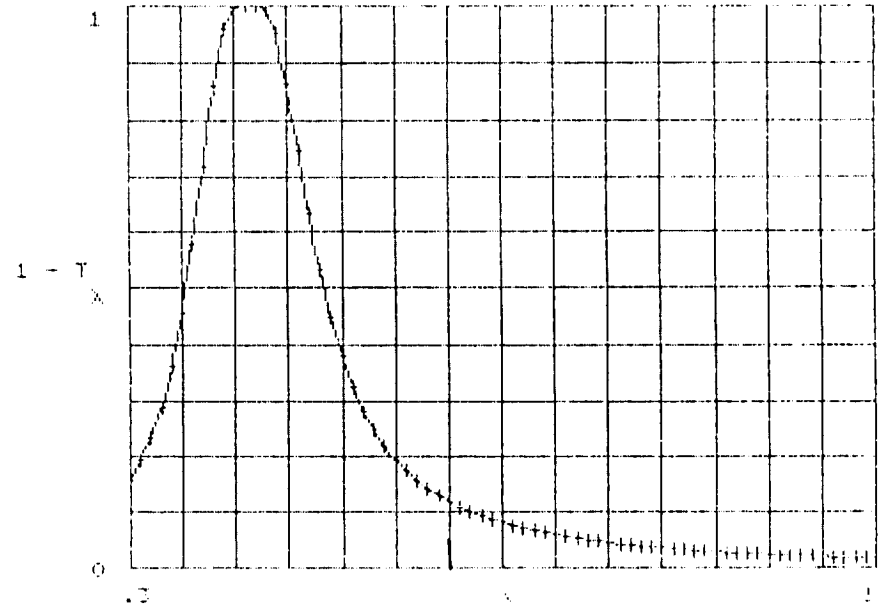

Wavelength in Microns

Figure 1.2-30

Section 1.3 Metal Particle Sizes and Shapes

Analysis of absorption characteristics of ideal silver prolate spheroids indicates that effective polarizers for the visible spectral region can be fabricated using arrays of these particles. There are two key issues which must be resolved in order to design an effective polarizing thin film once the aspect ratio is established for 600 nm peak resonance absorption. The first issue is particle volume V. The second issue is particle density N. Both of these factors enter the absorption equation through the term $\psi = 2\pi NV$. The first condition which must be met is that ψ be large enough to produce the desired contrast as indicated in Table 1.2-1. The product NV is actually the volume of silver in the optical path for a unit cross section of optical beam.

For high performance polarizers and polarizers used for visual or ophthalmic applications it is important to have a clear material which means that a hazy appearance caused by light scattering must be avoided. Investigators working with silver based photochromic glasses and silver based glass polarizer have reported that when silver particles are too large, scattering causes a hazy appearance in the material. There is also a lower limit on particle size which is set by the fact that for silver particles with diameter smaller than 5 to 10 nm, the mean free path of the conduction electrons is limited and the absorption peak is broadened.

The upper limit on particle size is set by the onset of significant scattering which causes a hazy or translucent appearance in the film. To avoid these effects the particles should have diameters less than 50 nm and preferably as small as 20 nm. Most experimental data on particle sizes was obtained from silver halide particles prior to reduction to metallic silver. Since silver occupies somewhat smaller volume than the precursor silver halide particles, these upper limits on particle size are only approximate. The range for particle diameter of an equivalent spherical volume of silver is in the diameter range form 20 nm to 50 nm. Effective polarization has, however, been observed with silver particles having a diameter as large as 500 nm.

PROLATE SPHEROID PARTICLES SIZE

Having bounded the volume V of equivalent spherical particles, it is now of interest to relate the volume V to the shape of a prolate spheroid which also has volume V. A sphere of diameter d = 2r has a volume V where

$$V = \frac{4\pi r^3}{3} = \frac{\pi d^3}{6} \quad . \tag{1.2-1}$$

A prolate spheroid of major axis a and minor axis b = c is formed by rotating an ellipse of major axis a and minor axis b about the a axis. The volume of prolate spheroid is

$$V = 4/3\ \pi a b^2 \quad . \tag{1.3-2}$$

The ratio a/b equals k where k = 5 for peak resonance absorption at 600 nm. Since the volume of the sphere and prolate spheroid are the same, by setting Eq. (1.3-1) and Eq. (1.3-2) equal, it is found that the length of the prolate spheroid 2a is given by

$$2a = (k)^{2/3}\, d \quad , \tag{1.3-3}$$

where d is diameter of sphere with volume identical to the prolate spheroid. This relationship will be used to estimate the volume of actual silver particles as determined by electron microscopy.

For the case where k = 5 for peak resonance absorption at 600 nm, the particle is 2.9 times longer than the diameter of a sphere of identical volume. Since good polarization characteristics have been found for particles with diameter d in the range from 20 nm to 50 nm, the silver prolate spheroids for k = 5 would be expected to fall in the length range (2a) from 60 nm to 150 nm.

PARTICLE DENSITY

The design goal is to cover the surface with parallel prolate spheroids with a/b = k = 5 and with length in the range from 60 nm to 150 nm. The next issue is the number of metal particles required to achieve effective polarization. This can be established by noting that the absorption cross section is proportional to ψ where $\psi = 2\pi NV$. Since V is specified by the equivalent diameter of the metal particles, we can select a contrast value $C = k_1/k_2$ and calculate the required value of ψ. Then N can be found from the expression

$$N = \psi/2\pi V \ . \qquad (1.2\text{-}4)$$

From Table 1.2-1, we find that, for a contrast of 997 at 600 nm, $\psi = 0.030$. For a contrast of 10,860, $\psi = 0.045$. For particles with a diameter of 50 n (0.05μ), the volume is $6.55 \times 10^{-5} \mu m^3$. For the case where $\psi = 0.045$, we found from Eq. 1.2-4 that N = 109 particles. Since our silver films are deposited on a flat surface, this is a density of 109 particles per square micron. Since the fractional covering of the surface is the critical issue, the individual particles in spherical form which can be contained in a single layer of spheres is $1\mu m^2/d^2$ or $1\mu m^2/0.0025\mu m^2$ or 400. Approximately 27% of the surface is blocked by metal particles. If the equivalent sphere has a diameter of 100 nm (0.1μm), only 14 particles are required, but 100 particles are required to cover the surface area of 1 square micron.

The design goal can be stated as covering the surface with a coating of aligned silver prolate spheroids having a/b = 5 and a length of 150 nm. The contrast would be expected to be of the order of 10^4. This is, of course, an ideal film.

NON-IDEAL FILMS

The film designed in this manner would have a contrast greater than 10,000 at 600 nm and absorption curves from T_a shown in Figure 1.2-10 and T_b shown in Figure 1.2-11. However a number of factors can cause experimental films to fail to achieve this ideal performance. We now examine these factors which can cause actual films to deviate from the ideal.

1. Inaccuracies in the Analytical Description

The analytical expression must accurately describe the polarization dependent absorption of a silver prolate spheroid. This implies that the mathematical expression for absorption is correct and the constants for silver are accurate for the wavelength region of interest. It is our opinion that these expressions and silver constants are accurate for silver particles based on agreement with experimental results.

2. Particles

The particles must meet the conditions for which the equations are valid, namely independent scattering. As discussed by van de Hulst (1957), a scattering event is one in which electromagnetic radiation interacts with a scattering center (in our case a submicroscopic prolate spheroid) to produce scattering or absorption. If such particles are sufficiently far from each other, it is possible to describe the scattering of one particle without reference to the others. This is called independent scattering and the equations used in Section 1 describe this case.

When the particles are close enough to interact, the problem is one of dependent scattering. The distance between particles to ensure independent scattering is given by van de Hulst as three times the radius. While not a general rule, it serves as a bench mark for analysis of actual structure in our experimental films. The goal is not to develop a mathematical description for dependent scattering, but rather we want to fabricate metal thin films which satisfy the conditions of independent scattering, since it is to be anticipated that contrast and transmission will degrade with increased dependent scattering.

3. Distribution in Particle Shape

Since we have assumed a single particle size and aspect ratio for 590 nm, performance will be degraded by variations is aspect ratio of the metal

spheroids. The wavelength of peak absorption varies with aspect ration, therefore a distribution of particles with different aspect ratios decreases the contrast ratio and broadens the resonance absorption curve. Using Eq. 1.1-9 we have calculated the wavelength of peak absorption (A_a) for a range of b/a between 0 and 1 as shown in Figure 1.3-1. The upper curve is for $N_0 = 1$ while the lower curve is for $N_0 = 1$. It can be seen that a 10% variation on b/a can cause variations of the order of 100 nm in the peak absorption wavelength. Our goal experimentally is to produce metal spheroids with a very small range of b/a values about the b/a design goal. Note that in the range of b/a between 0.8 and 1.0 the equation is not valid as seen in Figure 1.3-1 and a different expression for wavelength of peak resonance absorption is required as a ≅ b and the shape becomes spherical.

Section 1.4 Polarizing Filter Design Equation

The goal was to formulate an analytical expression for light transmitted by a polarizing filter made up of one or more polarizing metal thin films. In practice it is useful to fabricate the filter using two or more substrates, each coated with a polarizing metal film. The problems of mechanical alignment of two or more substrates will be deferred until Section 5. In this section the impact of thin film physics on filter design will be considered.

ABSORPTION

A light beam for polarizer evaluation is ideally unidirectional, lineally polarized, and monochromatic, i.e. confined to one frequency. The beam has intensity I_0 which indicates the total energy flux in the beam. Ideally, the effectiveness of a polarizing filter is judged by its extinction ability. The polarized beam of intensity I_0 enters the filter which is set for maximum extinction and leaves the filter diminished in intensity because of absorption, and has intensity $I_0 - \Delta I$. Here ΔI is the absorbed radiation. $A = \Delta I/I_0$ is the fractional absorption and $1 - \Delta I/I_0$ is the fractional transmission T. The case of maximum absorption is designated

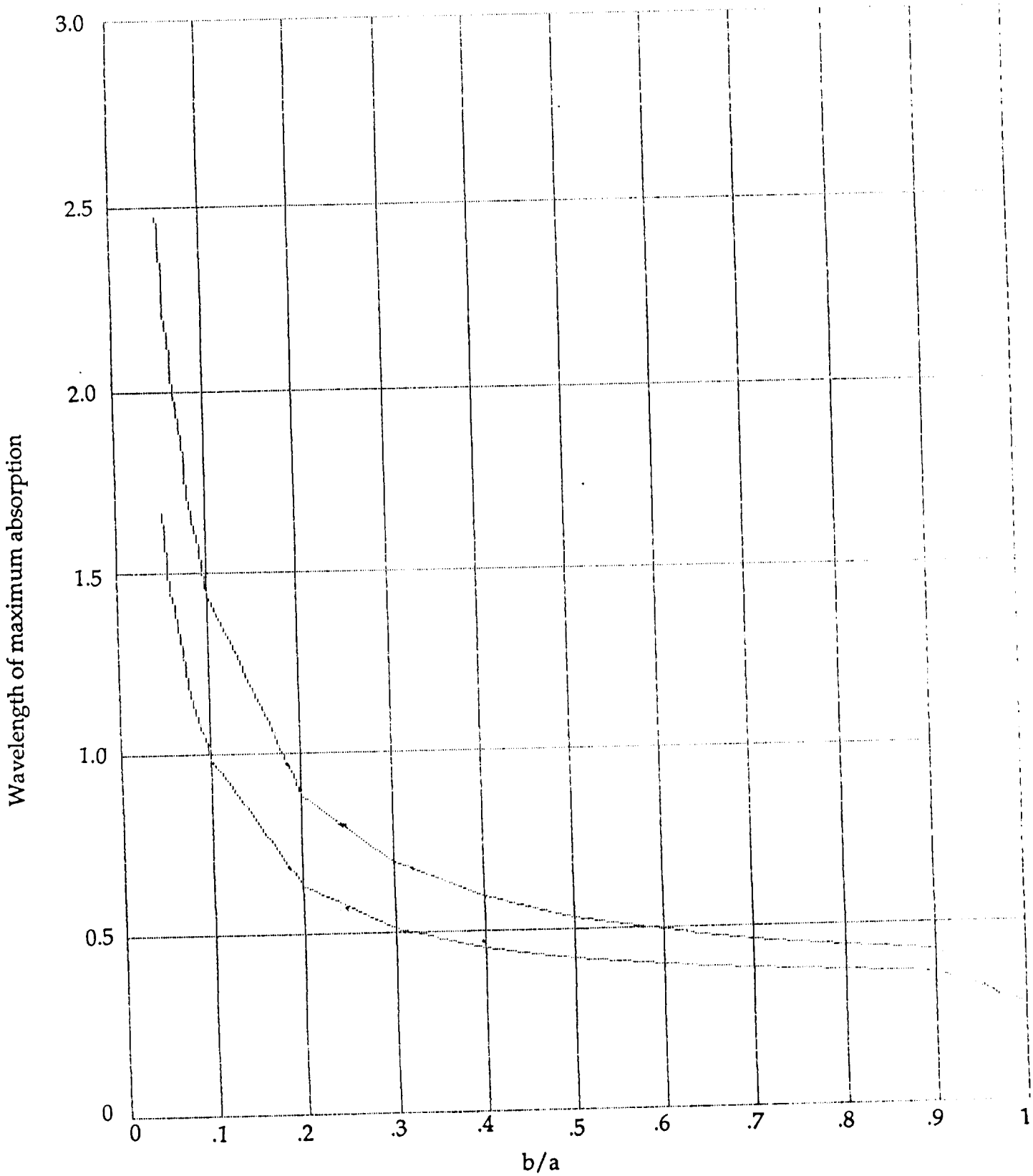

Figure 1.3-1 Dependence of wavelength of peak resonance absorption on b/a for prolate spheroid.

state 2 which is the case of the electric vector is parallel the major axis of the silver prolate spheroids. State 1 is the position where the electric vector is parallel the minor axis of the prolate spheroid. Principle transmittances are defined as $k_1 = (I_0 - \Delta I_1)/I_0$ and $k_2 = (I_0 - \Delta I_2)/I_0$. Useful indicators of polarizer performance are k_1, k_2 and contrast $C = k_1/k_2$ measured at a specific wavelength, normally the wavelength of peak resonance absorption. A second measure of polarizer performance is absorbance which is defined as

$$\text{absorbance} = -\log_{10}(T), \tag{1.4-1}$$

where T is the transmittance. Normally the absorbance of a filter is stated for $T = k_2$ at a specific wavelength.

By placing a light detector after the beam, we measure the effect of extinction of the test beam by the polarizing filter. It is assumed up to this point that the extinction is due to absorption, but in fact it is necessary to include the effects of reflection and scattering of light from the test beam.

REFLECTION

Each silver film is deposited on a glass substrate which is usually a thin disc of BK-7 glass. Each surface reflects approximately 4% of the indecent light. The beam passing through a disc will no metal film present would lose 8% of its intensity. The loss of intensity of the beam ΔI would have an absorption term $\Delta I(A)$ and a reflection term $\Delta I(R)$. For evaluation of experimental thin films the surface reflectance was usually neglected. However, in the evaluation of polarizing filters described in Section 5 the surface reflection terms were taken into account.

A second reflection effect can occur when very dense metal films are used. Although we were not able to measure this effect directly, reflection is thought to occur when the particles are dense enough to cause dependent scattering. This reflection effect should be eliminated when the particles are separated by a distance great enough to eliminate dependent scattering. It would, however, be

expected to be different for axis 1 and axis 2. The term $\Delta I_1(R) = \Delta I_1(R_S) + \Delta I_1(R_f)$. Where subscript s indicates surface reflection and subscript f indicates reflection from the metal film. We have then:

$$I = I_0 - \Delta I_1 = I_0 - \Delta I_1(A) - \Delta I_1(R_s) - \Delta I_1(R_f) \ , \qquad (1.4\text{-}2)$$

where I is the transmitted beam intensity in orientation 1. A similar equation can be written for light polarized along axis 2.

SCATTERING

The last effect to be included in the observed extinction observation is scattering by the metal particles. An individual particle has both an absorption cross section and a scattering cross section. For polarizers used in applications for human vision, scattering effects must be reduced to a negligible level or the material appears hazy or translucent. Scattering is also harmful in high performance polarizers. A major technical issue is the design and manufacture of high performance crystal polarizers is eliminating of scatter within the polarizer to achieve a contrast of 10^6 or better.

The problem for thin film polarizers is not only scattering from the polarizer package but scatter from the metal particles which make up the polarizing film. There are three major effects of particle scattering. The first is scatter of the incident light out of the transmitted beam which can be written $\Delta I_2(S_a)$. This effect actually improves the extinction of the filter by an amount $\Delta I_2(S_a)$. The second effect is forward scatter in the direction of the beam. The term $\Delta I_2(S_f)$ indicates the forward scatter into the solid angle subtended by the light detector. The forward scattering effect which degrades polarizing filter performance is cross polarization scattering. Cross-polarization scattering occurs when a linearly polarized beam with electric vector along the particle a axis (condition for maximum absorption) is scattered by the silver particles into the polarization state with electric vector along the b axis. This transfer of radiation from polarization state a to polarization state b, lowers the effective contrast since an analyzer polarizer crossed with the metal film polarizer would see the cross-

polarization as effectively increasing k_2. The cross-polarization effect can be eliminated, we believe, by reducing the volume of silver particles. This reduction was beyond the scope of the current contract. However, the scatter effect was eliminated during actual extinction measurements by locating the laser light detector at least one meter from the metal film polarizer.

Section 2: Optical and Structural Investigations of Metal Thin Films and Filters

The technical objectives of Task 2 included development of procedures for investigating the structure of metal thin films and the anistropic polarization dependent absorption characteristics of metal thin films. The technical goal is to correlate the film structure with the optical absorption characteristics in Section 3. In addition to these general characterization procedures, a method and apparatus is required for measuring the performance of polarizers with contrast ratios in excess of 10^5 at 590 nm wavelength.

The technical approach, measurement procedures, and resulting instrumentation used to meet each of these objectives are described in the following three subsections. Specifically, we selected a spectrometer and instrumentation which allowed us to measure polarization dependent absorption in the spectral band from 450 nm to 1550 nm. In order to observe the microscopic structure of metal thin films we obtained transmission electron microscope (TEM) images from the University of Central Florida and scanning electron microscope images from the University of Arizona. The University of Central Florida had a series of technical problems meeting their contractual obligations and were eleminated from the technical team after 12 months. A special HeNe laser which emitted radiation at 594 nm was used as a light source in a special apparatus assembled to evaluate polarizers with contrast greater than 10^5. We demonstrated this evaluation unit with a pair of crystal polarizers obtained from JPL for calibration.

Section 2.1 Polarization Dependent Absorption Spectrum

A method was required for evaluating the polarization dependent absorption spectrum of thin metal films which is accurate and reproducable. A special spectrometer was assembled for this task. A schematic representation of the spectrometer is shown in Figure 2.1-1. The wavelength of light is selected by a Beckman DK-7 Duel Beam Spectrophotometer. Radiation is provided by a high brightness halogen bulb located in the source optics of the Beckman DK-7. The light is passed through a light chopper in preparation for narrow band detection by a lock-in amplifier. A beam splitter is placed in the sample chamber of the

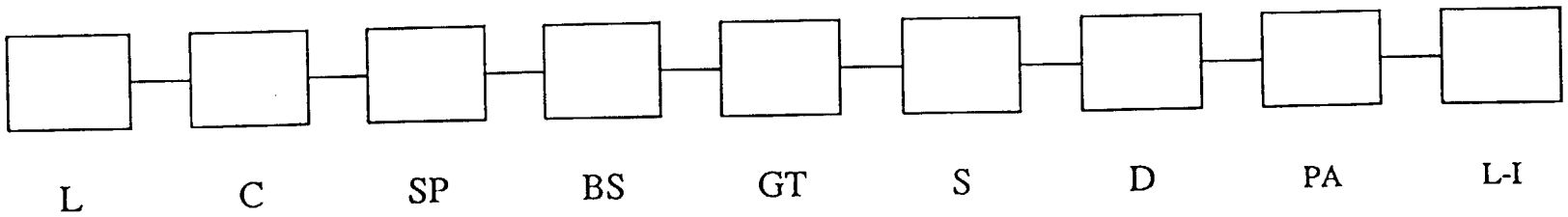

L = HALOGEN LAMP

C = LIGHT CHOPPER

SP = SPECTROPHOTOMETER

BS = BEAM SPLITTER

GT = GLAN-TAYLOR POLARIZER

S = SAMPLE

D = DETECTOR

PA = PRE-AMPLIFIER

L-I = LOCK-IN AMPLIFIER

Spectrometer for measuring polarization dependent absorption.

Figure 2.1-1

spectrophotometer in order to direct the horizontal light beam in a vertical direction. A Glan-Taylor prism is placed in the vertical beam to polarize the vertical beam of radiation.

A special sample holder is mounted on the spectrophotometer so that thin film samples deposited on glass discs can be placed in the path of the vertical polarized beam while resting flat on the sample mount. Special sample holders were designed so that the vertical beam passes through the center of the thin film sample. The Glan Taylor Polarizer is rotated until maximum absorption is observed. The sample is held in a square mount which can be rotated 90 degrees in order to observe minimum absorption.

The spectrometer can be tuned over a range from 400 nm to 1550 nm. Using the rotating sample method described above the principle transmittances of a metal thin film can be observed for a specific wavelength. The maximum transmittance k_1 is found by dividing the light at minimum absorption by the light incident on the detector when the sample is removed. The minimum transmittance is found by dividing the light at maximum absorption by the light transmitted when the sample is removed and the polarized reference beam is incident on the detector.

Throughout this investigation, metal thin films were optically characterized by the values of k_1 and k_2 at the wavelength of interest.

Section 2.2 Electron Microscope Structure Investigation

The technical objective was to develop scanning electron microscope (SEM) and transmission electron microscope (TEM) techniques for examining the structure of polarizing silver films. During the first 18 months of the project we attempted to use the University of Central Florida as a team member for TEM and SEM work. It became apparent that UCF had seriously over stated their electron microscope capabilities for analyzing silver films structure. Neither their TEM or SEM instruments could be used, even after much cost and delay were incurred.

The initial goal was to establish a correlation between the various deposition process parameters employed for making thin silver film polarizers and their anisotropic microstructure. These coatings were deposited in a way which resulted in small sized whiskers with a specific directional orientation. Several attempts were made with both Transmission and Scanning Electron Microscopes (TEM and SEM) to determine the size, density, and orientation of the whiskers. The results of the TEM and SEM investigations were delayed for many months because of equipment problems at UCF. The primary requirement for this project was the investigation of several silver films with a TEM. This study required sample preparation which involved carbon coatings. For this study, a used diffusion pumped system was acquired and fully rebuilt. For the directional shadowing of the thin film samples, a special T-shaped glass chamber was ordered from Blazers. Because of shipping delays and the amount of work required to rebuild the deposition system, specimen preparation was not possible until December, 1988. The TEM (Hatachi model HU-11E), which was located in the College of Engineering at UCF needed a full service before it was usable. This was completed in July, 1988. Because the TEM was an older model, it required extensive servicing to keep it operational. Therefore, to facilitate progress, a collaborative effort was established with the University of Florida (UF) in July 1989. Much of the TEM work was performed on the JEOL 2000 TEM system at the Major Analytical Instrumentation Center (MAIC)/UF with the help of Dr. Augusto Morrone. Further delays were caused by a period of rapid turnover in the undergraduate students involved in the project. The samples, which were supplied by Polatomic, were extremely delicate and had to be handled very carefully. The samples were also susceptible to moisture damage and were shipped sealed in plastic with desiccant. Upon arrival, the samples were transferred to vacuum desiccators.

TEM Sample Preparation

Three sample preparation techniques were used to make specimens for TEM imaging. The first was the microcleavage technique. This involved scratching the surface with a diamond scribe which created several small glass particles with the silver whiskers attached. There particles were transferred to a standard

copper grid used for specimen mounting in the electron microscope. It was hoped that it would be possible to determine the whiskers orientation from these images. Unfortunately, the substrate microroughness and the random orientation of the glass particles on the copper grid made an absolute angular determination impossible.

The technique that was used for the majority of the samples was a lift-off method. The samples were first coated with a thin carbon film doped with a small amount of platinum to increase the image contrast and then with another layer of plain carbon to strengthen the film. The carbon deposition was performed in a Varian vacuum system at 10^{-5} to 10^{-6} mbar. After coating, the samples were left in desiccators in a near-clean room environment to prevent further contamination and damage. The films were transferred to the copper grids by immersing the samples in a 10% HF solution at a shallow angle so that the HF acid creeps in between the carbon film and the substrate, etching the glass away. Surface tension causes the film to float off the substrate. Portions of the film are then placed onto the copper grids. To reduce the long term corrosion of the silver film, the HF solution was diluted to about 0.5% prior to removal of the specimens. This technique allowed for the preparation of both bulk surface and edge samples. The specimens were dried and placed in a desiccator.

The third technique attempted was the slicing of bonded samples for cross-section TEM (XTEM). This method should result in excellent edge shots providing the samples survive the preparation process. The samples were sliced with a diamond saw and the ground and polished until they were about 1 μm thick. The sample was then ion milled until it was transparent to the electron beam. This was a difficult and time consuming technique, which required durable samples.

TEM Analysis

Sixteen of the samples for normal incidence TEM imaging were prepared with method two (2) and investigated in the TEM at MAIC/UF with the help of Dr. Augusto Morrone. These samples had different whisker sizes and densities

(density information was provided as a scale form 1 to 10 with 10 being the highest density). Pictures of some of the samples (#7, $9 and #16) were not taken because of sample drift, which could not be eliminated. Sample #2 was not supplied. The TEM images of each sample were ordered by whisker size. The discrepancy may be a result of the deposition angle, which was not provided, or it may be some other process parameter. Three of the samples were not included in the listing: sample 1 appeared to be a bad sample, either from preparation or from deposition; samples 19 and 20 were not included in the initial list of densities. For the higher density samples the whiskers were elongated and had a definite orientation. The orientation corresponds to the deposition direction. For the low density samples, the whiskers were not elongated and there was a large size distribution. There were also a significant number of nucleation sites that had not formed into whiskers. Image processing of these micrographs should allow for the determination of film density as well as a determination of the size and aspect ratio distribution for each sample.

Edge shots were also attempted with some of the lift-off samples. Although it was possible to observe edges and see a definite angular orientation, this angle was probably rotated with respect to the image plane. Therefore, any angular measurement would be inaccurate. The tilt and rotation capabilities of the TEM specimen stage did not make it possible to resolve this problem. The best method for determining the angular orientation of the whisker was to view a cross-section cut from the bonded samples provided. The sample preparation time was estimated at 16 to 20 hours per sample provided the sample was durable enough to survive the process.

Electron Diffraction Analysis

Electron diffraction images were taken with the MAIC TEM for each of the above samples. The ring diffraction patterns were used to determine the crystalline phase of the silver. Table 2.2-1 shows the expected ring locations for the standard crystalline phases. By comparing the ring radii of our samples with those of Table 2.2-1, we can determine the crystal structure. To determine the crystal structure we need to relate $A(R_i/R_0)^2$ to allowed N for the different crystal

Crystal structure	Formula for interplanar spacing	Possible values of h, k, l for reflection (up to 20)	Criterion
simple cubic	$\frac{1}{d^2} = \frac{h^2 + k^2 + l^2}{a^2} = \frac{N}{a^2}$	N an integer except 7 or 15	ratios of squares of radii $\propto N$
f.c.c.	$\frac{1}{d^2} = \frac{h^2 + k^2 + l^2}{a^2} = \frac{N}{a^2}$	$N = 3, 4, 8, 11, 12, 16, 19, 20$	ratios $\propto N$
b.c.c.	$\frac{1}{d^2} = \frac{h^2 + k^2 + l^2}{a^2} = \frac{N}{a^2}$	$N = 2, 4, 6, 8, 10, 12, 14, 16, 18, 20$	ratios $\propto N$
diamond structure	$\frac{1}{d^2} = \frac{h^2 + k^2 + l^2}{a^2} = \frac{N}{a^2}$	$N = 2, 8, 11, 16, 19$	ratios $\propto N$
tetragonal	$\frac{1}{d^2} = \frac{h^2 + k^2}{a^2} + \frac{l^2}{c^2}$	$h^2 + k^2 = 1, 2, 4, 5, 8, 9, 10, 13, 16, 17, 18, 20$	ratios frequently proportional to 2; use Bunn chart, see Henry *et al.* (1951)
hexagonal	$\frac{1}{d^2} = \frac{4}{3}\frac{h^2 + hk + k^2}{a^2} + \frac{l^2}{c^2}$	$h^2 + hk + l^2 = 1, 3, 4, 7, 9, 12, 13, 16, 19$	ratios frequently proportional to 3; use Bunn chart, see Henry *et al.* (1951)

Table 2.2-1 Proportionalities of the ratios of the radii of ring patterns for different crystal structures.

phases indicated in Table 2.2-1. For our data this required multiplying the ratios by three (3) to form integers (within measurement error). Comparison of the experiment values with Table 2.2-1 shows that the Ag films have an fcc crystal structure. Comparison of the ring structures for the other samples shows that they are all fcc. As the size and density of the whiskers decreases, the intensity of the diffraction ring decreases. Also, the number of distinct diffraction spots decreases. This result is expected because there is less crystalline material to diffract the electrons. To obtain any further information from these images would require exact determination of the ring locations and thicknesses. With this knowledge it my be possible to estimate crystallite size and film stress levels. Unfortunately, it is not possible to measure the ring properties accurately without image processing. One diffraction image was digitized and the digital image was analyzed with the UCF Gould computer. A histogram of the image shows that the image consists of 12-15 gray levels out of a possible 256. This makes it possible to accurately determining diameters and widths.

SEM Analysis

SEM micrographs were taken of the surface of four of the samples that were also used for TEM investigations at UCF. This allowed for comparisons of the two techniques. Because these samples were not deposited onto conductive substrates, they were coated with a gold-palladium layer to increase electron conductivity. Although a magnification of 50,000 was possible, it was easily seen that the SEM photos did not have the high resolution of the TEM micrographics. It was difficult to distinguish individual whiskers, and in some cases orientation was hard to see. With the resolution of the TEM available, SEM analysis of the film surface did not provide any additional information. Samples deposited onto conductive substrates were also analyzed with the SEM. The results were similar to the samples discussed above.

Two technique were attempted to determine the angular orientation of the whiskers. The first required cleaving a sample on a conductive substrate. The sample was broken parallel to the whisker direction and prepared for SEM analysis. Because the sample was on a conductive substrate, it was not coated.

Note that there is a strong possibility that the film was damaged from the cleaving. Unfortunately, because of strong charging no imaging was possible. A second method, which viewed the whiskers at oblique incidence near a scratch, was used. From the picture, we see that an accurate determination of the whisker angle was not possible.

Because of the failure of UCF to produce SEM images, a new source was sought. Dr. V. A. Lindly of Electron Microscope Consultants at the University if Arizona was selected. Dr. Lindly provided all usable SEM micrographs used to analyze film development techniques in Sections 3 and 4.

Section 2.3 High Contrast Polarizer Evaluation

TEST APPARATUS

The project goal is production of polarizing filters with contrast greater than 10^5 at 589 nm. It was necessary, therefore, to design and assemble a test apparatus capable of making accurate measurements of this level. A preliminary design for the apparatus called for a laser light source. The design was evaluated at 800 nm using a High Brightness Spectra Diode semiconductor laser and a broad band Glan Taylor crystal polarizer with contrast in excess of 100,000:1.

The apparatus can be configured as an AC detection or DC detection system. The DC detection system is shown schematically in Figure 2.3-1. The laser light source is a PMS HeNe laser which delivers 2.5 mW of unpolarized radiation at 594 nm. A beam expander is used to increase the beam diameter from 2 mm to 5 mm. The beam is polarized by a Karl Lambrecht crystal polarizer of the Glan Taylor type. For calibration purposes a polarizer analyzer was inserted in place of a thin film polarizer. A light shield was added to shield the detector, a Si photovoltaic device from Oriel. A beam power meter from Newport Research Corporation was calibrated to read from 0.002μW to 1.0×10^4μW.

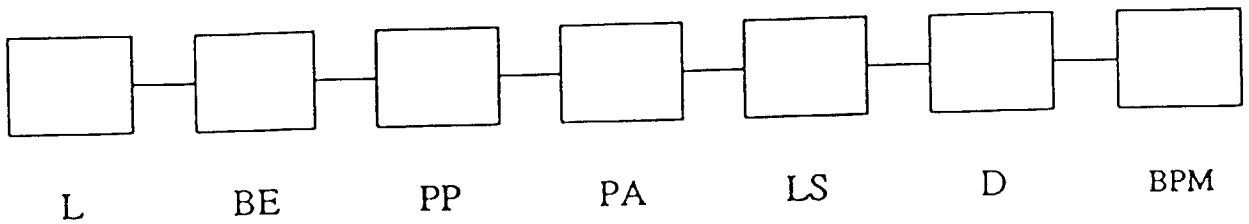

L = PMS λ594 nm 2,5 nm Random Polarized Laser

BE = Beam Expander

PP = Polarizer

PA = Polarizer Analyzer

LS = Room Light Shield

D = Oriel SiPV Detector

BP = Beam Power Meter Newport Research Corp.

Figure 2.3-1 High Contrast Polarizer Evaluation Apparatus - DC System

The optical components were mounted to an optical rail. The sample or analyzer crystal polarizer was mounted in a machined holder which permitted rotation over 360° about the beam axis. A micrometer screw adjustment permitted reading the angular position to 0.1 minute of arc.

The AC detection system, shown in Figure 2.3-2, contains the laser, beam expander, polarizer, light shield and silicon detector which are in common with the DC system. However, a light chopper and reference generator is added after the laser. A neutral density filter is used to set the light level into the Ithaco lock-in amplifier. A preamp is added between the detector and the lock-in amplifier. The following sources were identified for test equipment and critical components:

1. Laser Model 0250 M 594.1nm, 2.5 mw Random Polarized. P.M.S.Electro Optics, 1855 South 57th Court, Boulder, CO 80301

2. Glan Thompson Prism Polarizer #MGT3S10, with visible A/R coat. Karl Lambrecht Corp., 4202 N. Lincoln Ave., Chicago, IL 60618.

3. Photovoltaic Detector, STD#7182. Oriel Corp., 250 Long Beach Blvd., P.O.Box 672, Stratford, CT 06497

4. Laser Power Meter, Model 820, Newport Research Corp., 18235 Mt. Badly Circle, Fountain Valley, CA 92708

5. a.) Lock-In Amplifier, Model 3921, b.) Preamp cable #3921V1, c.) Current Sensitive Preamplifier Model 1642, ITHACO, 735 Clinton St., P.O.Box 6437, Ithaca, NY 14851-6437

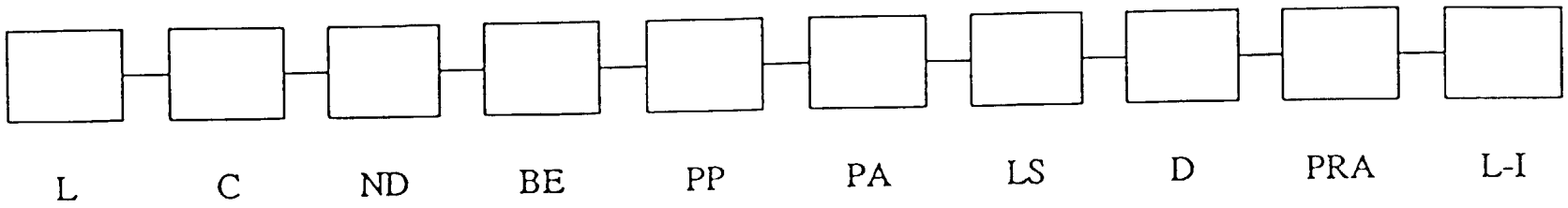

L = PMS λ594 nm 2.5 nm Random Polarized Laser

C = Chopper & Reference Generator

ND = Neutral Density Filter

BE = Beam Expander

PP = Polarizer

PA = Polarizer Analyzer

LS = Room Light Shield

D = Oriel SiPV Detector

PRA = Pre-Amplifier

L-I = Lock-In Phase Detector

Figure 2.3-2 High Contrast Polarizer Evaluation Apparatus - AC System

SYSTEM LINEARITY

To measure the system linearity requires that the light power be variable and its relative power be known over a six orders of magnitude range. The light detector and the readout electronics must be also linear over six orders of magnitude. When two polarizers are aligned and their polarization axis are rotated with respect to each other by an angle θ, the amplitude I of the light vector in the beam varies as $\cos\theta$, or

$$I = k\, I_o \cos\theta \qquad (2.3\text{-}1)$$

where:

k = a constant
I_o = amplitude of incident light
θ = angle between the polarization axes of the two polarizers

The power P in the radiation is proportional to the square of the amplitude (electric or magnetic), so

$$P = I^2$$
$$= k^2 I_o^2 \cos^2\theta \qquad (2.3\text{-}2)$$

When $\theta = 0$, then the transmitted power has its maximum value. When $\theta = 90°$ the transmitted power has its minimum value. The holder of the analyzer polarizer is calibrated in the range 0 - 360°, and its micrometer screw permitted reading θ to within 0.1°.

The Si photovoltic detector is linear over many orders of magnitude provided it is operated in the current mode as it was here. The electronics following the detector was a.) The Newport Research Corporation Power meter and b.) the ITHACO Lock-In Amplifier. Both of the systems are designed to be linear to at least six orders of magnitude.

The light power value was calculated to be proportional to $\cos^2\theta$ and the value of θ was read to within 0.1 minutes of arc. The value of $\cos^2\theta$ was plotted along the X-axis. The relative light power was read on the electronic read out systems

which were calibrated individually. The relative light power was plotted on the Y-axis.

LINEARITY OF THE DC SYSTEM

Two JPL polarizers, each labeled MGTYE20-BB580-780, were supplied for evaluation. For these tests one was further identified as #1, the other as #2. The assumption is made that they are identical in performance. The data for them is plotted the Figure 2.3-3. At the low end of the data there are great changes in light power as θ approaches 90°. The value of $\cos^2(\theta \rightarrow 90°)$ cannot be plotted since at $\theta=90°$ $\cos^2\theta=0$ and the point is off the log scale. In addition as θ approaches 90°, its value could be read with less accuracy. In addition the value of the light power is at the lowest range of the power meter and its value was estimated. Nevertheless the system is linear over a range approaching six orders of magnitude. Within this range the system can be used with confidence to measure the polarization values k_1 and k_2 of any polarizer.

The Karl Lambrecht Glan Thompson polarizer was the best quality availaable. The cross sectional area was smaller than those of JPL but adequate for our application. Preliminary tests showed that it had a k_1 orientation light power transmission that was higher than that of the JPL polarizers. In addition when it was crossed with the JPL#2, the minimum value of transmission, k_2 orientation, had a lower value than that for the 2 JPL polarizers. In fact the light power was at the limit of the Newport meter and was estimated. The linearity of the K.L. and the JPL #2 combination is plotted in Figure 2.3-4. The D.C. system is comfortably linear over six orders of magnitude. It is possible to approach the 7th order at the low end by estimating the meter reading at the very low end of the scale. The D.C. system is linear and would be suitable for measuring k_1, k_2 for most polarizers.

LINEARITY OF THE AC SYSTEM

Here we used the Karl Lambrecht as the radiation polarizer and the JPL #2 as the analyzer. Data is plotted in Figure 2.3-5. The Lock-In preamplifier makes possible the extension of reading to very low values. It was found that there is a zero

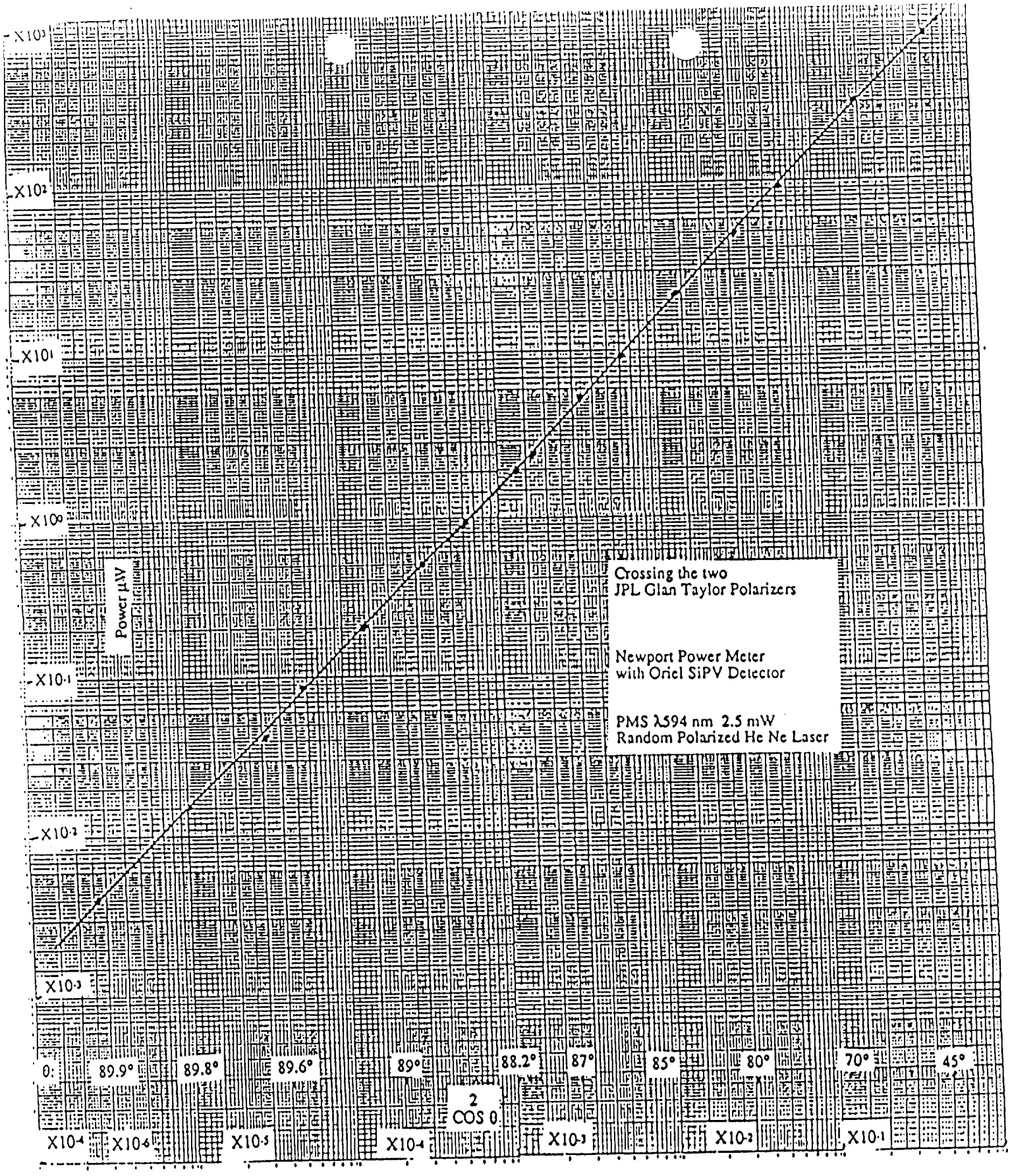

Figure 2.3-3 Linearity of DC System - JPL Polarizers

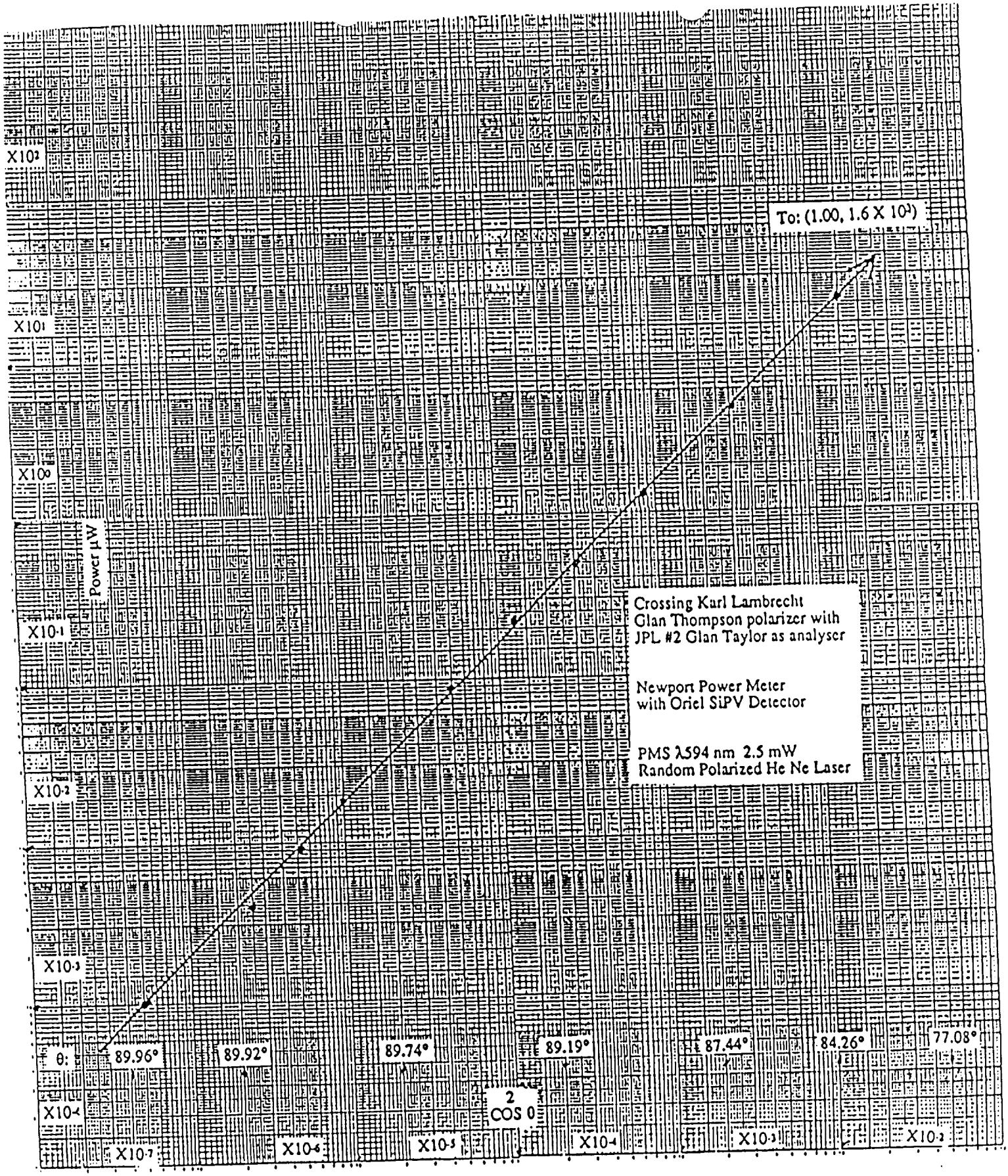

Figure 2.3-4 Linearity of DC System - Karl Lambrecht and JPL Polarizer

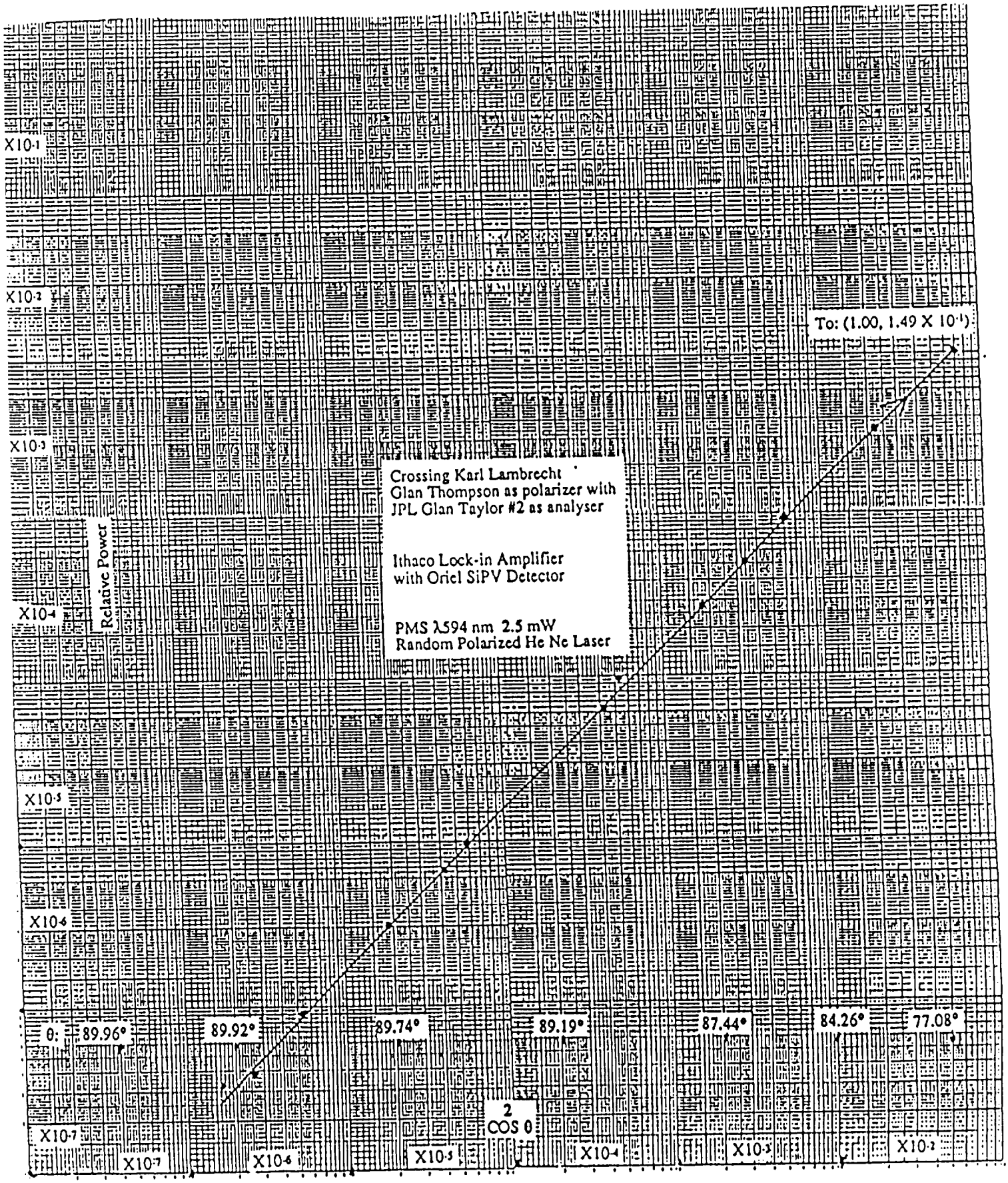

Figure 2.3-5 Linearity of AC System - Karl Lambrecht and JPL Polarizer

reading that can be subtracted from the experimental reading to extend linear range to seven orders of magnitude. This is adequate for all situations we encountered. Decreasing the gain of the preamplifier could possibly extend the linearity to eight orders of magnitude. The A. C. system is linear to seven orders of magnitude and is suitable for measuring k_1, k_2 for most polarizers to be encountered.

MEASURING THE POLARIZATION PARAMETERS OF THE JPL AND KARL LAMBRECHT POLARIZERS

A. Theory

This technique developed by Rupprecht (1962) requires two identical polarizers. Let the emission of the laser be

$$1/2\ Pt_v + 1/2\ Pt_h = P_o \quad , \tag{2.3-3}$$

where

P_o = Total emission of the laser

$1/2\ Pt_v$ = component polarized in the vertical plane

$1/2\ Pt_h$ = component polarized in the horizontal plane

Inserting a polarizer and rotating it in the vertically and horizontally planes yields measured values:

$$P_v = 1/2\ P\ (t_vT_1 + t_hT_2) \tag{2.3-4}$$

$$P_h = 1/2\ P\ (t_vT_2 + t_hT_1) \tag{2.3-5}$$

and combining (3), (4) and (5) yields:

$$(P_v + P_h)/P_o = T_1 + T_2 \quad . \tag{2.3-6}$$

Adding the second identical polarizer in series with the first but rotating the second one so it is crossed with the first, and making measurements yields $P_\perp$ where:

$$P_\perp = 1/2\ P(t_vT_1T_2 + t_hT_1T_2)$$

$$= 1/2\ P(t_v+t_h)\ T_1T_2$$

from which:

$$P_\perp / P_o = T_1\ T_2 \quad . \tag{2.3-7}$$

Combining Eq. (2.3-6) and Eq. (2.3-7) and solving for T_1 yields a quadratic in T_1 from which:

$$T_1 = \frac{(P_h+P_v)}{2P_o}\left\{1 + \left[1-4\,\frac{P_\perp P_o}{(P_h+P_v)^2}\right]^{1/2}\right\} \cong \frac{P_h+P_v}{P_o} - \frac{P_\perp}{P_h+P_v} \quad . \text{(2-8)}$$

Substating in Eq. (2.3-7) and solving for T_2 yields:

$$T_2 = \frac{(P_h+P_v)}{2P_o}\left\{1 - \left[1-4\,\frac{P_\perp P_o}{(P_h+P_v)^2}\right]^{1/2}\right\} \cong \frac{P_\perp}{P_h+P_v} \quad . \text{(2-9)}$$

T_1 and T_2 are calculated from measured values.

B. Measurement and calculations, JPL Polarizers

Measurements were made on the DC system. Data and calculations are presented in tabular form.

Table I JPL Polarizers (first run)

P_o $\mu wX10^4$	P_v $\mu wX10^4$	P_h $\mu wX10^4$	$P_\perp$ μw
$0.388X10^4$	$0.168X10^4$	$0.171X10^4$	0.005

These yield: $T_1 = 0.874$

$T_2 = 1.47 \times 10^{-7}$

Repeating gave:

Table II JPL Polarizers (second run)

P_o $\mu wX10^4$	P_v $\mu wX10^4$	P_h $\mu wX10^4$	$P_\perp$ μw
$0.391X10^4$	$0.169X10^4$	$0.177X10^4$	0.005

These yield: $T_1 = 0.880$

$T_2 = 1.45 \times 10^{-7}$

Averaging results of Table I and II give:

$\overline{T_1} = 0.880$

$\overline{T_2} = 1.46X10^{-7}$

and

$\overline{T_1/T_2} = 6.01 \times 10^6$

C. Karl Lambrecht Glan Thompson Polarizer

T_1 values are determined from P_v and P_h measurements but do not require a second identical polarizer. To obtain T_2, the JPL #2 polarizer was used to determine $P_\perp$ for which the value was at the lower limit estimation allowed. Had another similar polarizer been available the estimated value would have been probably cut in half. The alternative would have been to use the AC system. This was not done.

The results of one measurement are given in Table III.

Table III Measured values for Karl Lambrecht polarizer

P_o	P_v	P_h	$P_\perp$
μw	μw	μw	μw
$0.393X10^4$	$0.186X10^4$	$0.180X10^4$	0.0002

From these values we calculate:

$T_1 = 0.931$

$T_2 = 5.46 \times 10^{-8}$

$T_1/T_2 = 17.1 \times 10^6$

This polarizer will be used in measuring the polarizers produced by thin film methods.

Section 3 Development of Polarizing Metal Films

The technical objective of the effort reported in Section 3 is development of a technique for fabricating metal films made up of metal particles having a correct shape factor and density for polarizing light in the visible spectral region. Specifically these films must be developed for use in high performance polarizing filters peaked at 589 nm. Having presented an analytical discussion of such films in Section 1, it must be pointed out that the experimental work predated the analytical work by 18 months and followed a "cut and try method" for evaluating a wide variety of experimental approaches for producing visible polarizing metal thin films of silver.

The starting point was a know deposition technique for producing a wide-band polarizing silver film covering the spectral range from 780 nm to 1250 nm with peak resonance absorption at 1050 nm. The technical approach described in Section 3 describes variations in amount of silver, directional sequence for deposition, variation of deposition parameters and substrate condition. All variations were evaluated for effectiveness in improving the films polarization characteristics at 589 nm. Our initial intention to investigate other metals besides silver was deferred at first and later abandoned because of continued success with silver.

The technique used to deposit silver is a grazing angle incidence deposition using standard evaporative vacuum deposition methods. The three essential innovations for producing polarizing films at 589 nm are:

(1.) Selection of the correct amount of silver.

(2.) Correct division of the silver into alternating directions of depositions.

(3.) Preparation of the substrate with a precoat of silver which is heat treated to shape the particles.

The experimental work leading to the development of the polarizing thin film for visible light will be reviewed in the following sections.

Section 3.1 Shaping of Metal Particles

Vacuum Deposition System and Fixtures

A vacuum system with a six-inch oil diffusion pump, cryogenic trap and 18 inch bell jar was installed in our laboratory. Silver was evaporated from a graphite boat with dc current controlled by a Variac. Silver was purchased in the form of a ribbon with a rectangular cross-section with sides of 0.25 mm and 1.0 mm. For convenience, the silver length was indicated in inches of ribbon. Silver was deposited at a vacuum approaching 10^{-6} torr. Reproducible results were regularly achieved by specifying silver ribbon length and Variac setting for deposition.

The schematic representation of the vacuum are shown in Figure 3.1-1. The substrates were 25 mm diameter polished discs of BK-7 glass. Each disc was mounted to a disc carrier which could be placed in the positioning fixture in the vacuum chamber. A fixture was built so that 14 discs at a time could be mounted in the chamber. A precision adjustment of each of the 14 stations could position each disc so that the normal to the surface was normal to the incident beam of silver. The angle between the normal to the glass surface and the incident beam of silver could be varied between 85° and 89°. An optical indicator was used to position the tilt of a disc at positions of 0, ± 1 1/2, ±1 around a standard position near grazing angle.

Our standard experimental procedure is to divide the length of silver into a even number of segments and alternate the direction of deposition on the disc. Position 1 is the position defined by the direction of the beam onto the disc surface for the first coating. Position 2 is defined by rotating the disc 180° about the normal to the disc extended from the center of the disc. The deposition in Position 2 is in a direction essentially opposite that of Position 1. It is implied that, when a division of silver is made into an even number of segments, the

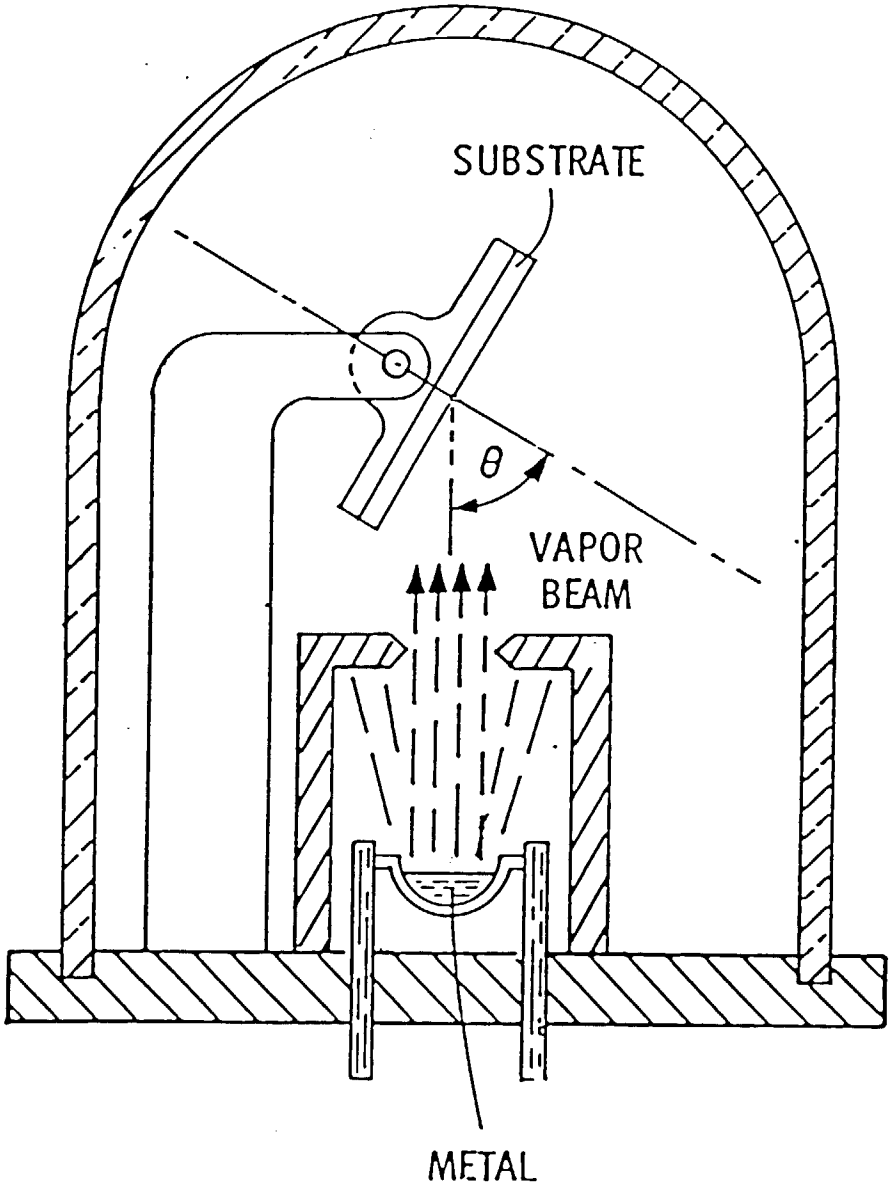

Figure 3.1-1 Schematic of grazing angle evaporative deposition system.

segments will be deposited in a sequence alternating between Position 1 and Position 2 unless otherwise indicated.

Silver Films: Optical and Structural Features

The experimental results reported in this section will summarize the optical characteristics and structural characteristics of the basic silver films. The optical characteristics are the measured principle transmittance k_1 and k_2 recorded using the polarizing spectrophotometer described in Section 2.1. Although scores of discs were coated during the evaporation process, the results can be summarized by the typical TEM pictures and principle transmittances for 4, 6, 8 and 10 segment depositions.

A. 4 Segment - 21.0 inches Ag

A typical 4 segment transmittance plot is shown in Figure 3.1-2. A TEM picture is shown in Figure 3.2-3. Many of the prominent spheroids have a length of the order of 0.5 micron. Peak absorption occurs at 700 nm.

B. 6 Segment - 21.0 inches Ag

A typical 6 segment transmittance plot is shown in Figure 3.1-4. A contrast of 46 is achieved at the 600 nm peak. A TEM picture of a 6 segment film is shown in Figure 3.1-5. A typical length a silver prolate spheroid is 0.15 micron.

C. 8 Segment - 26.4 inches Ag

A typical 8 segment transmittance plot is shown in Figure 3.1-6. A contrast of 122 is achieved at 600 nm while the peak resonance absorption occurs at 575 nm with a contrast of 144. A SEM picture of a very poor quality is shown in Figure 3.1-7. A TEM micrograph of the same sample is shown after 6 of the 8 segments are deposited in Figure 3.1-8.

POLARIZER DATA

Date: 09/24/90 Job Number: 8801 Run Number:
Disk Number: 1

A:	4.5 inch Ag, 4 shots	D:	
	2.5 min at 110, Tilt -1		
B:	Plain Disc	E:	
C:		F:	

K1/K2

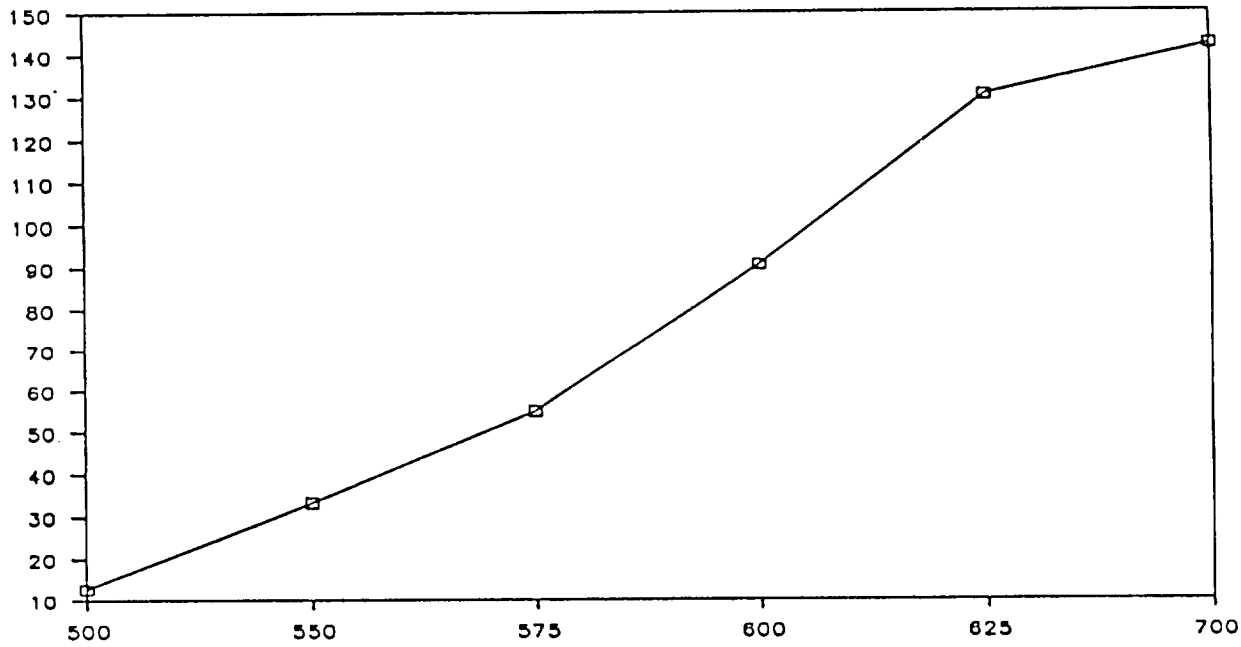

K1 = □ K2 = +

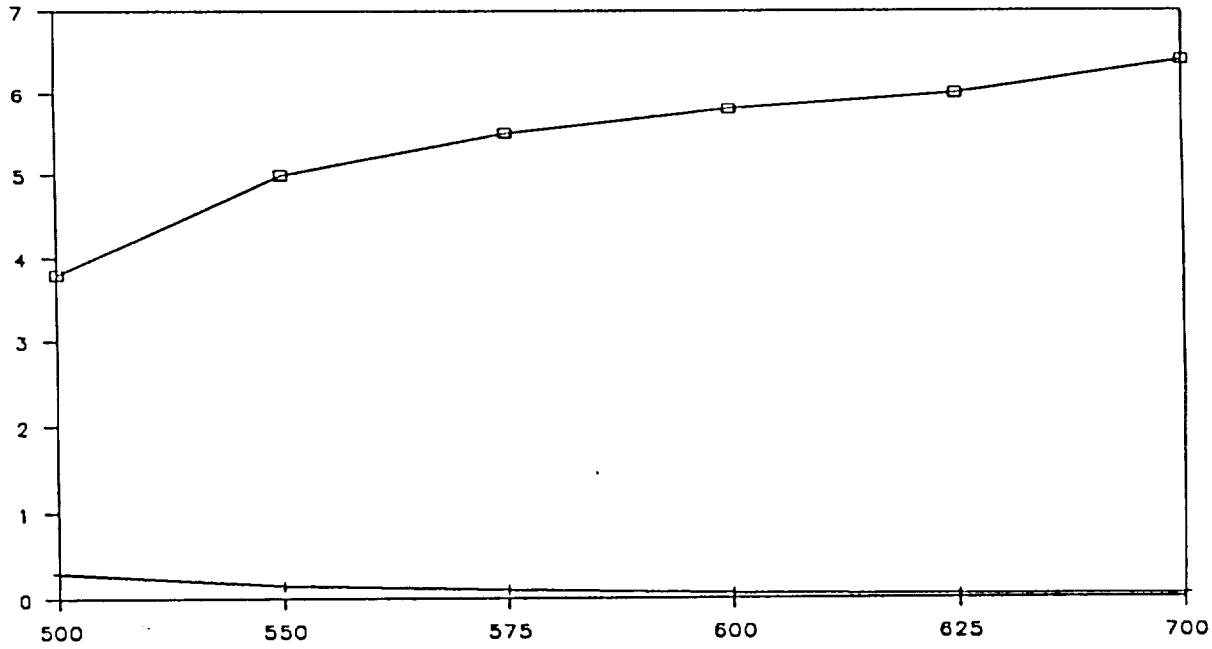

Figure 3.1-2 Transmittances and contrast for 4 segment film

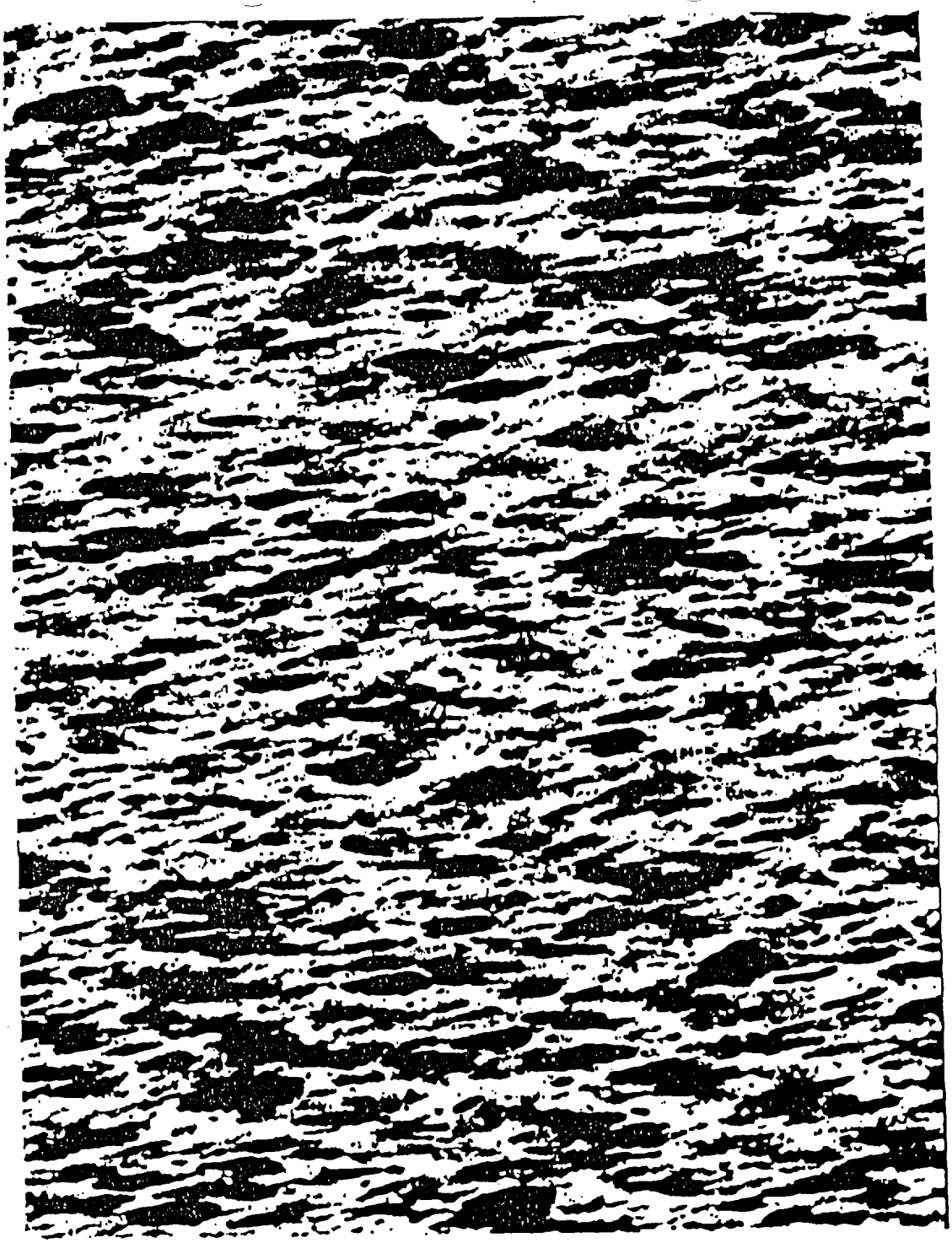

Figure 3.1-3 TEM image of 4 segment film

POLARIZER DATA

Date: 07/09/90 — Job Number: 8801 — Run Number: 2
Disk Number: 2

A:	6 shots, 3.3" AG each	D:	
	2.5 minutes at 110		
B:	Evap. Direction Alternation	E:	
	AB AB AB		
C:	Tilt: -1 F.U.	F:	

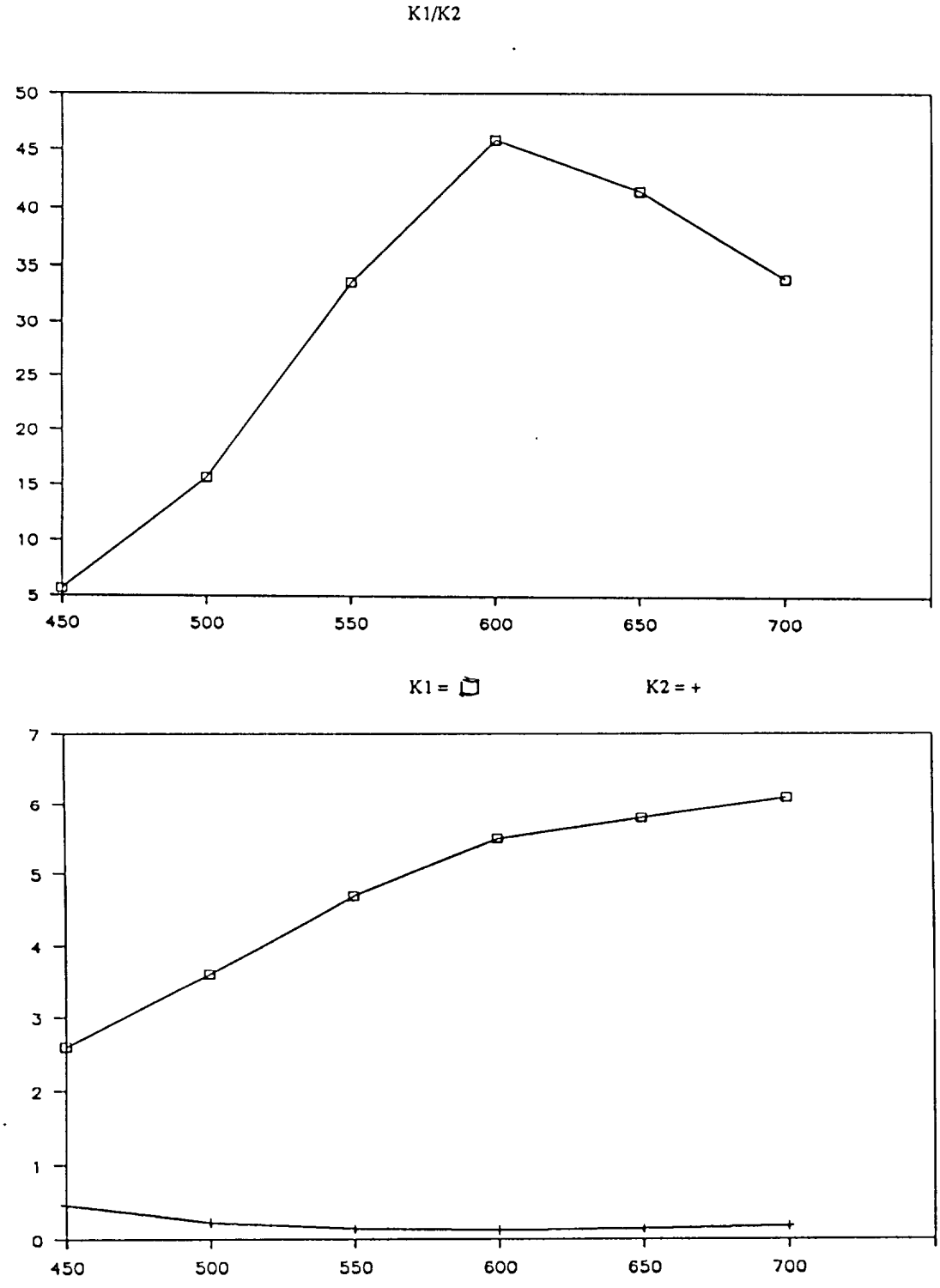

Figure 3.1-4 Transmittances and contrast for 6 segment film

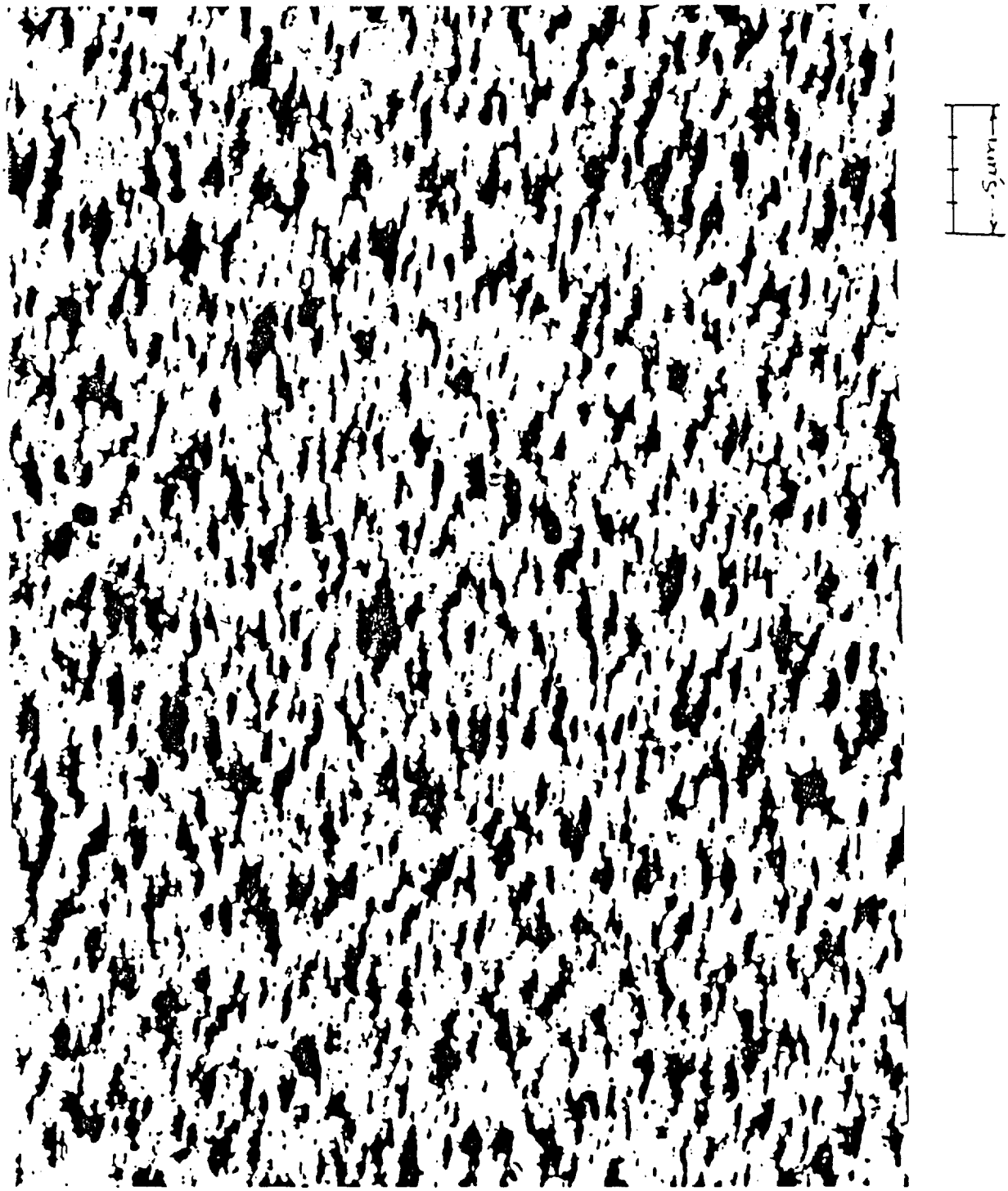

Figure 3.1-5 TEM image of 6 segment film

POLARIZER DATA

Date: 08/08/90 Job Number: 8801 Run Number: 1
Disk Number: 5

A:	3.3 Ag x8 (AB)4	D:	
	2.5 min at 110		
B:	Tilt: -0-	E:	
C:	Plain discs (10 ea.)	F:	

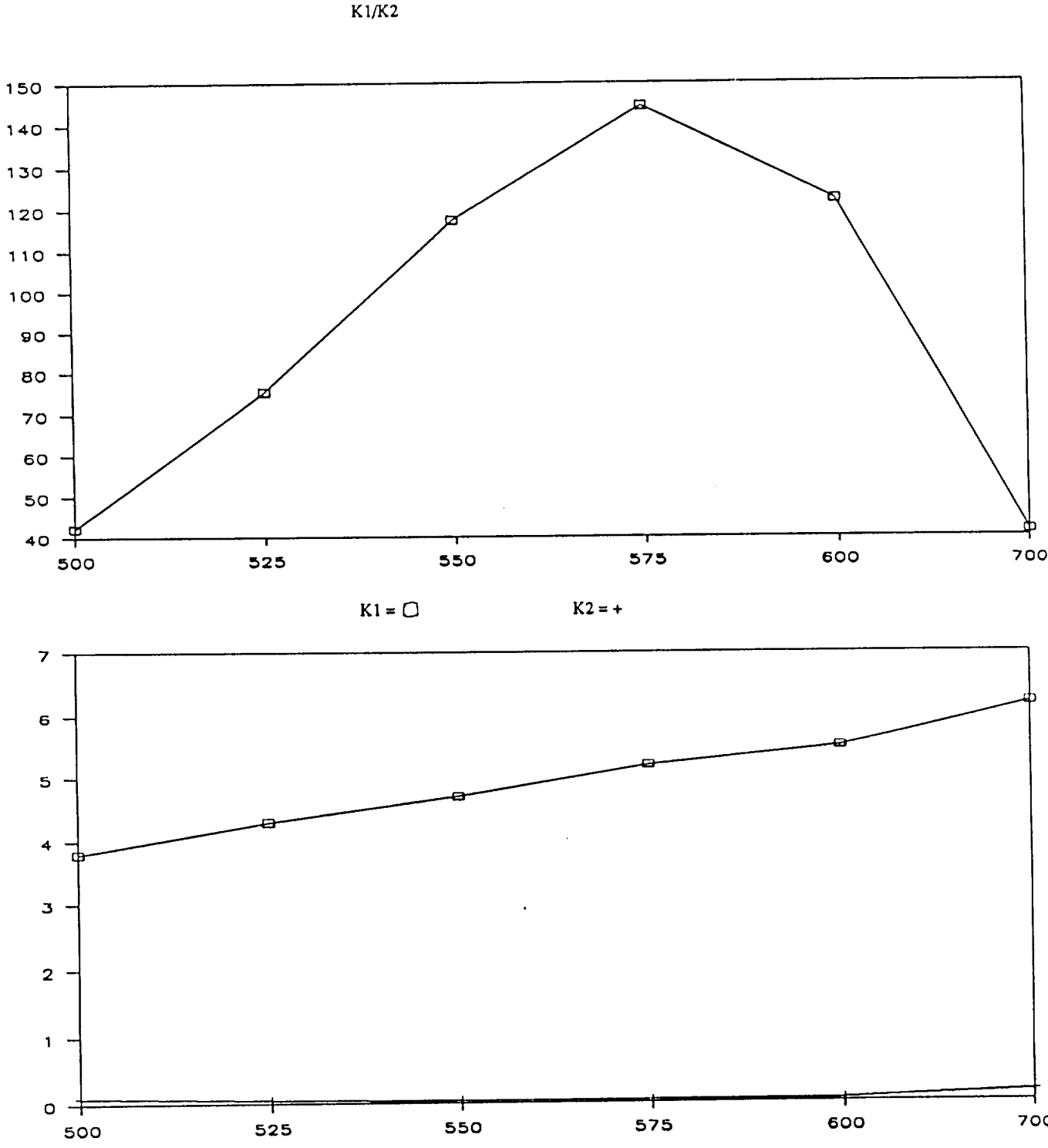

Figure 3.1-6 Transmittances and contrast for 8 segment film

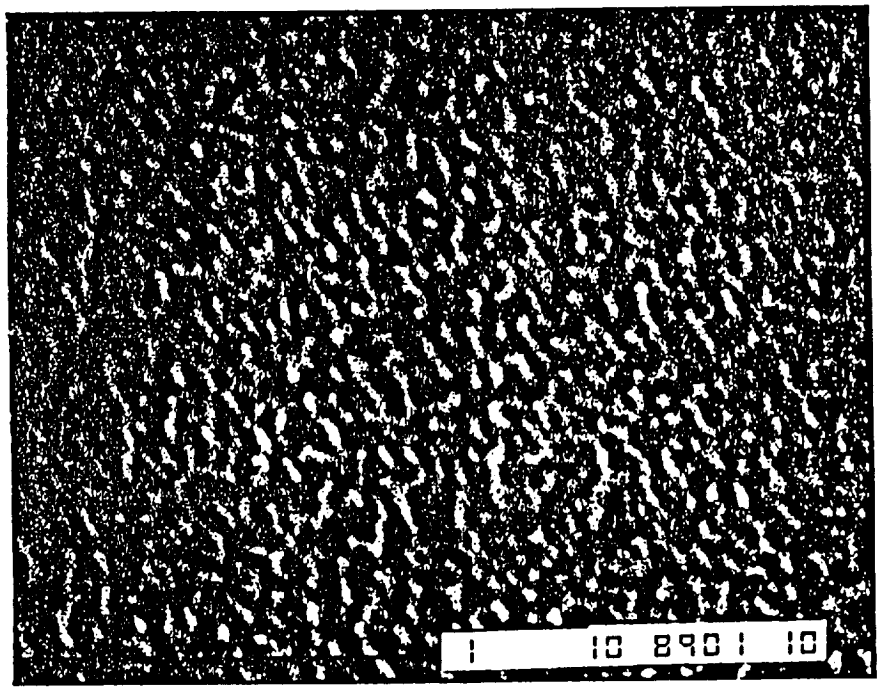

Figure 3.1-7 SEM image of 8 segment film

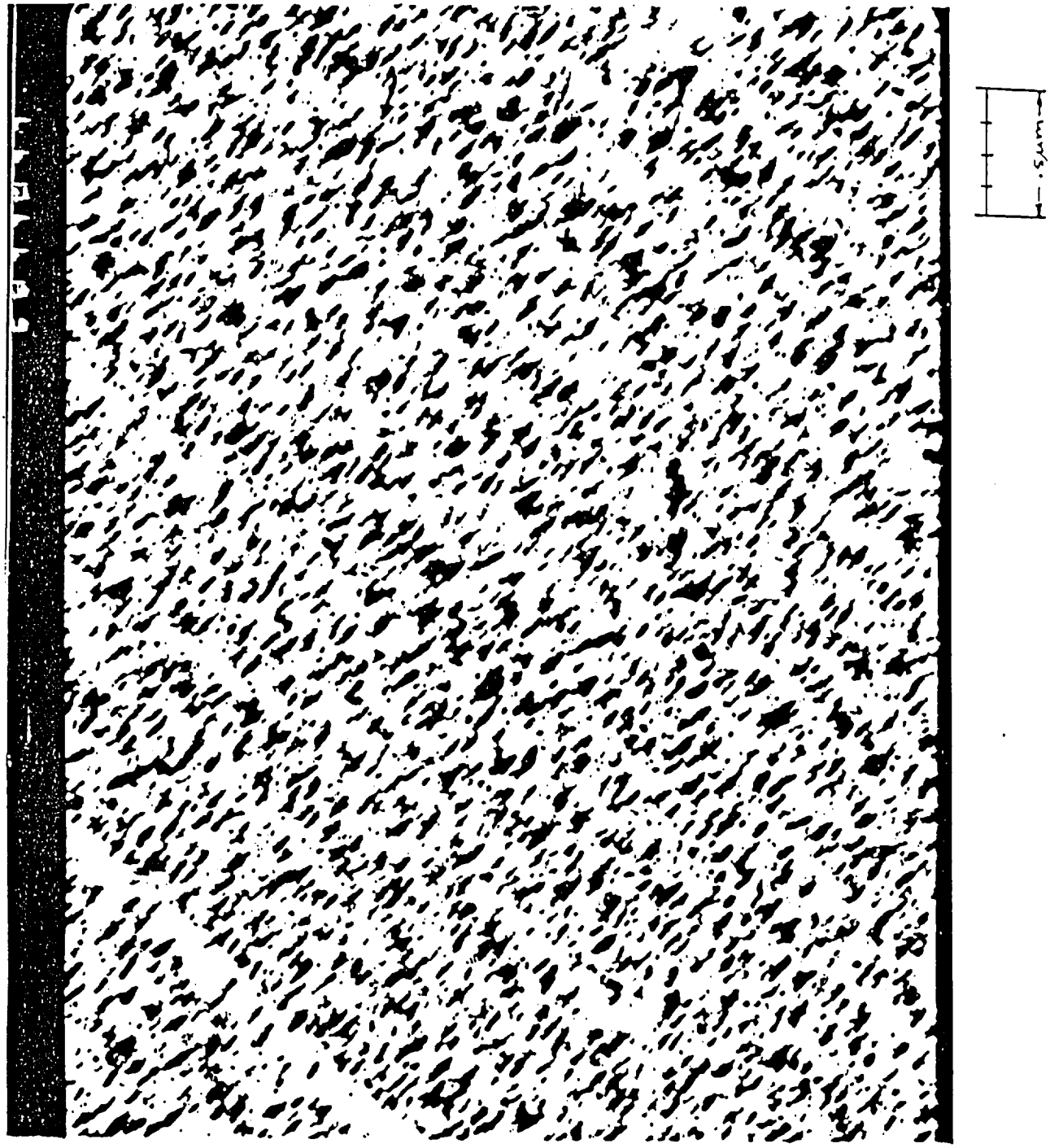

Figure 3.1-8 TEM image of 8 segment film after 6 segments

D. 10 Segment - 26.0 inches Ag

A typical 10 segment transmittance plot is shown in Figure 3.1-9. Contrast greater than 61 is achieved at both 550 nm and 575 nm. It is apparent that the resonance peak is shifted to even shorter wavelength in the visible spectrum. No electron microscopy was performed on the 10 segment sample.

E. Summary

It is evident from the transmittance data that the increase in the number of segments increases the density of silver spheroids, decreases the size of the spheroids and increases the ratio b/a of typical prolate spheroids. All effects contribute to shifting the resonance peak to shorter wavelength according to the analytical description of Section 1. It is also apparent that the resonance peaks are very broad. The electron micrographs reveal a variety of particle shapes and sizes which serves to decrease k_1 and broaden the peak absorption of k_2. These results clearly indicate the potential for fabricating effective polarizing films for the visible spectral region.

Section 3.2 Substrate Surfaces

The technical objective of this task was investigation of methods of coating or preparing the surface prior to silver deposition in order to improve polarization characteristics of the silver film. A variety of technical approaches were investigated with one very significant success. This technique consisted of depositing a light silver film as a precoat followed by heat treating in a vacuum prior to depositing the multisegment silver film in the normal fashion. This technique was incorporated in the film fabrication technique which produced our best polarizing films.

At the start of the program the standard substrate was a 25 mm diameter disc of Corning 7059 glass, a low sodium glass which is drawn rather than polished. A change was made to 25 mm diameter disc of BK-7 glass which was ground and polished. The BK-7 glass gave improved and more reproducible results.

POLARIZER DATA

Date: 07/19/90 Job Number: 8801 Run Number: 1
Disk Number: 1

A:	AG 2.6" x 10	D:	Tilt: -1
	2.5 minutes at 110		
B:	Deposit alternate: (AB)5	E:	
C:	Plain disks, 6	F:	

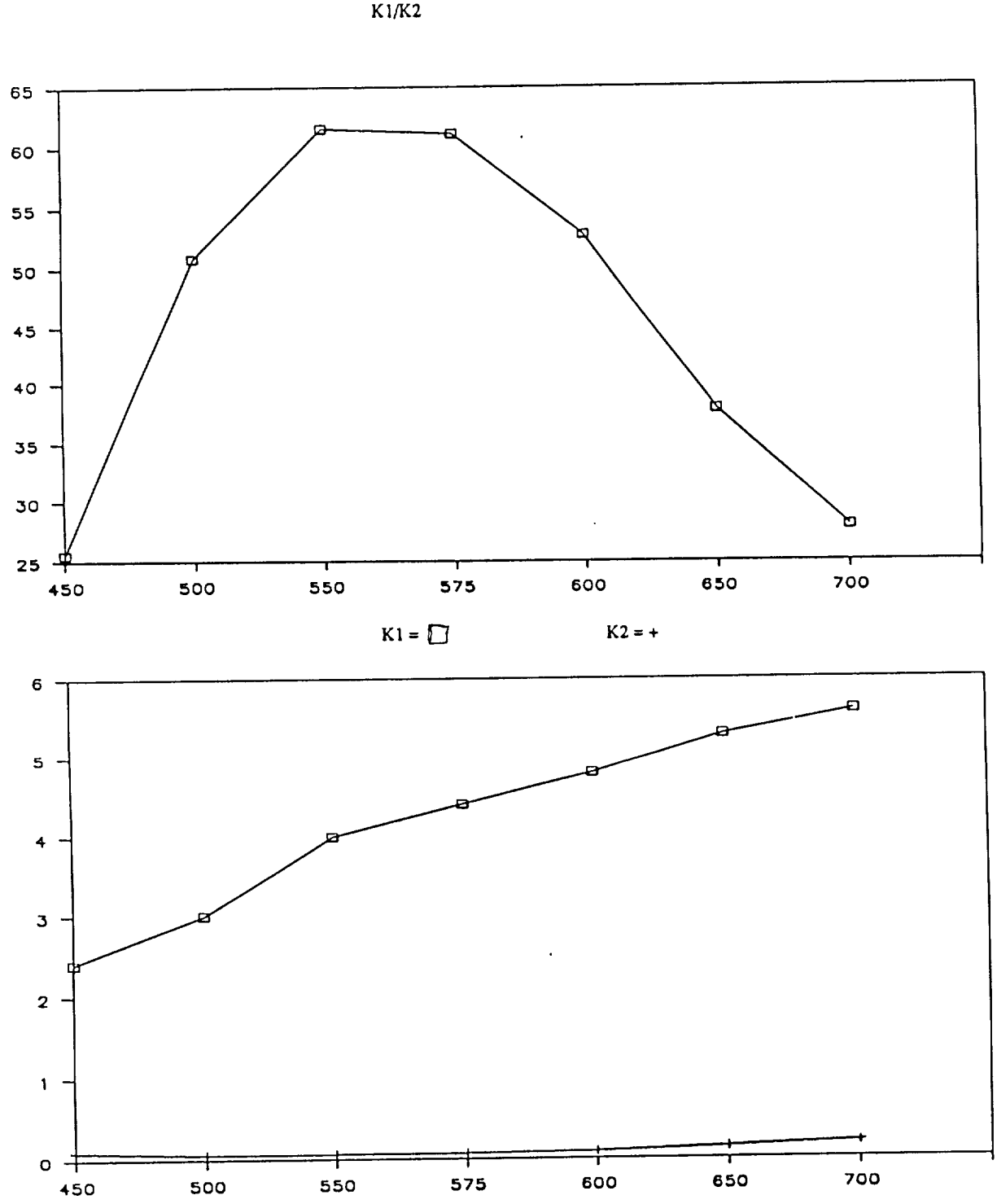

Figure 3.1-9 Transmittances and contrast for 10 segment film

A second part of the effort was investigation of the effects of precoating the BK-7 discs. A sputter deposition machine was used to coat the discs with Teflon, SiO_2, MgF_2, and SnO. No improvements were observed in the performance of films deposited on these coated substrates. A third technique investigated under this task was the effect of sputter etch of the silver films. This appeared to have the same effect as heating and did not improve polarization of the film.

Silver Precoat and Heating

The investigation of silver precoat began with observations of silver deposited on glass discs without grazing incidence. The silver particles are essentially spherical. The discs were placed on the bottom of the vacuum system and precoated with silver which was vaporized by the heated crucible and cooled by multiple collisions of the vapor within the vacuum chamber while normal deposition is in progress. This cooling process was termed "blow by". These "slow" atoms were deposited as a precoat on the disc. Although theory specifies the particle dimensions for desired polarization parameters, it does not dictate the deposition condition. The effect on the polarizer parameter due to deposition condition must be determined experimentally. We evaporated 3.3 inches of silver from the crucible to create the precoat on the disc. The disc rested on the bottom plate in the vacuum chamber. Only silver atom cooled by scattering deposited on the glass disc.

The disc was next heated by the hot crucible for 2.5 minutes. The structure of the precoat silver particles is shown in Figure 3.2-1. The particles are very small, but their average diameter and distribution can be determined by count and measurement. The silver deposition for the polarizing particles on the disc was done by 8 deposits of 3.3 inches of silver strip. The evaporation direction was alternated 180° for each deposit. The crucible was heated by the variac at 110 VAC for 2.5 minutes. The disc tilt was -1. The silver deposited on this precoated heated disc is shown in Figure 3.2-2. The shape and size may be determined by count and measurement since 2.0 inches on the micrograph covers 1.0 micron.

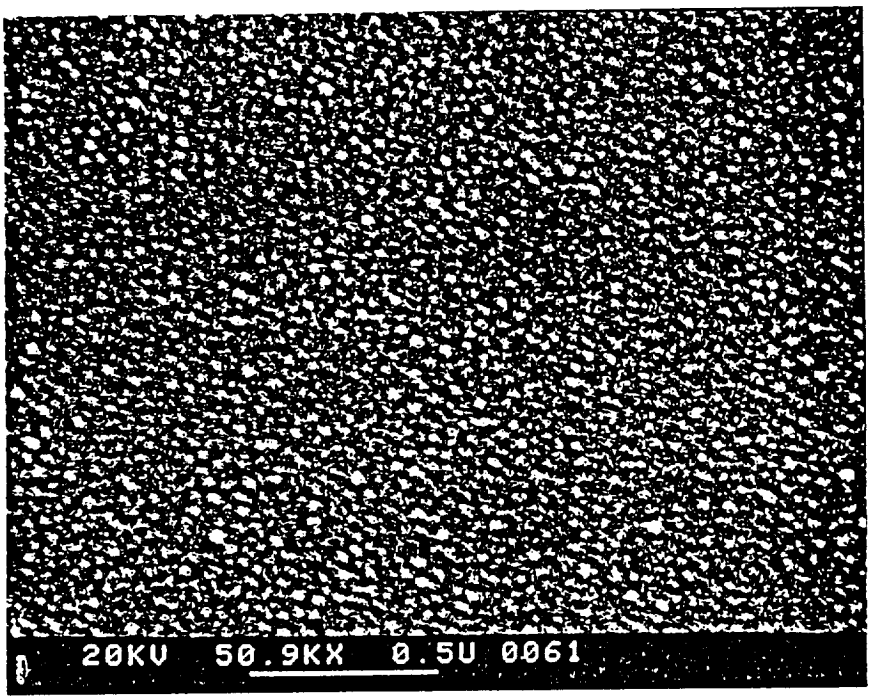

Figure 3.2-1 Blowby Silver Film

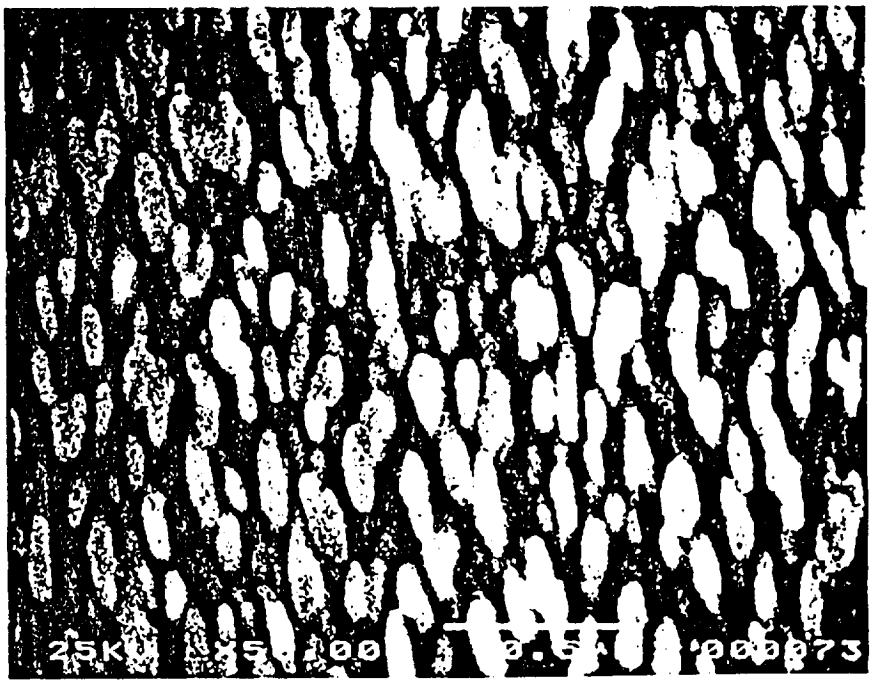

Figure 3.2-2 Ag deposited on heat treated precoat.

The Polarizer data is given in Figure 3.2-3. It shows a marked change in k_1/k_2 being 1600 at 500 nm. Also the curve is sharp and extends from 450 to 550 nm, trailing to about 100 at 700 nm. The polarizer characteristics can be altered radically by changing the deposition conditions. The selection of other conditions are a continuing challenge to the imagination, ingenuity, and trial and error of the experimenters.

The SEM photo micrograph in Figure 3.2-4 shows the appearance of the silver fibers when 4 inches of Ag is deposited in 1 shot at a tilt angle of -1 units. The fibers are not symmetrical, are elongated and show a range in size distribution. A second SEM photo micrograph shown in Figure 3.2-5 shows the shape of the particles after these Ag coated glass substrates were heated in a vacuum at a distance of 2.5 inches from the graphite deposition crucible heated by a current using a Variac at 110 VAC for a period of 2.5 minutes. The Ag particles have coalesced into larger particles whose size distribution is more uniform. The space between particles has been cleared of small particles. This leaves more clear glass exposed, thereby permitting a larger value for k_1 after the final silver has been deposited. This effect was investigated for a number of deposition conditions as a result the precoat and preheat step have become an important step in the polarizer fabrication. The precoated preheated discs were placed in the next process step where 4 shots each of 4.25 inches of silver strip were deposited on these discs at a tilt angle of -1. The discs were rotated 180° between shots to produce particles whose shapes were symmetrical about their centers. This is shown in the SEM photo micrograph in Figure 3.2-6. There is a small amount of small particle deposition in the area between the optically polarizing particles. These small particles do not contribute to the polarizer performance but may act adversely by reducing k_1 and increasing k_2. A method for their elimination has not been found.

POLARIZER DATA

Date: 07/11/90 Job Number: 8801 Run Number: 1
Disk Number: 10

A:	Ag 3.3" x 8	D:	Tilt = -1
	2.5 minutes at 110		
B:	Evap. Direction Alternation	E:	
	A B (4 times)		
C:	06-18-90 Blow by, 3.3" Ag	F:	
	Bottom plate, heated 2.5 minutes		

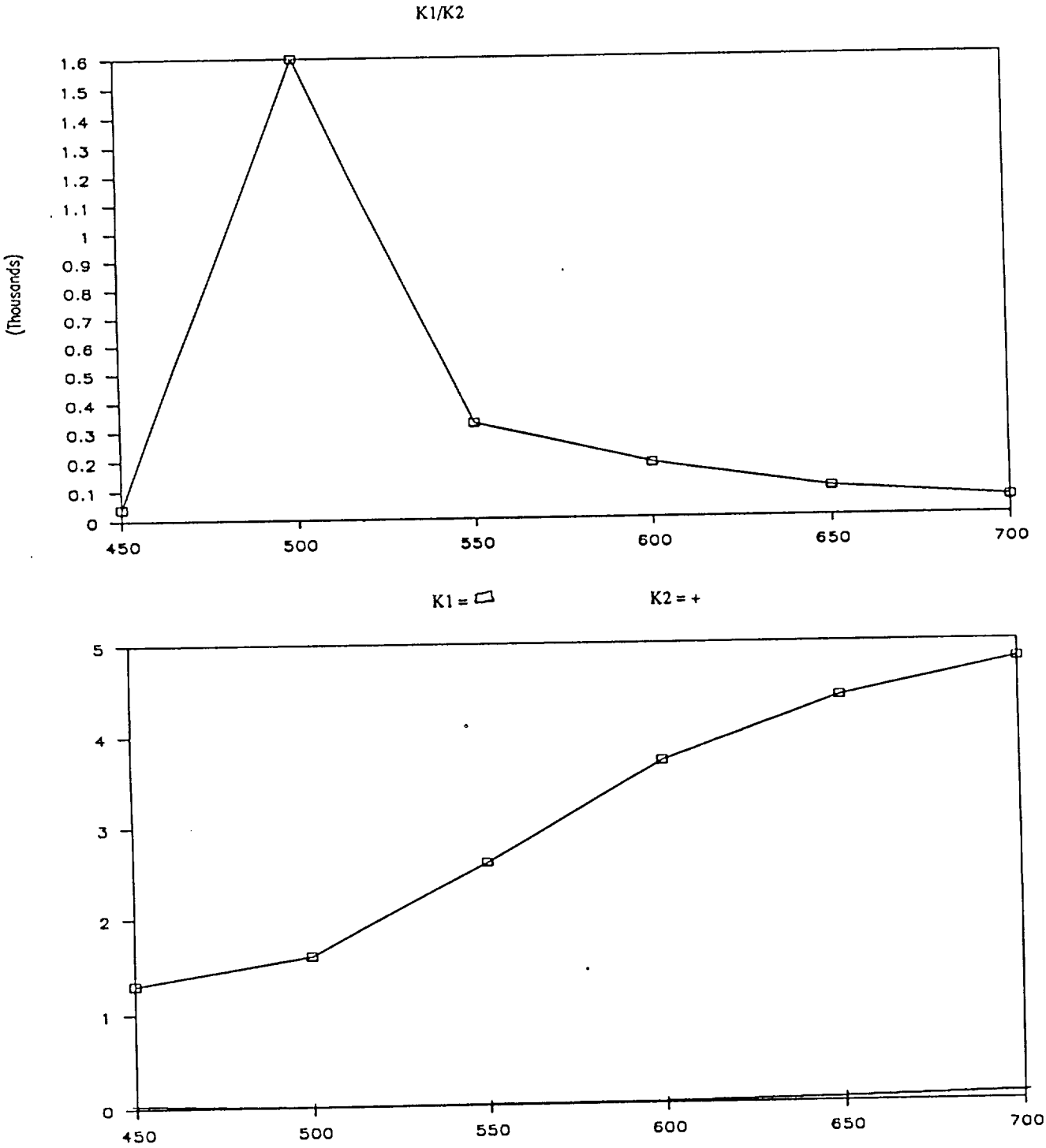

Figure 3.2-3

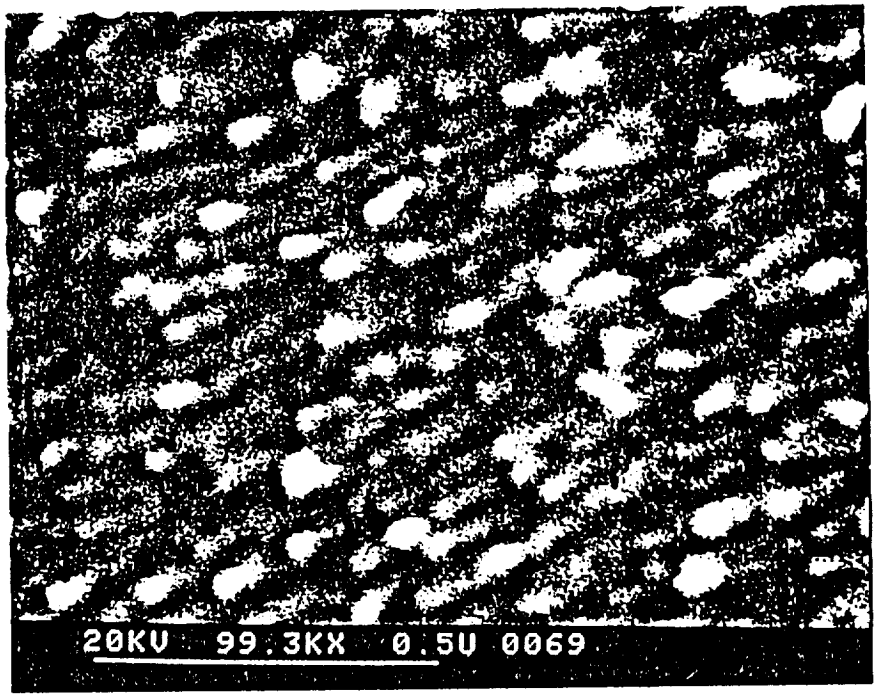

Figure 3.2-4

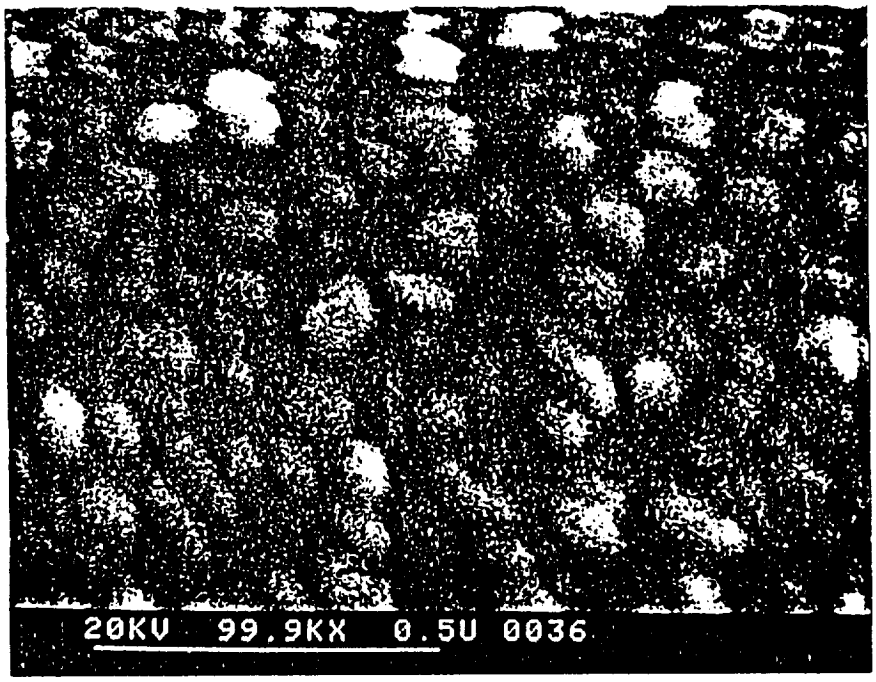

Figure 3.2-5

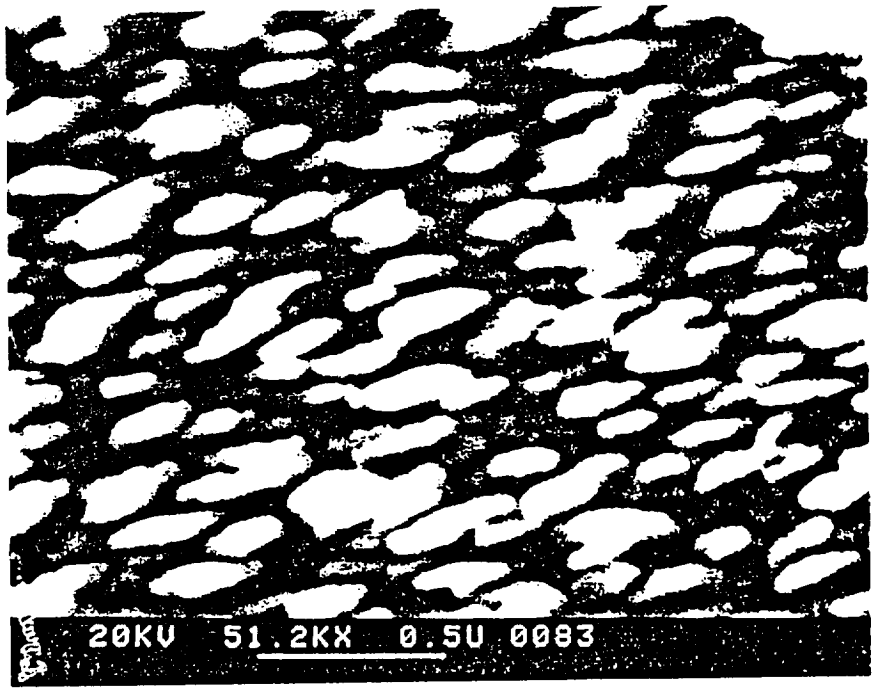

Figure 3.2-6

Polarizer Performance

Figure 3.2-7 dated 09-09-90 give the k_1, k_2, and k_1/k_2 values for the following deposition condition:

Precoat: 2 inches Ag, Tilt (-1)

Heat: Distance 2.5 inches, crucible Variac power 110 VAC, 3 minutes

Ag Deposition: Ag 16 inches, 4 shots, direction orientation alternated 180°, deposition time each 2.5 minutes, crucible Variac power 110 VAC, disc tilt -1.

Figure 3.2-7 shows variation of k_1, k_2, and k_1/k_2 with wavelength. Peak k_1/k_2 of 146 occurs at 600 nm. The values drop both directions from the peaks. The spectral range was 500 to 700 nm. The effect on the k_1, k_2, k_1/k_2 values of the deposition parameters were studied over a wide range, in the search for conditions that would give high k_1/k_2 and k_1 values at 600 nm.

Section 3.3 Materials for Metal Particles

Our technical goal was identification of the metal most likely to form a film with polarization characteristics which meet the filter contrast goal of 10^5 or greater. Our initial theoretical investigations predicted in Section 1 that silver would meet our requirements. It was not necessary to initiate studies of other materials. Our preliminary investigation indicated that gold and lead had strong plasmon resonances which would lead to a polarization effect for spheroidal particles. In addition, we were prepared to investigate films of Al, Cr, Pt, Ta and W at the University of Central Florida. This did not prove necessary since we were able to validate the theoretical predictions for silver. If investigations of other materials had been required, the work would not have been performed at UCF as proposed but would have been mover to another laboratory because of UCF's inability to satisfy their contractual requirements on their proposed electron microscopy tasks.

POLARIZER DATA

Date: 05/15/91 Job Number: 8801 Run Number: 1
Disk: #7

A:	Precoat 2" + 2" Ag	D:	
B:	Heat 3 min at 110	E:	
C:	Tilt (-1)	F:	

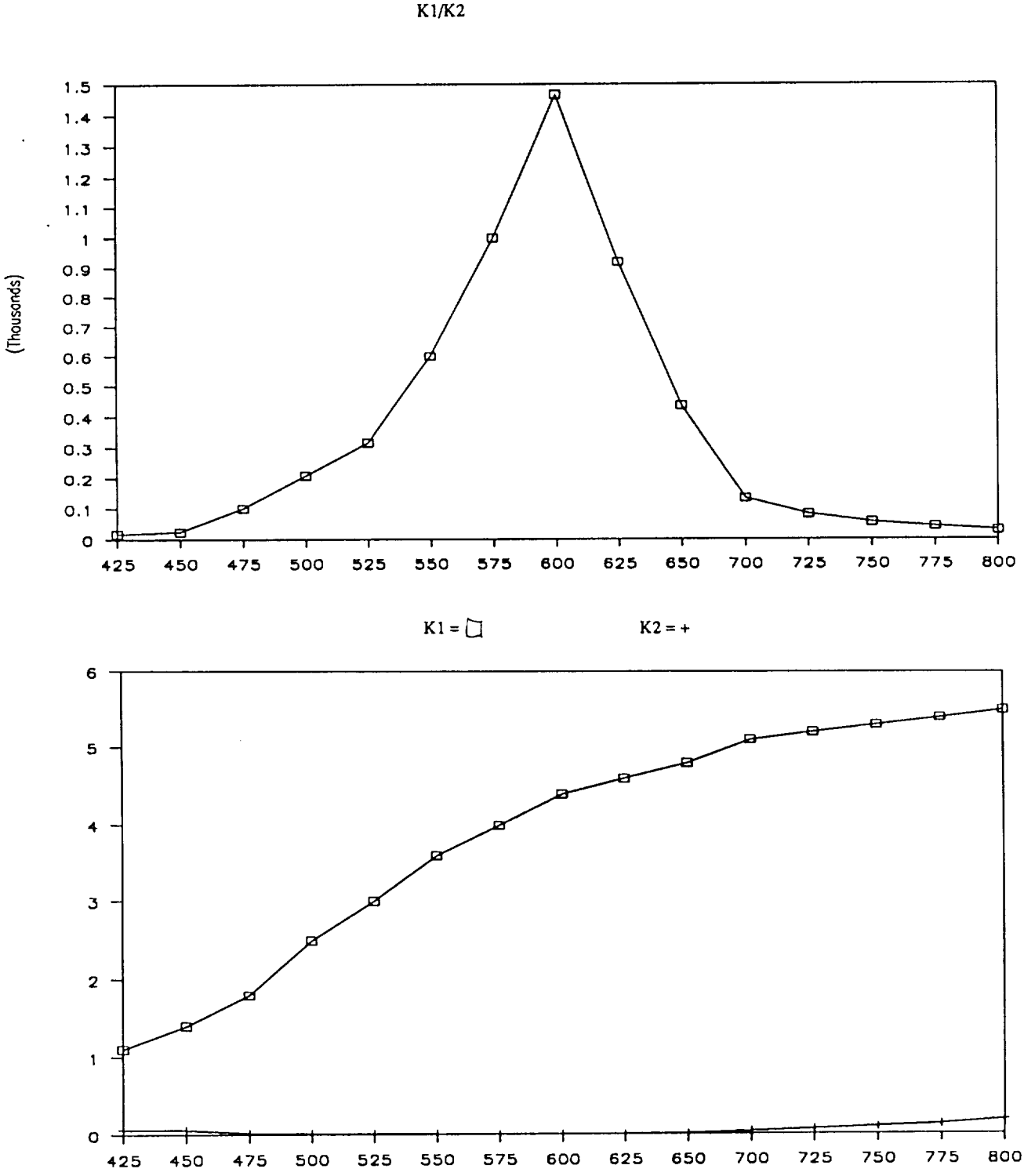

Figure 3.2-7

Section 4 Multilayer Film Methods

In section 4 we report efforts to develop multiple layers of the metal thin film structure composed of silver prolate spheroids. The technical objective can be clearly stated based on the theoretical analysis of Section 1. Three requirements for a high performance polarizer consisting of an array of silver prolate spheroids are:

1. The number of particles in the optical path must be large enough to produce a significant absorption cross-section.

2. The volume of the particles must be small enough to prevent excessive scattering ($d \leq 100$ nm).

3. The spacing between particles must be at least 3 radii of a sphere of equivalent particle volume.

The conceptual design solution is to space the particles at distances which satisfy condition 3. Adjust the particle size to meet condition 2. And finally, add layers to the film until the desired number of particles is achieved to produce effective polarization.

We will report three approaches to spacing the particles by multilayer spacing. The first approach to be described in Section 4.1 proposes the use of a polarizing glass, designated Polacor by Corning, as the substrate. The second approach discussed in Section 4.2, evaluates use of a layer of transparent adhesive between layers of the silver films. The third approach, discussed in Section 4.3, proposes the use of an evaporatively deposited transparent layer to separate metal films. In attempting to experimentally simulate this third approach, an effective technique was developed for depositing multilayer silver films on a single substrate and achieving contrast in excess of 40,000. We will discuss the experiment and the outstanding results.

Section 4.1 Polarizing Substrates

Our first approach to fabricating a multilayer polarizer calls for use of a substrate of polarizing glass manufactured under the trademark Polacor by Corning. The design approach called for aligning the polarization axis of the deposited silver film with the polarization axis of the Polacor substrate. The substrate would be axially aligned with the deposition direction and, therefore, the axis of the silver film. The polarization effect in Polacor glass is produced by silver prolate spheroids disbursed in a glass matrix.

Today commercially available Polacor glass has absorption peaks only in the near-infrared spectral region. Corning agreed to make available two samples of experimental Polacor glass which has a resonance absorption peak near 633 nm. We have evaluated the principle transmittances and contrast of these two Polacor samples which we numbered #15 and #16. In Section 5.1 we report performance results for a multilayer design evaluation using the better Polacor sample with silver film samples. We did not attempt to go beyond this point and deposit silver films directily on the Polacor substrate because we were unable to obtain by purchase Polacor samples peaked near 600 nm in the 25 mm diameter required for our filter design. We were regretfully informed by Corning that no new Polacor glass was available in any size for loan or purchase that peaked in the visible spectral region.

Polacor Polarization Characteristics

Two polarizing glass discs were received from Corning which were numbered #702M37015 and #702M37016. Both were 15 mm in diameter and were designated for use at 633 nm. The principle transmittances and contrast for each disc were measured using the polarizing spectrometer described in Section 2.1 and are shown in Figures 4.1-1 and 4.1-2. Although designated for use at 633 nm, the two filters were found to have contrast of 718 and 942 respectively at 590.

POLARIZER DATA

Date: 07/18/90 Job Number: 8801 Run Number: 1
Disk: #

A:	Corning #702M37015	D:	
	G.T.P.		
B:	Silicone detector	E:	
C:		F:	

K1/K2

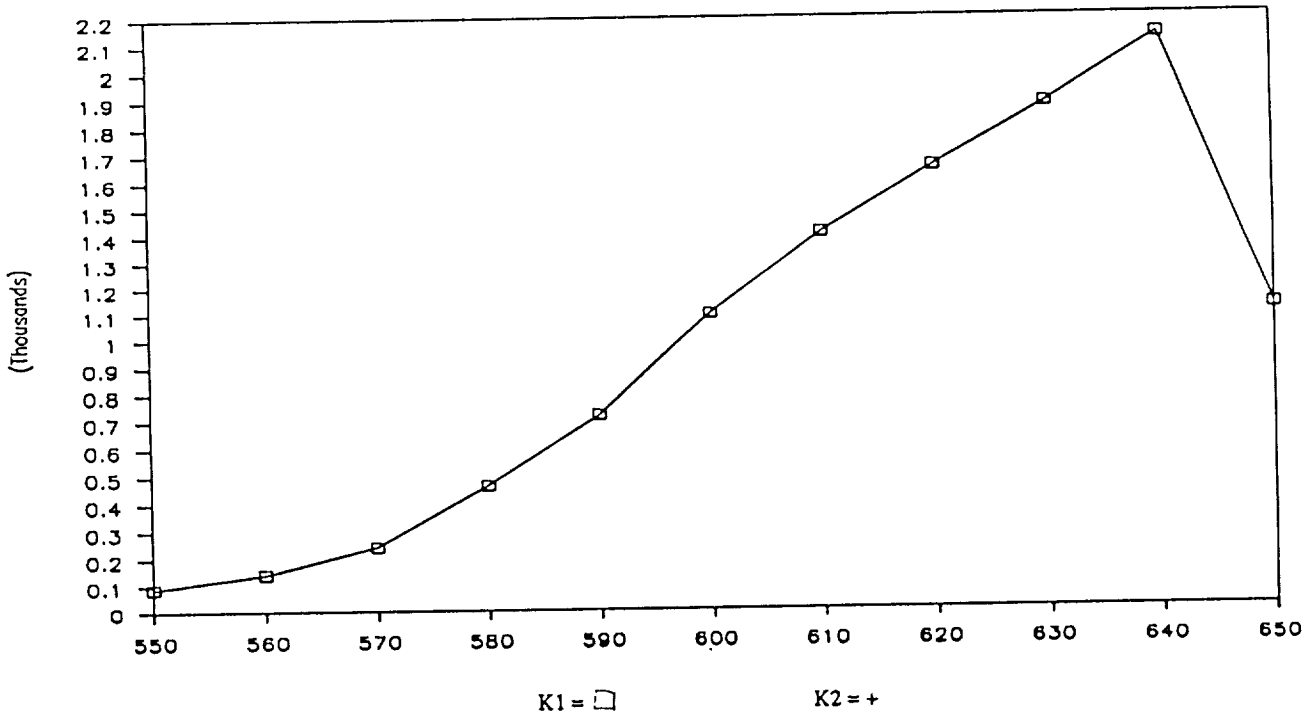

K1 = □ K2 = +

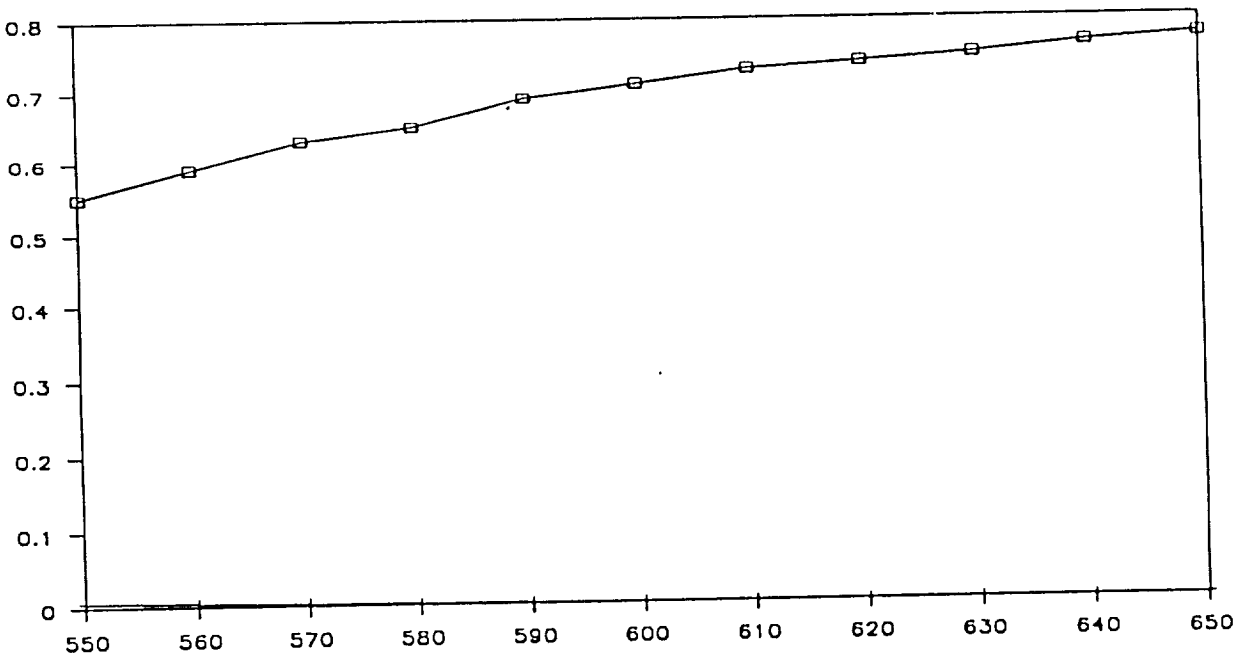

Figure 4.1-1

 Q-2

POLARIZER DATA

Date: 07/18/90 Job Number: 8801 Run Number: 1
Disk: #

A:	Corning #702M37016	D:	
	G.T.P.		
B:	Silicone detector	E:	
C:		F:	

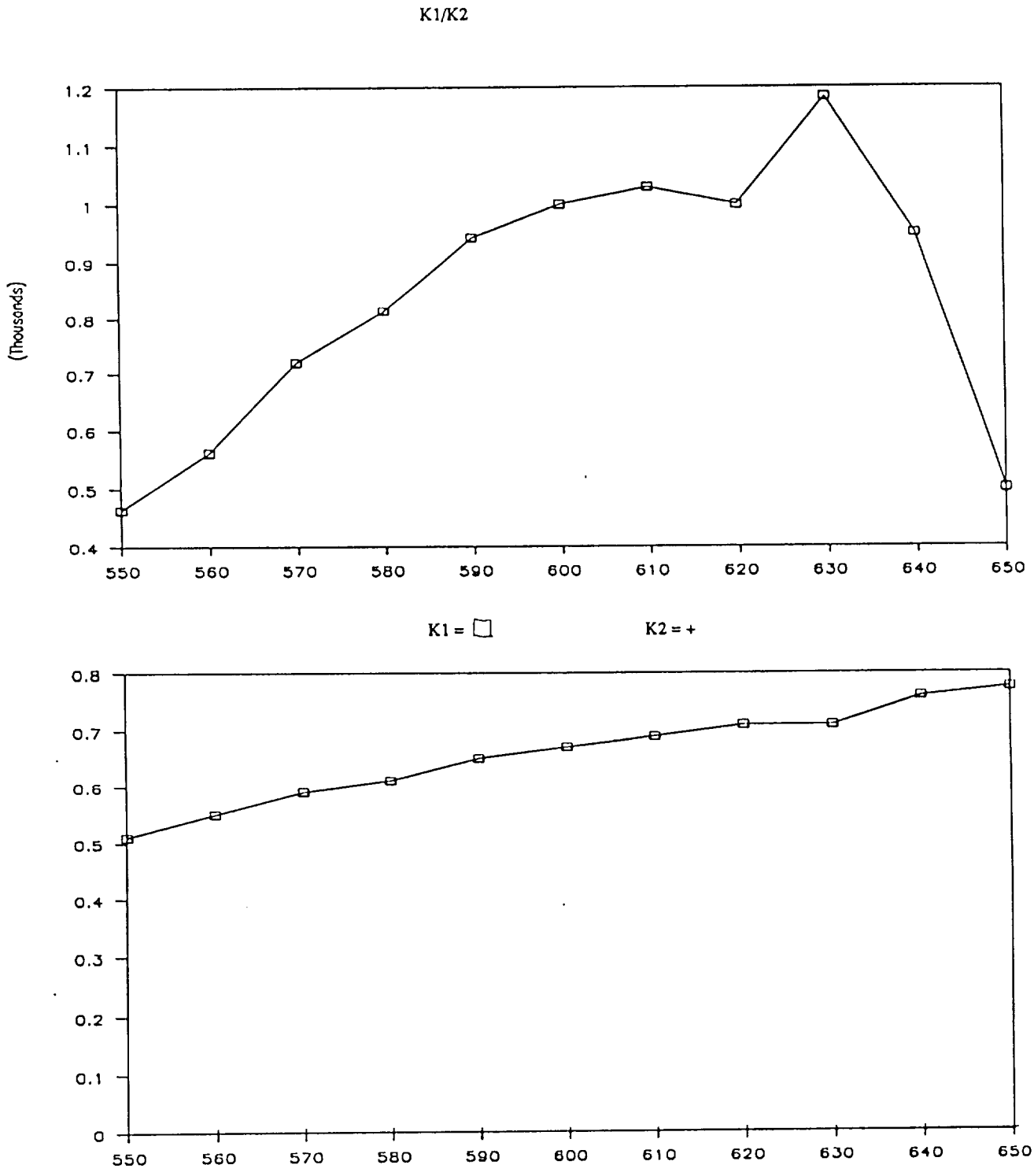

Figure 4.1-2

Section 4.2 Chemical Bonding

One approach to achieving the high density of particles required for high contrast is separation of multiple silver films with a transparent chemical adhesive. As demonstrated in Section 1, the resonance absorption peak for a particle in air (refractive index $N_0 = 1.0$) is shifted by a factor of N_0/N_2 where N_2 is the refractive index of the second higher index medium. The design implication is that the b/a ratio for a material with refractive index 1.5 must be twice that for refractive index 1.0 when the absorption peak is at 600 nm. We were able to demonstrate the bonding with two discs, one coated with a silver film which has a resonance absorption peak near 600 nm and the other a plain disc. The Norlin Optical Cement used as an adhesive has a refractive index of 1.5. The design concept calls for depositing a silver polarizing film on a transparent substrate, covering the film with a higher index transparent optical coating, and depositing a second silver film on the flat surface of the transparent surface, and repeating the process until a number of silver films are deposited sufficient to achieve the desired density of silver particles. This process requires that the transparent chemical adhesive be formed into an optically flat layer. Two experimental methods were evaluated for producing a flat layer of adhesive.

First, an adhesive was spread on a glass disc coated with a light layer of Teflon. The disc was pressed against the silver film and UV cured. It was difficult to separate the disc without fracturing the discs. However, patches of adhesive coated silver film were observed which indicates that this "lift off" method has promise. In the second approach the adhesive was spread on a smooth disc of Teflon material, pressed against a silver film and UV cured. Again the lift off was patchy, but good areas could be observed. If Teflon surfaces polished to optical flatness were used, the method probably would work.

The effect of the high refractive index adhesive can be observed by measuring the principle transmittances and contrast of silver film, bonding a clear disc to the film, and remeasuring. An example of a near-infrared polarizing film is shown in Figure 4.2-1. By cementing a clear disc to the film with an adhesive having a refractive index of 1.5, the point of peak contrast is shifted form 900 nm to 1350 nm as shown in Figure 4.2-2. The effect of directly bonding two films

POLARIZER DATA

Date: 07/18/90 Job Number: 8801 Run Number: 1
Disk Number: 10

A: Special RES Run	D:
B:	E:
C:	F:

K1/K2

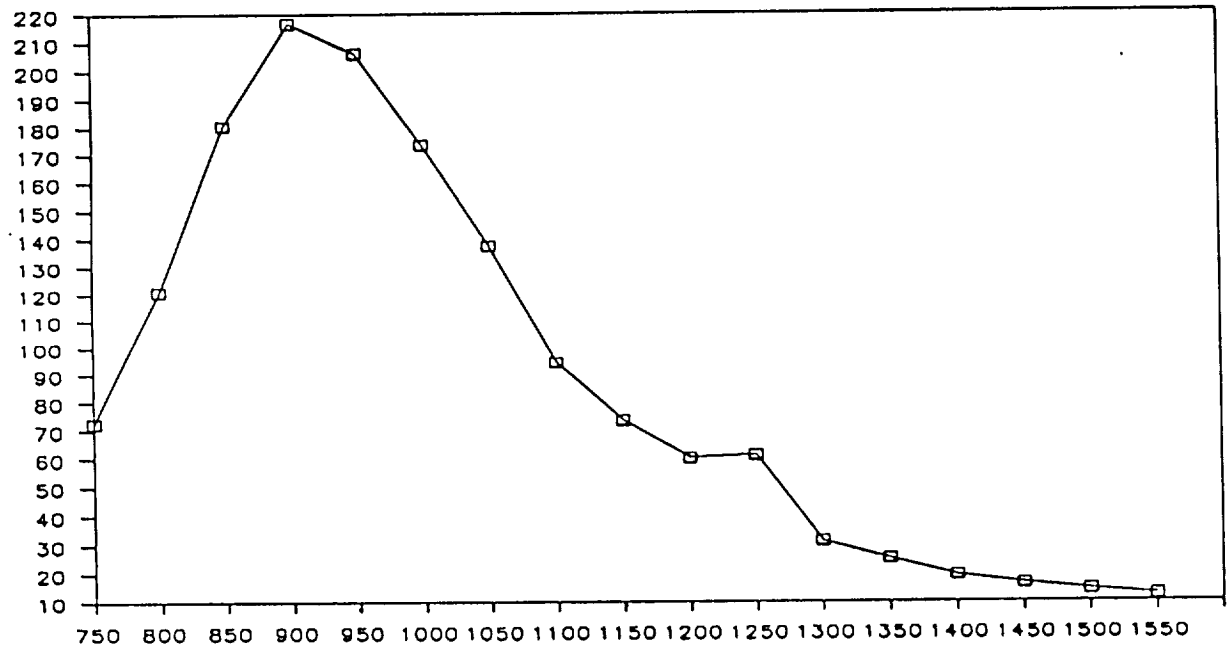

K1 = □ K2 = +

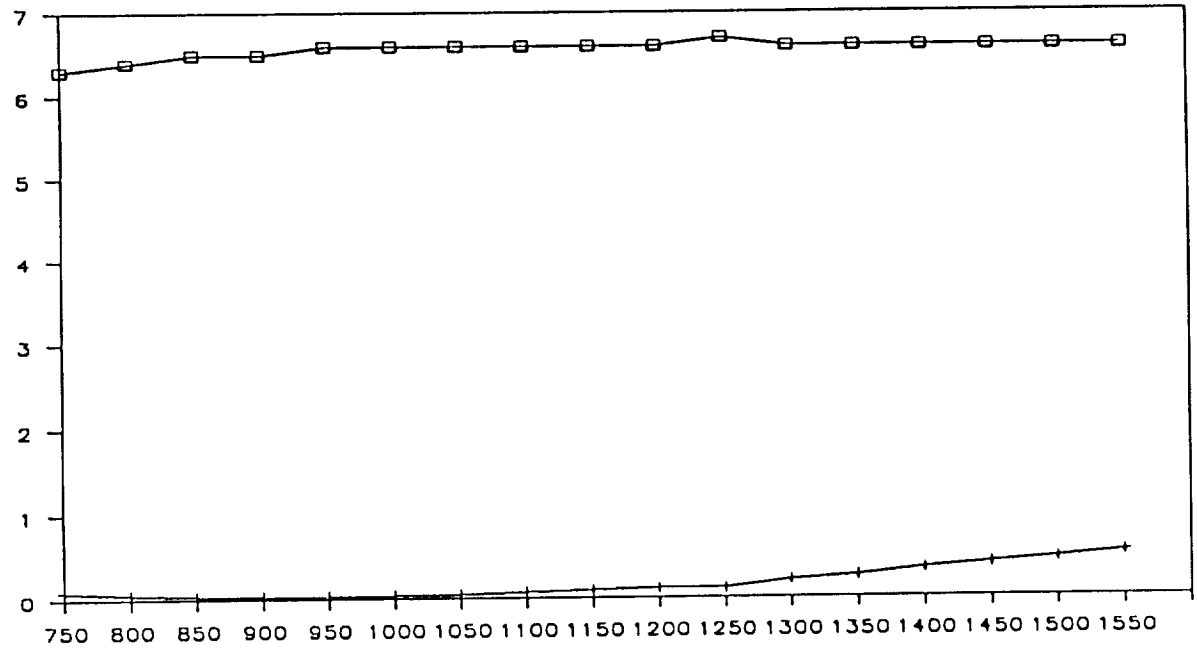

Figure 4.2-1

POLARIZER DATA

Date: 07/18/90 — Job Number: 8801 — Run Number: 2
Disk Number: 10

A: Special RES run	D:
B: #10 bonded to plalin disk (UV)	E:
C:	F:

K1/K2

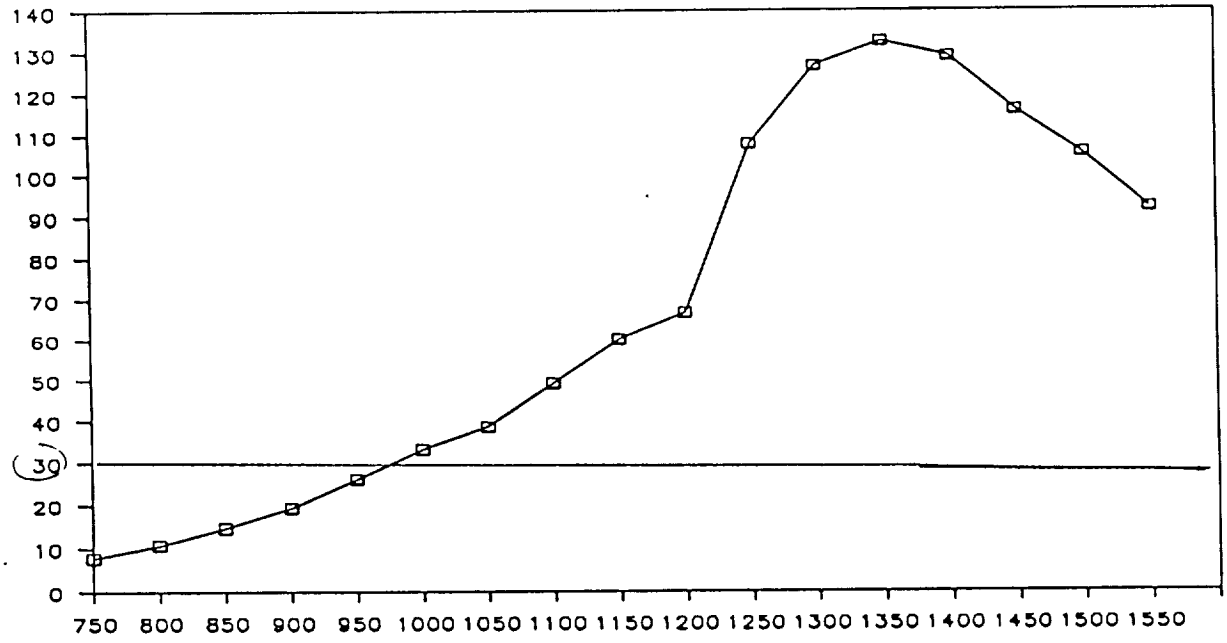

K1 = □ K2 = +

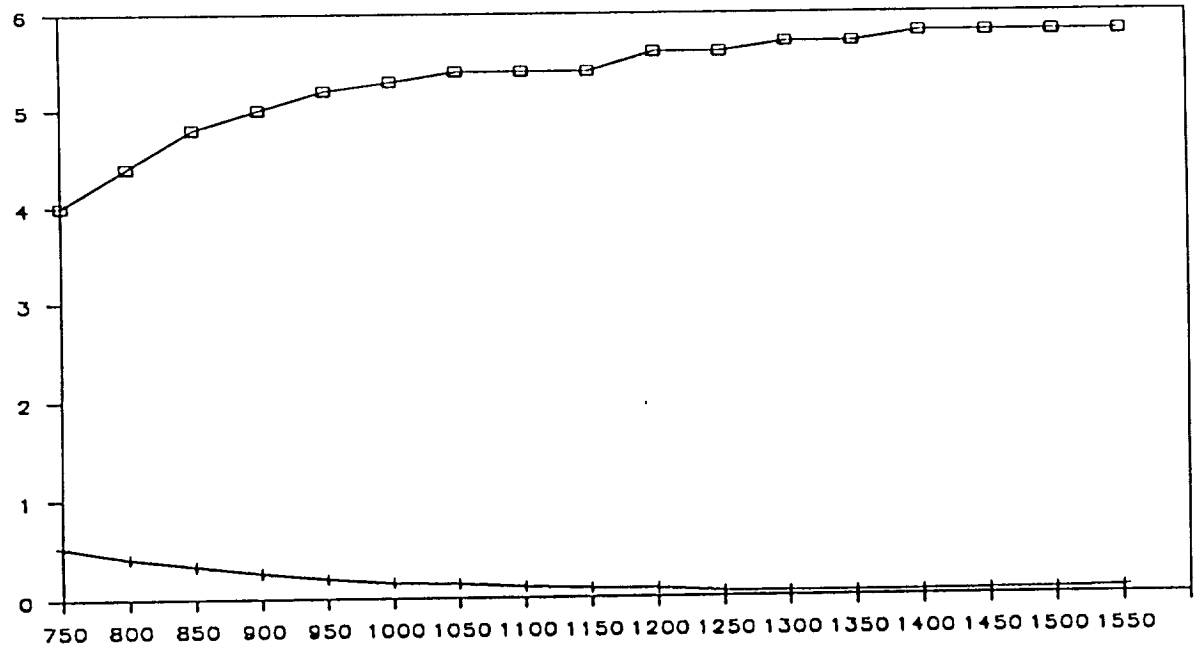

Figure 4.2-2

with resonance peaks in the visible region can be illustrated using two films whose optical characteristics are shown in Figure 4.2-3 and Figure 4.2-4. The resulting optical characteristics are shown in Figure 4.2-5.

It can be concluded that there is a good probability that multilayer films can be fabricated using chemical adhesive/lift off techniques. A key technical issue is formation of films composed of particles whose resonance absorption peaks at 600 nm when immersed in a material with refractive index 1.5.

Section 4.3 Evaporatively Deposited Bonding Layer

This approach to multilayer films calls for depositing a silver film on a glass substrate and over-coating the metal film with a layer of smooth, evaporatively deposited transparent material such as MgF_2 or SiO_2. A second layer of metal would be applied on the surface of the transparent layer. This process would continue until the desired density of metal particles is achieved. A number of attempts were made to over coat a polarizing silver film with SiO_2. We were unable to gain control of the temperature and deposition rate, and the results were inconclusive. Refinement of this method is a key technical object for the fabrication of robust, durable silver film polarizers.

A simple evaluation of the layer spacing concept resulted in a significant improvement in film fabrication for 600 nm light. At the end of the program the deposition process has evolved to the concept of a film consisting of eight 4 inch segments of Ag deposited on an annealed precoat of two 2 inch Ag segments. Transmittances and contrast for a typical film is shown in Figure 4.3-1. Polarization at 600 nm is 2933. In order to demonstrate the concept of a high index separation layer, we applied an annealed precoat to both sides of a single BK-7 glass blank and applied four 4 inch segments to each side of a disc. The results, shown in Figure 4.3-2, indicate a peak contrast of 11,250 at 650 nm on a single disc and a contrast of 9750 at 600 nm. This represents the "best effort" of the program for a single disc and indicates the potential of separating particles with high index layers as spacing.

POLARIZER DATA

Date: 08/09/90 Job Number: 8801 Run Number: 1
Disk: #4

A:	3.5" Ag - 6 shots	D:	
B:	2.5 Minutes at 110	E:	
C:	Tilt -0-	F:	

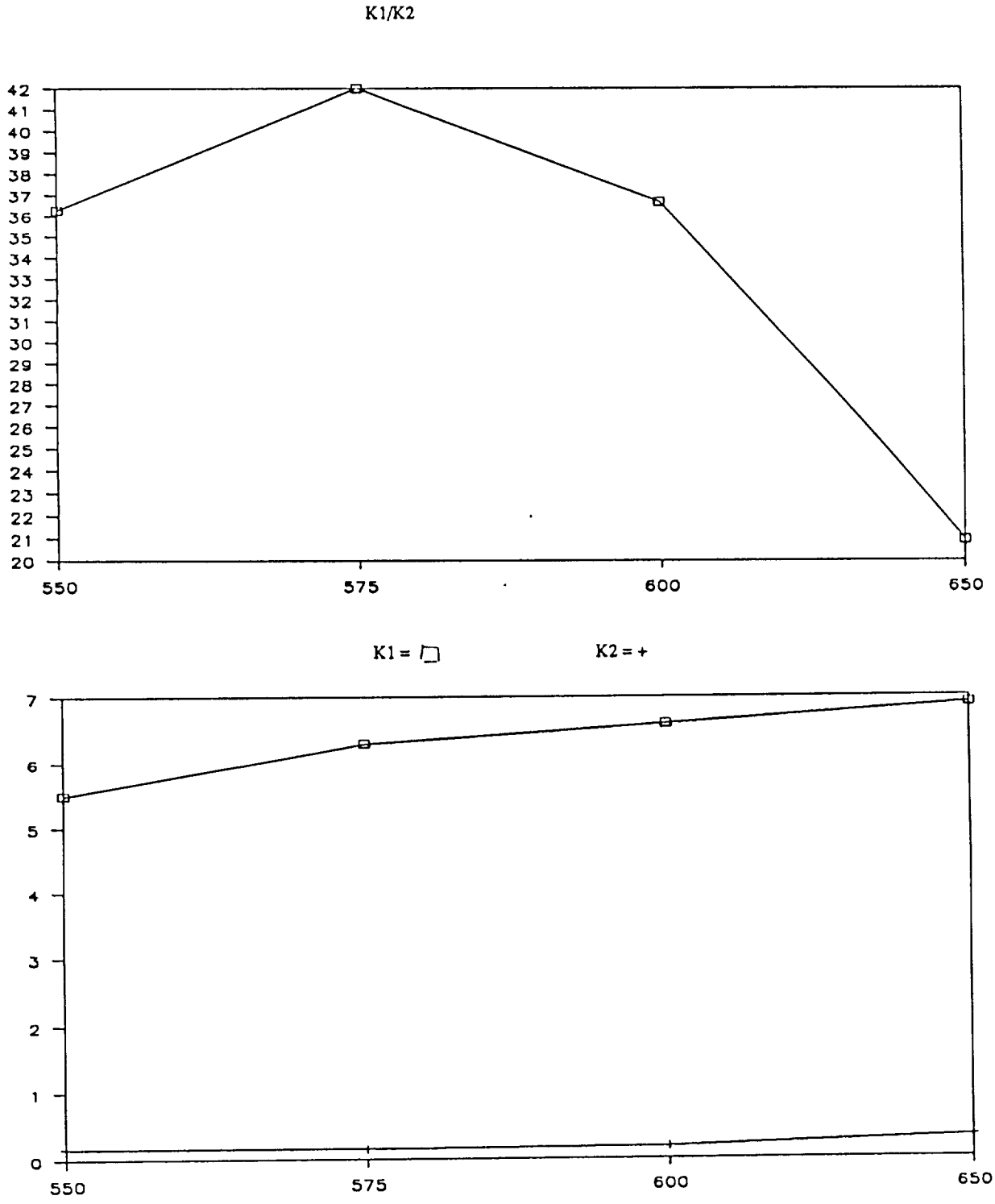

Figure 4.2-3

POLARIZER DATA

Date: 08/09/90 Job Number: 8801 Run Number: 1
Disk: #5

A:	3.5" Ag - 6 shots	D:	
B:	2.5 Minutes at 110	E:	
C:	Tilt -0-	F:	

K1/K2

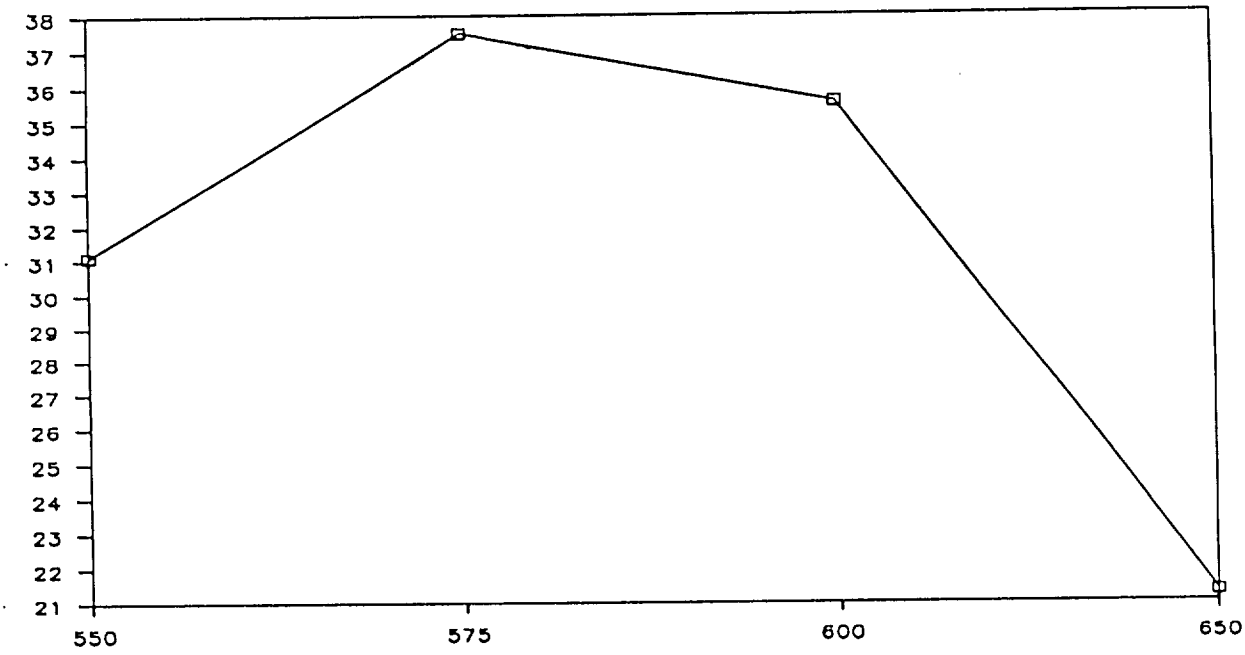

K1 = □ K2 = +

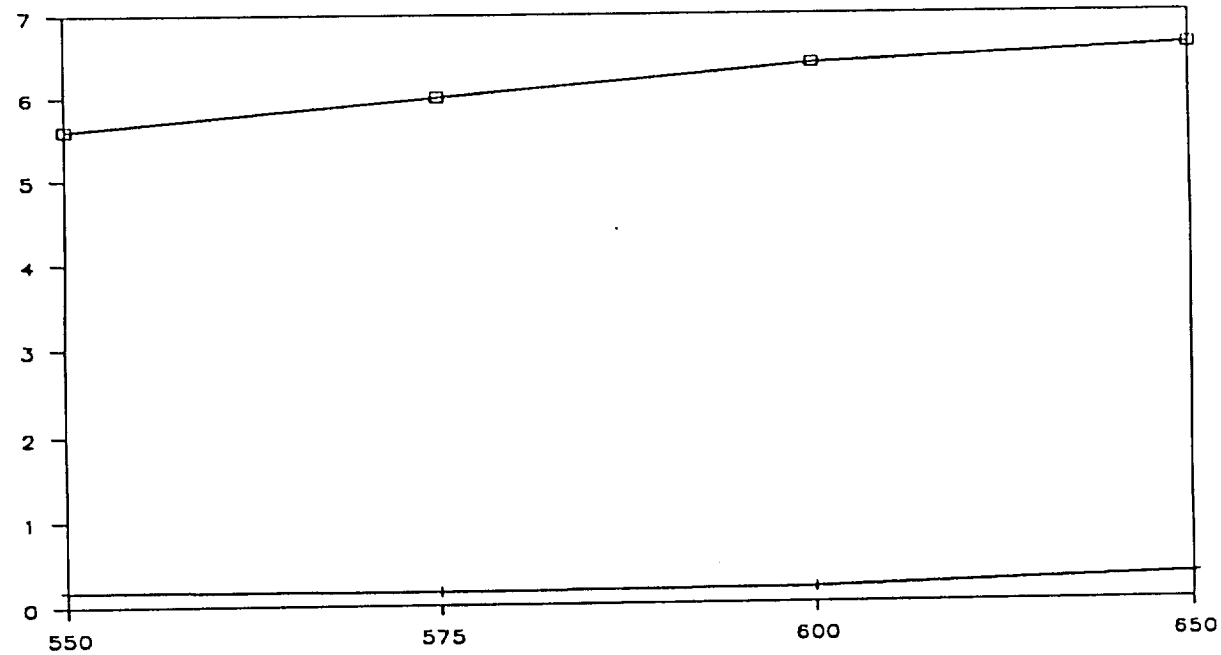

Figure 4.2-4

POLARIZER DATA

Date: 08/09/90 Job Number: 8801 Run Number: 1
Disk: #4 & 5

A:	3.5" Ag - 6 shots	D:	
B:	2.5 minutes at 110	E:	
C:	Tilt -0-	F:	

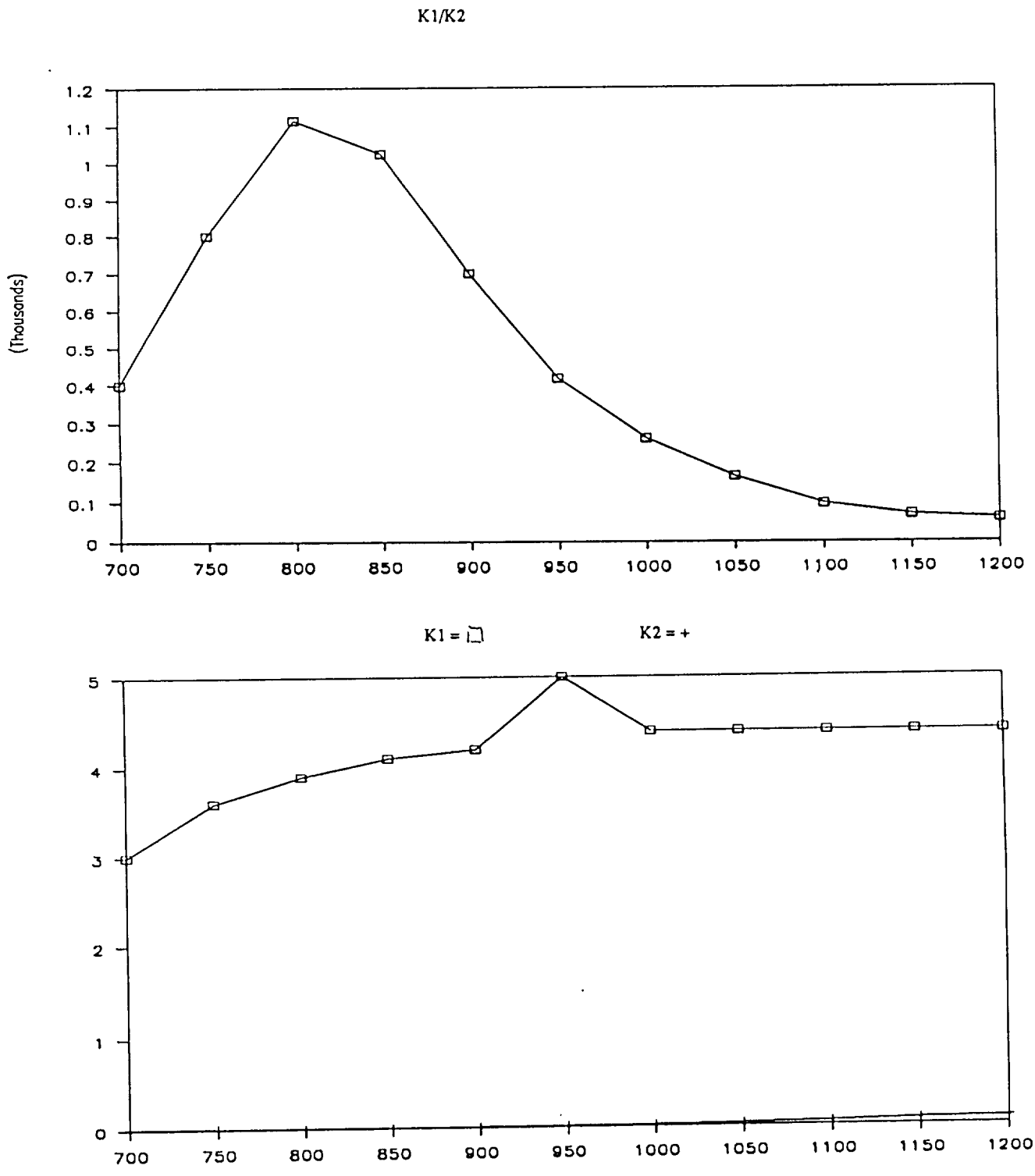

Figure 4.2-5

POLARIZER DATA

Date: 02/18/91 Job Number: 8801 Run Number: 1
Disk: #7

A: 4" Ag - 8 shots	D:
B: 2.5 Minutes at 110	E:
C:	F:

K1/K2

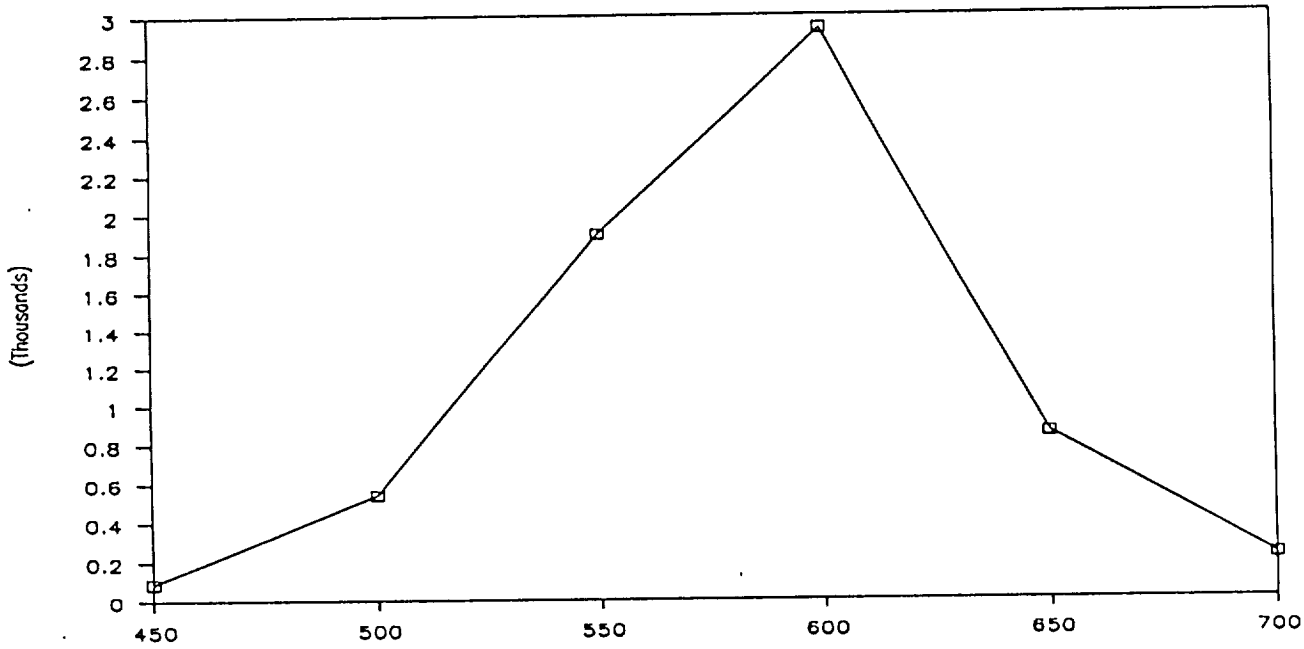

K1 = □ K2 = +

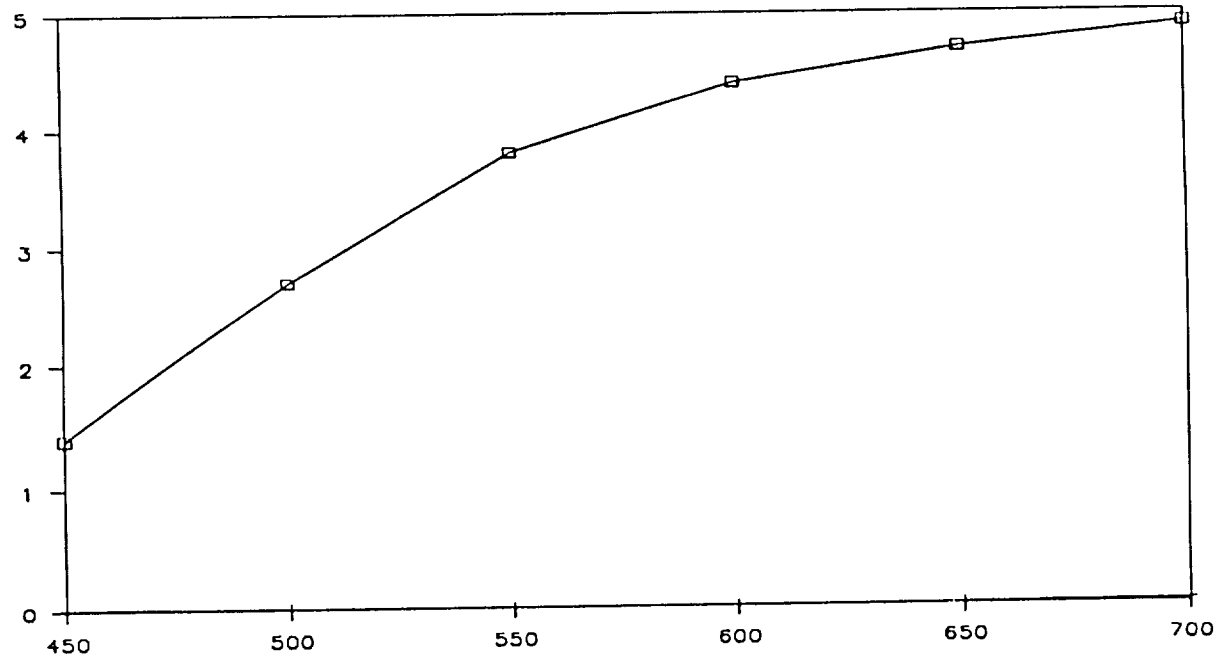

Figure 4.3-1

POLARIZER DATA

Date: 03/07/91 Job Number: 8801 Run Number: 1
Disk: #1

A:	2" x 2" Precoat	D:	Tilt (-1)
	2.5 min at 110		
B:	4" x 4 each side	E:	
C:	Heat 3 minutes at 110	F:	

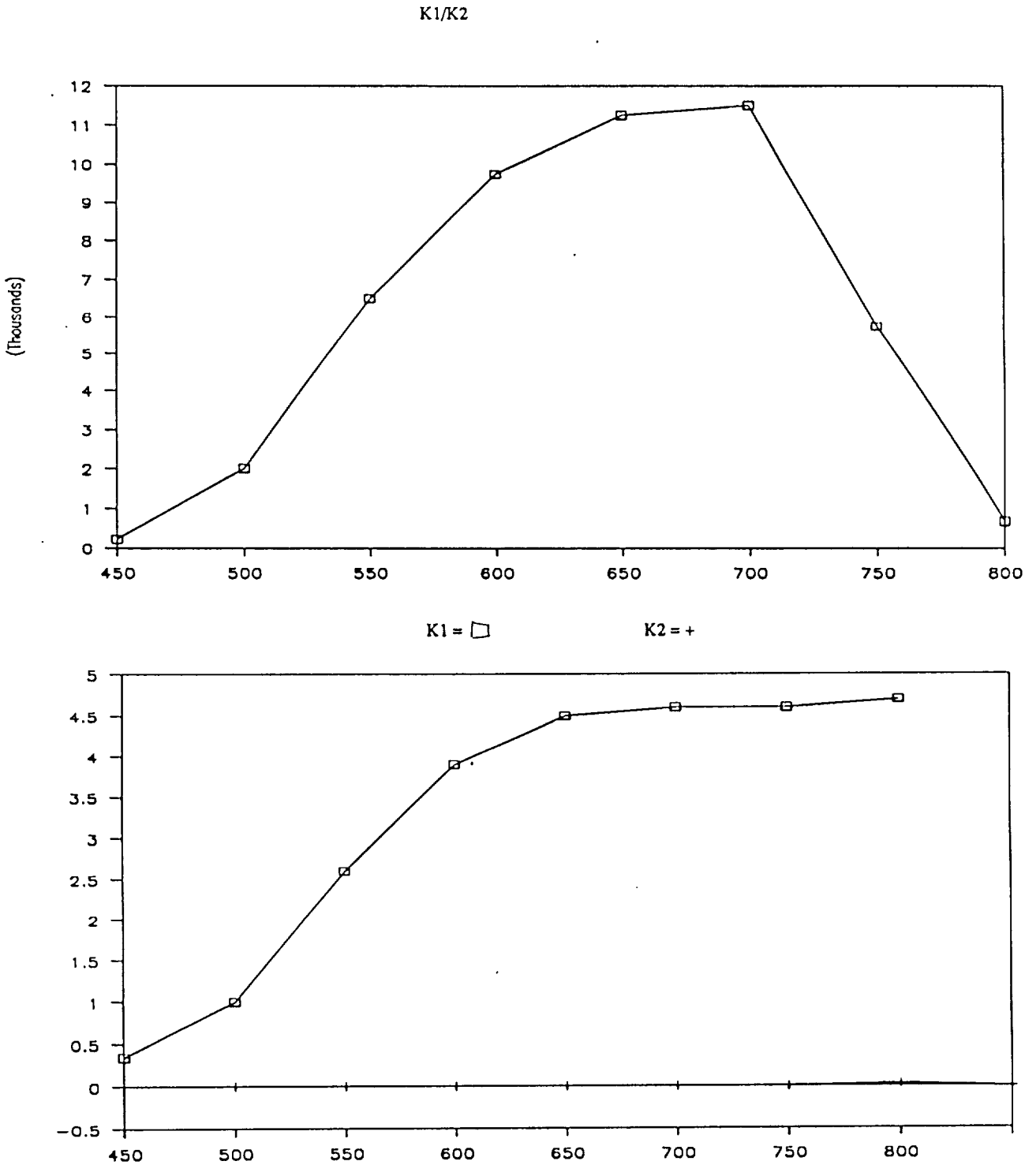

Figure 4.3-2

Section 5 Fabrication of Polarizing Filters

The technical objective of Task 5 was evaluation of the thin film polarizer technology as it developed throughout the program. This was to be accomplished by fabrication of a "best effort" thin film polarizer at six month intervals over the 24 month program. Since technical advances could not be scheduled, we report here the more significant polarizer fabrications and evaluations which took place immediately following the availability of an improved thin film technology or component. We will describe the performance of polarizers at 594 nm determined with the test apparatus described in Section 2.3. In Section 5.1, the performance results for a multilayer polarizer concept using polarizing glass substrates will be described. In Section 5.2, the performance of the best polarizer components using all multilayer silver films will be described. Because of the success with silver films, no other metals for polarizing metal films were considered for polarizer fabrication.

Finally, the design, assembly and evaluation of two "best effort" polarizing filters are described in Section 5.4. Two units were assembled in a filter package and achieved contrast of 10^5 at 594 nm. These filters use two multilayer silver polarizing discs to achieve this value. There two filters will be delivered to JPL with the Final Report.

Section 5.1 Polarizing Glass Substrate Polarizer

The technical goal of Section 5.1 was evaluation of a "hybrid" polarizer composed of a polarizing glass filter supplied by Corning and silver film polarizer developed at Polatomic. The design concept was to utilize the Polacor disc, described in Section 4.1, as a substrate for silver film deposition. Unfortunately this was not possible since Corning supplied only two small samples for evaluation, but no further samplers of polarizing glass for 589 nm was made available for purchase or evaluation. We were able to evaluate several combinations of Polacor glass/silver film elements using the laser polarization checker described in Section 2.3 and validate the design concept. The optical bench holders were used to place the polarizing optical elements in series and

rotate the parts to optimum orientation. Contrast in excess of 200,000 were obtained with one of these hybrid combinations.

COMPONENTS

A. Corning #15 polarizer disc (Polacor)

B. Silver film discs in set # 01-31-91 (Single side deposition)

1. Fabrication

a.) Precoat deposit: Ag 2 in. + 2 in. counter deposited at 2 1/2 minutes with heater Variac at 110 VAC, Tilt -1.

b.) Precoated discs heated in vacuum by placing discs in holder 2 1/2 inches from graphite crucible heated for 3 minutes with heater Variac at 110 VAC.

c.) Ag deposit, 2 1/2 minutes at crucible Variac at 108 VAC. Deposits were alternated in direction incident on disc by disc rotation of 180°.

Ag (inches) =

3 1/2 + 3 1/2 + 4 1/2 + 4 1/2 + 3 1/2 + 3 1/2 + 4 1/2 + 4 1/2

for discs 1-4 tilt was -1/2
for discs 5-9 tilt was -1
for discs 10-14 tilt was 0.

d.) All coatings deposited on one side of disc

Polarizer Measurements

1. Corning #15

I_0	k_1	k_2	k_1/k_2
100	68	0.034	2000

2. Disc: 01-31-91 #14

Light enters glass side

100	48	.058	828

Light enters Ag side

100	48	.054	889

3. Disc: 01-31-91 #13

Light enters glass side

100	48	.048	1000

Light enters Ag side

100	48	.038	1263

4. Disc: 01-31-91 (#13+#14)

100	22	.0017	12,941

5. Corning 15 + 01-31-91 (#13+#14)

100	16	.00009	178,000

6. Disc: 01-31-91 #6, light enters Ag side

100	40	.0048	8333

7. Corning #15 + 01-31-91 #6

100	28	.00024	116,700

8. #01-31-91 #4

100	39	.0039	10,000

9. Corning #15 + 01-31-91 #6 + 01-31-91 #4

100	10.2	.00004	255,000

Section 5.2 Advanced Multilayer Polarizing Filter

The technical goal of Section 5.2 was evaluation of a polarizer design consisting exclusively of silver film polarizing discs. We selected the best results for the case where silver films were applied to a single side of the glass discs and the case where silver films were applied to both sides of the glass discs. The laser polarization checker was used to position the discs and orient them for optimum performance. Using silver films exclusively, we were able to achieve contrast in excess of 135,000.

COMPONENTS

A. Silver Film Discs in Set #03-07-91 (double side deposition)

The objective was to deposit the polarizing film on both sides of a single disc. This permitted the Ag material to be separated by glass having a refractive index of 1.5 instead of 1.0 that of air.

The Ag deposition on each side was as follows:

a.) Ag precoat

Ag: 2 in. + 2 in. with crucible Variac at 110 Vac for 2 1/2 minutes

b.) Pre-heat

After both sides were coated with 2 + 2 inch Ag, discs were heated for 3 minutes in vacuum by crucible heated with Variac at 110 VAC.

c.) Ag deposit

Each side was coated with 4 inches Ag for 4 shots. Disc was rotated 180° between shots.

Polarization Measurement

1. Disc 03-07-91 #1

I_0	k_1	k_2	k_1/k_2
100	39.5	0.00066	59,800

2. Corning #15 + 03-07-91 #1

100	27	.00008	337,500

3. Disc 03-07-91 #2

100	42	.001	42,000

4. Disc 03-07-91 #4

100	38.2	.00096	39,800

5. Disc 03-07-91 #4 + 03-07-91 #2

100	16	.000149	107,400

Note that k_1/k_2 = 107,400 was achieved only with the two 03-07-91 Polatomic discs.

B. Silver film discs set #03-14-91 (single side deposition)

Discs coated with Ag on both sides presented handling problems during fabrication. The objective for these discs was to deposit the Ag on one side only and then bonding the two discs with Norland Optical Adhesive (U.V. #61) thereby eliminating the reflection from two surfaces.

a.) Precoat: Ag: 2 in + 2 in on one side
b.) Heat: 3 min at 110 VAC
c.) Ag coat: Ag: 4 in two shots in reverse order

Polarization Measurements

#03-14-91 (#11 + #12) U.V. Bonded

I_0	k_1	k_2	k_1/k_2
100	56	.15	373

#03-14-91 (#2 + #8) U.V. Bonded

100	48	.15	320

#03-14-91: (#2+#8 U.V.Bonded)+(#11+#12 U.V. Bonded)

100	27	.0003	90,000

The $k_1/k_2 > 100{,}000$ was not reached.

C. Silver film disc Set #03-12-91 (single side deposition)

1.) Precoat: Ag 2 in + 2 in one side

2.) Heated 3 minutes at 110 VAC

3.) Coated one side: Ag: 4 in long strip, deposited 8 times in alternate direction by rotating discs 180° between shots.

4.) Polarization Measurements:

03-12-91 #4

100	31	.00095	32,600

03-12-91 #4 + 03-14-91 (#11+#12 U.V. Bonded)

100	19	.00014	135,700

Note that only three silver film discs were used to give $k_1/k_2 = 135{,}700$.

Section 5.3 Advanced Concepts Polarizing Filter

In the event that silver films were unable to achieve the required polarization performance, other types of metal thin films were to be investigated under the Phase II plan. Because of the success achieved with silver films at 590 nm, our technical effort was concentrated on silver and no other materials were required to achieve the contrast goal of 10^5.

Section 5.4 State-of-the-Art Metal Thin Film Polarizers

The technical objective of this section is demonstration of the silver film polarizer design and fabrication technology for fabricating and assembling two polarizing filters. These two filters will be delivered to JPL for inspection along with the Final Report. This step required design and fabrication of a unit to hold the individual discs and permit alignment of the discs. The discs were difficult to align and mount in the holder, however contrast of 100,000 and 97,000 were achieved with the final filters.

A new set of discs were fabricated for the final assembly. The deposition conditions were:

Precoat: Ag 2 inches two shots in alternate directions. Discs were coated on both sides.

Heat: Discs were heated in the vacuum at a distance of 2.5 inches from the crucible (heated by 110 VAC).

Silver Deposits: 4 inches of Ag strip shot 4 times in alternate directions were deposited in each side of the disc. 14 discs were prepared. The k_1/k_2 ratio is 5000 or better on the discs in this set.

Disc holder

Two discs were used per polarizer. Each disc (1 inch OD) is bonded into a lipped ring with Norland Optical Adhesive (UV 61). The outer edge of the disc is wiped to remove the silver at a distance of 1/8 inch on the radius. This prevents the bonding fluid from creeping and destroying the silver performance. An outer holder is black anodized aluminum having an inside diameter large enough to hold the ring with the polarizer disc. An axial section of the holder is illustrated in Figure 5.4-1.

A ring-mounted polarizer is placed on one side of the partition ring in the disc holder. The ring is bonded to the holder with 24 hour curing Epoxy. The disc

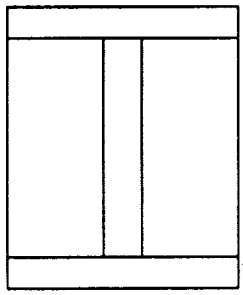

Figure 5.4-1 Disc Holder Cross-section

holder is clamped into the mount which is a part of the laser polarizer measuring system described in Section 2.3. The disc holder is rotated to the correct k_2 orientation. The second disc with polarizer is mounted into the other half of the disc holder, and again bonded loosely with the 24 hour curing Epoxy. Notches were made on the disc to permit its rotation with respect to the disc in the first half of the holder to give the lowest k_2 reading obtainable. This k_2 reading was obtained as well as the k_1 reading. If the k_1/k_2 was less than 100,000 the disc were replaced with another set until a k_1/k_2 reading approached 100,000. This was the most difficult and sensitive step in the polarizing filter assembly. It was observed that the silver particles did produce crosspolarization scattering. The detector was located 1m from the filter in order to eliminate this effect. Reduction in particle size would reduce scattering to a negligible level, however this improvement was beyond the scope of the present program.

When the polarization ratio remained constant over a few days, the assembly was completed. The completion step was to seal both halves of the disc holder with metal mounted antireflective coated glass disc using epoxy.

Polarization Measurement

Two polarizing filters were assembled. Their polarization values were:

Filter	k_1	k_2	k_1/k_2
#1	22	.00022	100,000
#2	29	.00030	97,000

These two filters will be delivered to JPL with the final report. A final measurement was made of the variation of transmittances with wavelength. The polarizing spectrophotometer described in Section 2.1 was used for the measurements. The variation of contrast with wavelength is shown in Figure 5.4-2 for silver film filter #1.

POLARIZER DATA

Date: 05/15/91 Job Number: 8801 Run Number: 1
Disk: #1 Assembly

A:	D:
B:	E:
C:	F:

K1/K2

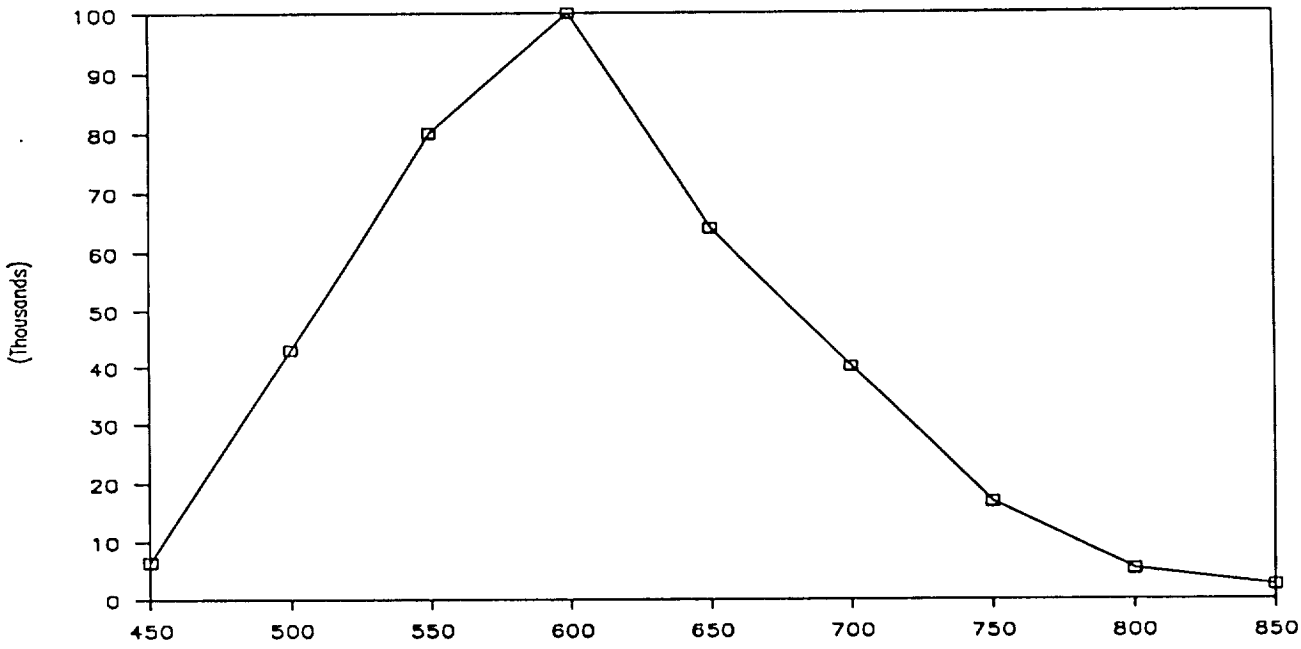

Figure 5.4-2 Dependence of contrast on wavelength for silver film filter #1.

Having achieved a contrast of 10^5, future polarizing filters could achieve even higher contrast and larger k_1 if the following improvements were incorporated. First, experience with assembly of the filter unit would lead to improved methods for adjusting the orientation of films for optimum performance inside in the final package. Second, smaller particles would reduce scattering. Examination of a SEM micrograph of the film indicates that particle density is approximately 50 per square micron with half of these in the equivalent diameter range between 150 nm and 300 nm. A goal would be to increase density and reduce volume.

REFERENCES

Abushagur, M. A. G., (1984), Nicholas George; Polarization and Wavelength Effects On The Scattering from Dielectric Cylinders; Applied Optics; Vol. 24, No. 23, Page 4141

Allara, D. L., (1982) A. F. Hebard, F. J. Padden, R. G. Nuzzo, D. R. Falcone; Chemically Induced Enhancement of Nucleation in Noble Metal Deposition; J. Vac. Science Technol., Vol. 1, No. 2, Page 376

Bennett, H. E., (1969), R. L. Peck, D. K. Burge and J. M. Bennett; Formation and Growth of Tarnish on Evaporated Silver Films; Journal of Applied Physics; Vol. 40, No. 8, Page 3351

Bennett, Jean M., (1985), H. H. Hurt, J. P. Rahn, J. M. Elson, K. H. Guenther, M. Rasigni and F. Varnier; Relation Between Optical Scattering, Microstructure and Topography of Thin Silver Films; Applied Optics; Vol. 24, No. 16, Page 2701

Bergman, J. G., (1981), D. S. Chemla, P. F. Liao, A. M. Glass, A. Pinczuk, R. M. Hart, and D. H. Olson; Relationship between Surface-enhanced Raman Scattering and The Dielectric Properties of Aggregated Silver Films; Optical Society of America; Vol. 6, No. 1, Page 33

Bird, G. R. (1971), M. Morse, H. Rodriguez, P. E. Bastian, J. Johnson and W. E. Gray; Diffusion Transfer Images of Pure and Impure Silver in Model Systems; Photographic Science and Engineering; Vol. 15, No. 5, Page 356

Bloemer, M. J. (1988), M. C. Buncick, R. J. Warmack, and T. L. Farrell; Surface Electromagnetic Models in Prolate Spheroids of Gold, Aluminum and Copper. Optical Society of America; Vol. 5, No. 12, Page 2552

Bloemer, M. J. (1988), M. C. Buncick, R. J. Warmack, and T. L. Farrell; Optical Properties of Submicrometer-size Silver Needles; Physical Review/American Physical Society; Vol. 37, No. 14, Page 8015

Borrelli, N. F. (1978), Thomas P. Seward III; Optically Induced Anisotropy In Photochromic Glasses; Americal Institute of Physics; September 1979, Page 5979

Borrelli, N. F. (1978), Thomas P. Seward III; Photoinduced Optical Anisotropy and Color Adaptation in Silver-Containing Glasses; American Institute of Physics; March 1979, Page 395

Buncick, M. C., (1987), R. J. Warmack and T. L. Ferrell; Optical Absorbance of Silver Ellipsoidal Particles; Journal of Optical Society of America B; Vol. 4, No. 6, Page 927

Chernov, S. F. (1984); Color Centers Arising in Highly Disperse Microcrystals of Some Silver Salts; Optical Society of America; September 1985, Page 341

Chernov, S. F. (1984); Smallest Metallic Particles of Silver in A Dielectric Medium; Optical Society of America; July 1985, Page 141

Cline, M. P. (1986), P. W. Barber and R. K. Chang; Surface-Enhanced Electric Intensities on Transition and Noble-Metal Spheroids; Journal of Optical Society of America B; Vol. 3, No. 1; Page 15

Cohn, M. S. (1961) Anisotropy in Permalloy Films Evaporated at Grazing Incidence; Journal of Applied Physics, Vol. 32, No. 3, Page 87S

Craighead, H. G., (1981); A. M. Glass; Optical Absorption of Small Metal Particles With Adsorbed Dye Coats; Optics Letters; Vol. 6, No. 5, Page 248

de Bruijn, Helene E., (1989), Rob Kooyman and Jan Greve; Determination of Dielectric Permittivity and Thinkness of A Metal Layer From A Surface Plasmon Resonance Experiment; Applied Optics; Vol. 29, No. 13, Page 1974

Dobierzewska-Mozrzymas, Ewa, (1987), J. Peisert and P. Bieganski; Optical Properties of Gold and Aluminum Island Films With Regard To Grain Size and Interisland Spacing Distributions; Applied Optics; Vol. 27, No. 1, Page 181

Doremus, R. H., (1964); Optical Properties of Small Silver Particles; Journal of Chemical Physics; Vol. 42, No. 1, Page 414

Doremus, R. H., (1966); Optical Properties of Thin Metallic Films In Island Form; Journal of Applied Physics; Vol. 37, No. 7, Page 2775

Doremus, R. H., (1964); Plasma Resonances in Small Metallic Particles; Journal of Applied Physics, Vol. 35, No. 12, Page 3456

Doyle, W. T., (1959); Coagulation, Optical Absorption and Photoconductivity of Colloid Centres in Alkali Halides; Proc. Physical Society; Vol. 5, Page 649

Eagen, C. F. (1981); Nature of The Enhanced Optical Absorption of Dye-Coated Ag Island Films; Applied Optics, Vol. 20, No. 17, Page 3035

Garoff, S. (1981) D. A. Weitz, T. J. Gramila, and C. D. Hanson; Optical Absorption Resonances of Dye-Coated Silver-Island Films; Optics Letters, Optical Society of America; Vol. 6, No. 5, Page 245

Goudonnet, J. P., (1989), J. L. Bijeon, M. Pautyl A Method For Determining Shape and Volume of Ellipsoidal Silver Particles From Absorbance Measurements; Thin Solid Films; Vol. 177, Page 49

Granqvist, C. G., (1975); R. A. Buhrman; Statistical Model for Coalescence of Islands in Discontinuous Films; Applied Phisics Letters; Vol. 27, No. 12, Page 693

Jones, R. C., (1970), G. R. Bird; Effect of Aggregation On The Absorption of Particles of Silver; Photographic Science and Engineering; Vol. 16, No. 1, Page 16

King, R. J., (1970); S. P. Talim; Some Aspects of Polarizer Performance; Journal of Physics E: Scientific Instruments; Vol 4, Page 93

Klein, E. (1960), H. J. Metz; Color of Colloidal Silver Sols in Gelatin; Photographic Science and Engineering; Vol. 5, No. 1, Page 5

Land, E. H. (1934), C. D. West; Dichroism and Dichroic Polarizers; Colliod Chemistry; page 160

Lewis, B., (1967), D. S. Campbell; Nucleation and Initial-Growth Behavior of Thin-Film Deposits; Journal of Vacuum Science and Technology; Vol. 4, No. 5, Page 209

Liao, P. F. (1982), M. B. Stern; Surface-enhanced Raman Scattering on Fold And ALuminum Particle Arrays; Optical Society of America; Vol. 7, No. 10, Page 483

Little, J. W., (1982), T. L. Ferrell, T. A. Callott, and E. T. Arakawa; Radiative Decay of Surgace Plasmons on Oblate Spheroids; Physical Review B; Vol. 26, No. 10, Page 5953

McCarthy, S. L., (1976), Optical Properties of Ultrathin Ag Films; J. Vac. Science Technol., Vol. 13, No. 1, Page 135

Nakahara, S. (1983), A. F. Hebard; Microstructure Trends In Metal (Aluminum, Copper, Indium, Lead, Tin) - Metal Oxide Thin Films Prepared By Reactive Ion Beam Sputter Deposition; Thin Solid Films; Vol 102, Page 345

Oro, J. A., (1983), J. C. Wolfe; Fabrication of A High Density Storage Medium for Electron Beam Memory; Journal of Vacuum Society Technol.; Vol. 1, No. 4, Page 1088

Osborn, J. A. (1945) Demagnetizing Factors of the General Ellipsoid; Physical Review; Vol. 67, No. 11, Page 351

Padmabandu, G. G. (1989), D. Abromson and WIlliam S. Bickel; Light Scattering By Micron-Sized Conducting Fibers; An Experimental Determination; Applied Optics; Vol. 30, No. 1, Page 139

Ritchie, R. H., (1973); Surface Plasmons in Solids; Surface Science 34; Page 1

Ritchie, R. H., (1982); J. C. Ashley and T. L. Ferrell; The Interaction of Photons With Surface Plasmons; Electromagnetic Surface Modes; Page 119

Royer, P., (1986), J. P. Goudonnet, R. J. Warmack, T. L. Ferrell; Substrate Effects on Surface-Plasmon Spectra in Metal-Island Films; Physical Review; Vol. 35, No. 8, Page 3753

Rupprecht, G., (1962), Ginsberg, D.M., Leslie, J.D.; Pyrolytic Graphite Transmission Polarizer for Infrared Radiation; Journal of the Optical Society of America; Vol. 31, No. 62, Page 665

Seward, Thomas P. III, (1984); Glass Polarizers Containing Silver; SPIE; Vol. 464, Page 96

Skillman, D. C., (1967), C. R. Berry; Effect of Particle Shape on the Spectral Absorption of Colloidal Silver in Gelatin; Journal of Chemical Physics; Vol. 48, No. 7, Page 3207

Skillman, D. C., (1972), C. R. Berry; Spectral Extinction of Colloidal Silver; Journal of Optical Society of America; Vol. 63, No. 6, Page 707

Slocum, R. E., (1976) U.S.Patent #3,969,545; (1977) U.S.Patent #4,049,338; Light Polarizing Material Method and Apparatus

Smith, D. O., (1960), M. S. Cohen and G. P. Weiss; Oblique-Incidence Anisotropy in Evaporated Permalloy Films; Journal of Applied Physics; Vol. 31, No. 10, Page 1755

Song, Dar-Yuan, (1985); R. W. Sprague, H. Angus Macleod, and Michael R. Jacobson; Progress in The Development of a Durable Silver-Based High-Reflectance Coating for Astronomical Telescopes; Applied Optics; Vol. 24, No. 8, Page 1164

Stookey, S.D., (1968), R.J.Araujo; Selective Polarization of Light Due To Absorption by Small Elongated Silver Particles in Glass; Applied Optics, Vol. 7, No. 5, page 777

Stover, John C., (1988); Optical Scatter; Laser & Optronics; August 1988; Page 61

van de Hulst, H. C., (1957, 1981), Absorbing Spheres; Light Scattering by Small Particles; Chapter 14, page 267

Werner, Arend, (1989), Hartmut Hibst; Particulate Au and Ag Films for Optical Recording; Applied Optics; Vol. 28, No. 7, Page 1422

NASA
National Aeronautics and Space Administration

Report Documentation Page

1. Report No.	2. Government Accession No.	3. Recipient's Catalog No.

4. Title and Subtitle

Metal Thin-Film Polarizers for Space Applicatis

5. Report Date

May 28, 1991

6. Performing Organization Code

7. Author(s)

Robert E. Slocum (P.I.)

8. Performing Organization Report No.

10. Work Unit No.

9. Performing Organization Name and Address

Polatomic, Inc.
2201 Waterview Parkway, Suite 1.712
Richardson, TX 75080

11. Contract or Grant No.

NAS7-1037

13. Type of Report and Period Covered

Final Report
17 May 1988 - 17 April 1991

12. Sponsoring Agency Name and Address

NASA/JPL
4800 Oak Grove Drive
Pasadena, CA 91109

14. Sponsoring Agency Code

15. Supplementary Notes

16. Abstract

A light polarizing material was developed for wavelengths in the visible and near-infrared spectral band (400 nm to 3,000 nm). The material is comprised of ellipsoidal silver particles uniformly distributed and aligned on the surface of an optical material. A method is set forth for making polarizing material by evaporatively coating a smooth glass surface with ellipsoidal silver particles. The wavelength of peak absorption is chosen by selecting the aspect ratio of the ellipsoidal metal particles and the refractive index of the material surrounding the metal particles. The wavelength of peak absorption can be selected to fall at a desired wavelength in the range from 400 nm to 3,000 nm by control of the deposition process. This method is demonstrated by evaporative deposition of silver particles directly on to a smooth optical surface. By applying a multilayer silver coating on a glass disc, a contrast of greater than 40,000 was achieved at 590 nm. A polarizing filter was designed, fabricated and assembled which achieved contrast of 100,000 at 590 nm and can serve as a replacement for crystal polarizers.

17. Key Words (Suggested by Author(s))	18. Distribution Statement
Polarizers Thin-Fils	Unclassified

19. Security Classif. (of this report)	20. Security Classif. (of this page)	21. No. of pages	22. Price
Unclassified	unclassified	123	

NASA FORM 1626 OCT 86